NOAA TECHNICAL MEMORANDUM NMFS-SEFSC-748

Predicting the effects of low salinity associated with the MBSD project on resident common bottlenose dolphins (*Tursiops truncatus*) in Barataria Bay, LA.

Lance P. Garrison,[1] Jenny Litz[1], Carrie Sinclair[2]

U.S. Department of Commerce
National Oceanic and Atmospheric Administration
National Marine Fisheries Service
Southeast Fisheries Science Center
75 Virginia Beach Drive
Miami, Florida 33149

December 2020

NOAA TECHNICAL MEMORANDUM NMFS-SEFSC-748

Predicting the effects of low salinity associated with the MBSD project on resident common bottlenose dolphins (*Tursiops truncatus*) in Barataria Bay, LA.

By

Lance P. Garrison,[1] Jenny Litz[1], Carrie Sinclair[2]

[1]National Marine Fisheries Service, Southeast Fisheries Science Center,
Miami, FL 33149
[2]National Marine Fisheries Service, Southeast Fisheries Science Center,
Pascagoula, MS 39568

U.S. DEPARTMENT OF COMMERCE
Wilbur L Ross Jr., Secretary

NATIONAL OCEANIC AND ATMOSPHERIC ADMINISTRATION
Neil A. Jacobs, Ph.D.,
Acting NOAA Administrator

NATIONAL MARINE FISHERIES SERVICE
Chris Oliver
Assistant Administrator for Fisheries

December 2020

NOTICE

The National Marine Fisheries Service (NMFS) does not approve, recommend or endorse any proprietary product or material mentioned in this publication. No reference shall be made to NOAA Fisheries Service, or to this publication furnished by NOAA Fisheries Service, in any advertising or sales promotion which would indicate or imply that NOAA Fisheries Service approves, recommends or endorses any proprietary product or material herein or which has as its purpose any intent to cause or indirectly cause the advertised product to be used or purchased because of National Marine Fisheries Service publication.

This report should be cited as follows:

Garrison, L.P, Litz, J. and Sinclair, C. 2020. Predicting the effects of low salinity associated with the MBSD project on resident common bottlenose dolphins (*Tursiops truncatus*) in Barataria Bay, LA. NOAA Technical Memorandum NOAA NMFS-SEFSC-748: 97 p.

Copies of this report can be obtained from:

Director, Protected Resources and
Biodiversity Division
Southeast Fisheries Science Center
National Marine Fisheries Service
75 Virginia Beach Drive
Miami, FL 33149

Or online at:
https://repository.library.noaa.gov/

Executive Summary

In this analysis, we develop a simulation approach to evaluate the probable effects of changes in salinity in Barataria Bay, LA associated with the Mid-Barataria Sediment Diversion (MBSD) project on the resident common bottlenose dolphin stock. This population occurs throughout the Bay with a total estimated population size of 2,071 (95% CI: 1,832 – 2,309) animals. Dolphins occur in the highest densities near the barrier islands and the associated passes. Under various alternative diversion scenarios, the MBSD project is expected to reconnect the flows of freshwater, sediment, and nutrients from the Mississippi River into the northern portion of the Bay on an annual basis. This action is intended to rebuild marsh areas and reduce land loss. The preferred alternative (Applicant's Preferred Alternative) sets a maximum instantaneous inflow from the project at 75,000 cubic feet per second (CFS). Two additional alternatives of differing discharge capacities are being considered in addition to the "No Action Alternative," where the current and future conditions are considered without the project. Daily salinity surfaces from the Delft3D hydrodynamic model were used to assess the changes in the distribution of low salinity (< 5 ppt) in the Bay and subsequent projected impacts on the bottlenose dolphin population. We used information on the initial spatial distribution of dolphins, simulated dolphin movements, modelled exposure to low salinity, and an expert elicitation-based dose-response curve relating exposure to low salinity to survival to estimate expected annual survival rates for the bottlenose dolphin population.

This document includes three sections. Section 1 describes the results of a photo-identification capture-mark-recapture (CMR) survey of Barataria Bay conducted during spring 2019 and provides an updated abundance estimate and an assessment of dolphin spatial distribution. Section 2 describes an approach to quantify known prediction biases in the Delft3D outputs and account for them in our assessment of bottlenose dolphin survival. Finally, Section 3 describes the development and application of the model that projects the impacts of exposure to low salinity on the survivorship of bottlenose dolphins in the bay under various diversion scenarios. Several sources of uncertainty are included in the assessment; however, there remain unquantified sources of uncertainty and potential bias that cannot be accounted for in the model. These are discussed in detail in section 3.

The model projects that increasing freshwater input into Barataria Bay will result in substantial declines in bottlenose dolphin survival rates. Relative to the No Action Alternative, the model projects that the mean population survival rate will decline by an estimated 34% (95% CL: 15.3%-62.7%) in any given year in the first decade under the Applicant's Preferred Alternative based upon the representative hydrograph, and the greatest impacts would be on dolphins inhabiting the central and western portions of the Bay. The projected reductions in survival would likely result in substantial declines in bottlenose dolphin population size over the short-term.

Table of Contents

I. Photo-identification Capture-Mark-Recapture and Abundance Estimation

I.1 Overview and Objectives

The Barataria Bay Estuarine System (BBES) Stock of common bottlenose dolphins (*Tursiops truncatus*) is abundant and widely distributed in Barataria Bay where the most recent abundance estimate (~2,300 dolphins) was based on data collected from 2010–2014 for the DWH Natural Resource Damage Assessment (NRDA) (McDonald et al. 2017). Previous studies have demonstrated that this population maintains a small range and is primarily restricted to the waters inside Barataria Bay and in the adjacent coastal waters within 2km from shore (Hayes et al. 2019, Wells et al. 2017). A comparison of photo-identification databases between Barataria Bay and the adjacent Terrebone-Timbalier sound estuarine system demonstrated little movement between these neighboring populations (Mullin et al. 2018).

The most recent estimate of abundance for the BBES dolphin stock was made using data collected through 2014. In addition to being outdated, the surveys used for those estimates did not cover the entirety of the BBES stock areas and were concentrated in the central and western portions of the Bay (Figure I.1). Density estimates for the surveyed region were derived using spatially explicit capture-recapture models, and these densities were extrapolated to cover the entire range of the stock (McDonald et al. 2017). The objective of this study was to conduct capture-mark-recapture surveys of bottlenose dolphins to provide a current abundance estimate and characterize spatial distribution within the stock range. In particular, the survey area was expanded compared to previous surveys to include a larger extent of potential dolphin habitat in the northern and eastern portions of Barataria Bay.

I.2 Methods

Photo-identification Surveys

The surveyed area included modifications to western and central track-lines previously covered during studies related to the DWH NRDA (McDonald et al. 2017).

Survey effort was also expanded to include bayous and contours of marsh habitat where dolphins have been tracked or sighted using other methodologies including satellite telemetry and fecundity surveys (Wells et al. 2017, Lane et al. 2015), as well as far eastern portions of the BBES which had not been included in prior surveys (Figure I.1).

The survey window was 19 days from 14 March to 1 April 2019. Surveys were conducted using a closed population capture-mark-recapture (CMR) design (*e.g.* Balmer et al. 2019, Mullin et al. 2017, McDonald et al. 2017, Rosel et al. 2011, Speakman et al. 2010, Balmer et al. 2008). Each regional set of tracklines (Figure I.2) was fully covered in each of four "mark" sessions. Each mark session took three to four days to complete using three vessels.

Surveys were conducted from three outboard-powered small boats, the 7.5-m NOAA *R/V R2* (R2), the 7.3-m NOAA *R/V Top Notch* (TN) and the 6.4-m NOAA *R/V Sciaenops* (SC), operating in concert. The starting point was weather dependent. A combination of marsh contours and open water track-lines were followed to facilitate full coverage of the survey area

Surveys were conducted in Beaufort Sea state (BSS) ≤4 and survey speed was approximately 30 km/h. A Survey Effort Log (*e.g.* on- and off-effort distance segments) was completed for each survey and each vessel's track-line was recorded on a handheld global positioning system (GPS). Survey Conditions (i.e. excellent, good, fair, poor) were recorded when effort began and any time there was a substantial change in conditions.

The survey teams consisted of a minimum of three observers per vessel where operational duties were driving, photographing and recording data. Observers searched visually (with naked eye) for dolphins forward of the vessel's beam on both sides of the boat. When a dolphin group was sighted, it was approached for data collection. A dolphin group was defined as all dolphins in <100m proximity, moving in the same direction and/or exhibiting similar behavior (Shane 1990).

Dolphin sighting procedures are given in detail in Melancon et al. (2011), and summarized here. Three waypoints were recorded during every encounter: Boat, Start and End. The Boat waypoint recorded where the boat was when the dolphins were first sighted. It was recorded as soon as a dolphin group was sighted, before the vessel departed the trackline to approach the group. The Start waypoint was recorded when the

vessel reached the location of the group to begin data collection. The End waypoint was recorded when the encounter was over, before returning to the trackline. The Boat and End Distance (daily trip odometer) was recorded when the boat departed (same time as Boat waypoint) and returned to the track-line (before effort is resumed), respectively.

Data associated with each waypoint (waypoint number, time, and trip odometer (distance)) were recorded on the Sighting Form. Returning to the trackline depended on direction and movement during the sighting. If the sighting was made or moved in a direction of previous effort (*e.g*., sighted abeam, just aft of the beam or moving in a direction backwards over track-line already covered), the boat returned to the Boat waypoint before resuming effort and recording End Distance. If the sighting continued along the track-line and remained forward of the Boat waypoint, the boat returned to the track-line at a perpendicular angle once the sighting was complete. Once on track, the odometer distance was recorded as the "End Distance" and effort was resumed. Dolphin groups were approached within 2m at a shallow angle and steady speed. Once in the vicinity of the dolphin group, vessel speed and travel direction of the group were matched and drastic changes in speed avoided.

Images of dorsal fins were collected with digital cameras equipped with zoom lenses (*e.g.* Canon EOS 7D and a Canon 100-400mm image stabilizing telephoto lens). The goal was to collect high quality, left and right side dorsal fin images of every dolphin in the group, regardless of fin distinctiveness. A high quality dorsal fin image was defined as fully visible (*e.g.* not obstructed by water, other dorsal fins or *Xenobalanus spp*.), perpendicular to the camera and had good to excellent contrast (lighting) and focus (clarity) (Urian et al. 2015). Images other than dorsal fins were taken if any of the following were present (but not limited to): 1) aerial or interesting behaviors; 2) freeze brands, satellite tags or roto-tags; 3) skin disorders; 4) gear entanglements; and/or 5) body condition concerns. Image acquisition was suspended for any of the following reasons: 1) all group members were photographed; 2) intractable dolphins; 3) repeatedly adverse behavioral reactions by one or more members of the group; 4) weather or safety concerns. Maximum time with each sighting was limited to 35 minutes.

The Sighting Form was filled out during the encounter (*e.g.* survey/sighting number, crew, sighting conditions, behaviors, observations, freeze brands) and finalized

at the end of the encounter (*e.g.* salinity, group size estimates). Estimates of total dolphins included all dolphins within the sighting, calves and neonates included. The total calves estimate did not include neonates. Calves were defined as dolphins less than 2/3 of the presumed mother's length and observed surfacing in the "calf" or echelon position (Shane 1990). Neonates were characterized by fetal folds, dark coloration and uncoordinated surfacing pattern (Urian and Wells 1996, Shane 1990). Smaller animals not observed alongside a larger animal were noted as a possible calf or neonate.
In the BBES, mom/calf pairs are closely monitored for reproductive rates, including fecundity tracking of previous years' reproductive or pregnant females (Lane et al. 2015). In groups where calves and neonates were present, image frame numbers of presumed mothers and calves were recorded on the Sighting Form. Typically, this was accomplished by communication between the photographer and recorder during the encounter or at the end of the encounter, before resuming effort.

In addition to environmental parameters collected during sightings, additional salinity and temperature data points were collected along the tracklines at set stations (Figure I.3). Some of the points were pre-determined along east-west tracklines. Along marsh contours, points were collected at the extremities of the contours (*e.g.* east, west, north and south along the contour and at the opening to bays and deep channels). Data points were recorded on the Survey Effort Worksheet. Date, time, station, salinity [in parts per thousand (ppt)] and temperature [degrees Celsius (°C)] were recorded in the notes section. If there was a sighting within 500m of a salinity and temperature station, the temperature and salinity recorded during the sighting was used for that station.

Photo-identification and analysis

GPS data and digital images were downloaded daily to external hard drives (one working drive and one backup drive). Data sheets were compared to waypoints and camera information to ensure accuracy. All files (camera folders, GPS, data sheets, etc.) were named in the same format: survey number, year, month, day, vessel (Snnn_YYYY_MMDD_VV). Upon returning from the field, Survey and Sighting Forms and GPS files were entered into FinBase, a custom Microsoft Access database (Melancon et al. 2011, Adams et al. 2006). All data from salinity and temperature stations were

entered into a centralized spreadsheet. All data forms were scanned and saved in portable document format.

Digital images from all surveys were sorted by sighting to find the best right and/or left dorsal fin image of each unique individual. All images of the same individual were placed in a designated folder within the sighting folder. Poor quality images were placed in a separate folder. When necessary, the folder was also labeled with additional information pertaining to the individual (mom, calf, skin disorder, etc). Once all images were sorted into folders, the best right and/or left from each individuals' folder was given a temporary ID (e.g., A, B, C…Z). Sorted images were rated separately for quality (Q1 = excellent, Q2 = average, Q3 = low) (Urian et al. 2014) and distinctiveness (D1 = high, D2 = average, D3 = Low, D4 = not distinct) (Speakman et al. 2010).

The matching phase consisted of an initial comparison of the sorted images to the Barataria Bay master catalog using finFindR software [Western Ecosystems Technology, Incorporated (WEST, Inc.); Laramie, WY] (Mullin et al. 2018). Briefly, finFindR was used to trace the trailing edge of newly sorted images. Once the traces were saved, they were compared to the master catalog images and finFindR displayed a spreadsheet of the most similar catalog images to each sorted fin. The "1 per ID" checkbox was selected which limits the results table to only one image for each unique ID in the master catalog. The first 50 unique catalog images were compared side by side to the sorted fins. If a match was found, the existing catalog ID was recorded. If a match was not found, a tentative new catalog ID was assigned. Verification of potential matches and tentative new fins was performed by trained technicians with naked eye using a user-defined, attribute-based ranking system in FinBase.

Abundance Estimation

The 2019 CMR data were analyzed with the software package MARK version 9.0 (http://www.phidot.org/software/mark/index.html, accessed 12 Oct. 2019) using closed population capture-mark-recapture models. The dataset was limited to only images with excellent or average photo-quality scores (PQ1 and PQ2, respectively) and only fins with high or average distinctiveness (D1 and D2 respectively) were considered marked (Litz et al. 2019, Urian et al. 2015, Speakman et al. 2010). The models were analyzed using the

Full-Likelihood approach (Otis et al. 1978) and the conditional approach (Huggins 1989), and results were similar between these methods. The results of the Full-Likelihood approach are presented below. Several model structures were evaluated and the model providing the best explanatory power was selected using the minimum Akaike's Information Criterion (AIC, Burnham and Anderson 2004). Using the Otis et al. (Otis et al. 1978) notation, the evaluated model structure included: 1) the simple, M_0 model where capture probability (p) and recapture probability (c) are assumed to be equal and constant across mark sessions, 2) the M_t model where the capture probability (p) and the recapture probability (c) are assumed to be equal but vary across mark sessions, and 3) the M_{tb} model where p and c were allowed to vary across mark sessions and were not equal to each other, thus evaluating whether or not there was a behavioral difference between the probability of capture and the probability of recapture.

The derived abundance estimate of the marked animals was then divided by the proportion of distinct fins to generate an abundance estimate for the total individuals (marked and unmarked) in the sampled population. The proportion marked was calculated by dividing the number of marked fins (D1 & D2) in each sighting by the total number of animals cataloged in that sighting using the same dataset analyzed (PQ1 & PQ2). The proportion marked was calculated only from those sightings with complete photo coverage (photo completeness ≥ 1, calculated by the number of cataloged dolphins for a sighting divided by the field estimate of the number of dolphins present in that sighting; Litz et al. 2019, Balmer et al. 2013).

Spatial Distribution

The relative spatial distribution of bottlenose dolphins during the CMR surveys was modeled using a Generalized Additive Model (GAM; Wood et al. 2016, Wood 2017). Survey tracks were first coded into "on-effort" and "off-effort" segments. "On-effort" included periods when the vessel was moving along the planned survey tracklines and observers were actively searching for dolphin groups. "Off-effort" segments included time spent transiting to and from the survey area, during periods when photographic data was being collected, and other periods when the vessel was not involved in active surveys. A 500 x 500m grid was developed for the survey area, and the length of on

effort trackline, number of dolphin sightings, and total number of dolphins within each grid cell was summarized (Figure I.4). The "Sightings Per Unit Effort (SPUE)" metric was calculated as the number of dolphins per 100 meters of on-effort trackline. This is a metric of relative density assuming that detection probability and the searched strip width is consistent across all transect segments. SPUE was modeled as a function of spatial location in the Bay using the GAM model. The response variable was the number of dolphins observed in a given grid cell. The x and y coordinates (UTM15 projection) of the centroid of each grid cell and the distance from the Barataria Pass were included as smooth terms in the model along with an offset term for survey effort (log(trackline length). A Tweedie distribution was used to model the error structure as this is a flexible model for count data that allows for overdispersion typical of spatial count data of this type (Wood et al. 2016, Wood 2017). The distance from Barataria Pass was included in the model to account for high encounter rates of dolphins observed in the pass. Prior studies (McDonald et al. 2017) found very high densities of dolphins in passes of Barataria Bay and the habitat surrounding the barrier islands. The resulting GAM model was used to develop a predicted surface of relative bottlenose dolphin occurrence within the stock area including extrapolation to areas that were not surveyed where appropriate. The GAM model was conducted using package "mgcv" (Wood 2017, version 1.8-31) in the R statistical computing language.

I.3 Results

Photo-identification Surveys

A total of 37 surveys (Western: n = 11; Central: n = 13; Southeastern: n = 13) covering 4,195km of track-lines were conducted during 14 March – 30 March 2019 in Barataria Bay. The number of dolphin groups sighted per day was variable with a range of 2-24 groups. Overall there were 368 sightings of bottlenose dolphin groups composed of 2,046 dolphins (Table 1). Calves were present in 21% (n = 76) of total sightings and comprised 4.7% of the total number of dolphins encountered. Neonates were encountered 55 times during the survey.

Sightings were distributed throughout the survey area (Figure I.4). Few sightings were observed in the northern extent of the Western Area (e.g. Hackberry Bay). In the Central area, there were no sightings in the Barataria Waterway adjacent to Hackberry Bay. However, there were relatively frequent sightings in the northern portion of this area including Bay Batiste. In the Southeastern area, there were few sightings in the southeastern area near Bay Jacques (Figure I.4). Group sizes in each of the three regions of the study area were similar with a range of 1 to 40 animals and mean group size ranging from 4.6 to 6.4 (Table I.2, Figure I.5).

The lowest average salinity was observed in the Western survey area ($\bar{x}$ = 7.6‰, range = 0.4 – 18.2‰). Slightly higher average salinity was observed in the Central area ($\bar{x}$ = 9.2‰, range = 1.5 – 20.2‰) and average salinity was highest in the Southeastern area ($\bar{x}$ = 11.4‰, range = 0.6 – 31.0‰). Average temperature was similar amongst the three areas (Western: $\bar{x}$ = 18.9; Central: $\bar{x}$ = 18.1; Southeastern: $\bar{x}$ = 18.2). The largest range in temperature was observed in the Central area (range = 9.2 – 21.1) (Table I.3). Of interest, during the first week of the survey (mark session 1), the salinity in the Western area was higher in the northern extent of the survey area and lower in the southern extent, closer to the Gulf of Mexico.

Photo Analysis

A total of 27,365 digital photographs were collected during the four mark sessions in 97% of sightings (n = 358). Sorting the raw images yielded 1,977 unique dolphins for comparison to the Barataria Bay master catalog. A discovery curve indicated there was a sharp increase in number of new dolphins added to the master catalog (n = 586) from the 2019 field effort (Figure I.6).

Photo-identification data were examined to assess the movement of dolphins between survey regions including comparison to prior year surveys which did not survey the Southeast area (McDonald et al. 2017). For this comparison, we used the most conservative dataset, which included only photos with excellent or average photo quality (PQ1 & PQ2) and individuals with high or average distinct fins (marked animals D1 & D2). There were a total of 835 individuals in the dataset from surveys conducted during 2010-2014, and there were 477 new animals sighted for the first time in 2019 (57%). Of

these new animals, 46.5% (222/477) were first sighted in the southeastern survey area, and only 4 animals sighted in the southeastern area had been seen in prior years. Of the 227 animals that were seen in the southeastern survey area, only 6 animals had also been seen elsewhere in the Bay, and those additional sightings were all close to the boundary of the southeastern survey area. The 2019 data indicate little movement of animals between the newly surveyed eastern portion of Barataria Bay and the previously surveyed main portion of the Bay.

Abundance Estimation

The closed capture full-likelihood approach supported the M_t model with slight support for the M_{tb} model (Table I.4). The M_0 model was unsupported. The capture probabilities for the 4 secondary surveys ranged from 0.15 to 0.22 (Table I.5). The resulting abundance estimate was 1,491 marked animals (Standard Error = 64.9). Of the 210 sightings with complete photographs, the average proportion of individuals marked was 0.72 (SE = 0.031). Correcting for the proportion of marked fins, the resulting abundance estimate for Barataria Bay dolphins was 2,071 (95% CI: 1,832 – 2,309, Table I.6).

Spatial Distribution

The spatial GAM model indicated that all three smooth terms (East, North, and distance from Barataria pass) were statistically significant, and the model explained 14.6% of the residual deviance (Table I.7). The smooth function in the East parameter demonstrated lower densities at the eastern and western ends of the survey area with higher densities in the central portion. The North parameter indicated higher density in the southern portion of the surveyed area, lower density in the middle, and increasing density toward the northern portion of the range. Finally, the "distance from pass" parameter demonstrates rapidly increasing density at lower distances from the pass (Figure I.7). The rapid increase in uncertainty at the extreme ends of these plots is typical of models of this type and caution against extrapolation beyond the range of the collected data. This is particularly the case with the North function where the predicted density is

increasing with high uncertainty at extreme values of the explanatory variable (Figure I.7). Comparison of model predictions to observed data demonstrate overall good fit and explanation of the observed spatial patterns in relative density (Figure I.8). It is notable that the relative density increases rapidly near the pass with the SPUE parameter increasing from 0.1 dolphins per 100m of trackline at 10,000m from the pass to 0.4 dolphins per 100m of trackline near the pass (Figure I.8). The predicted spatial pattern in density comports well with the location of observed groups with higher relative densities in the southern, western, and central portions of the Bay and concentrated around the pass (Figure I.9). Higher encounter rates inside smaller embayments in the north-central portions of the Bay were also captured by the model (Figure I.9). The resulting surface is masked to exclude areas where the coefficient of variation (standard error/mean) exceeded 0.4. This level restricted the fitted surface to the data collection area and avoids unwarranted extrapolation given the high uncertainty in model predictions outside of this range.

I.4 Application

The outcomes from this analysis provide a current abundance estimate for the BBES model. The expansion of the survey area to regions in the northern and eastern portions of the Bay provides an improved understanding of dolphin spatial distribution and habitat use. The newly surveyed southeastern region is an area with generally lower densities of dolphins than the central region and areas around the passes. Based on the data collected during 2019, there was limited exchange of animals between the southeastern area and other portions of the Bay and very few of these animals had previously been sighted prior to this survey. Additional surveys would be required to confirm that these general patterns are consistent over time. This is consistent with previous findings that there is partitioning of the Bay by sub-groups of dolphins and home-ranges are relatively small. The spatial model also demonstrates that the highest concentrations of dolphins are centered around the Barataria Pass, but it does not appear that these very high densities extend all the way along the barrier Island chain to the eastern portion of the Bay. Relatively high densities inside small embayments in the

north-central portion of the Bay also had not been documented by previous surveys that did not include these habitats. In the dolphin low salinity exposure model, in the initial time step, the starting point for the simulated movement patterns are randomly selected from the spatial domain of the GAM model. The relative density surface developed in this analysis provides a probability weighting for this random selection so that the simulated starting positions reflects the observed spatial distribution of the population. The movement model is weighted to result in relatively small movements away from these starting points, which is consistent with the limited exchange of dolphins between regions observed in this study and prior studies showing that animals within the Bay have relatively small home ranges. Because the change in salinity expected from the MBSD is highly dependent on the location in the Bay, this simulated dolphin spatial distribution is an important factor in the model outcomes.

II. Prediction Bias and Uncertainty in Delft3D Outputs

II.1 Overview and Objectives

Accurate projection of the effects of alternative MBSD scenarios on the future survival of Barataria Bay bottlenose dolphins depends upon the accuracy of the projected salinity fields produced by the Delft3D model. However, there are several known sources of bias and uncertainty in these outputs. If the Delft3D model consistently over- or under-estimates salinity, then the resulting prediction projection of future mortality rates will be similarly biased. There are two primary types of bias and uncertainty in the Delft3D predictions: retrospective prediction bias and future prediction bias.

Retrospective prediction bias reflects the capability of the model to accurately predict salinity fields under known conditions within the range of environmental variability that has been observed during the historical time series. This type of bias may result from simplification in the model formulation relative to the real world (e.g., using depth-averaged salinity and thereby ignoring vertical structure in the water column), inaccuracy in the boundary conditions used in the model (e.g., time-averaged wind and salinity in offshore waters), or inability to capture the influence of short-term or stochastic events that influence the salinity within the bay in a given year or shorter time interval. The Delft3D model uses external data from salinity stations within the bay to calibrate model outputs to minimize these potential retrospective biases. Evaluation of the effectiveness of this calibration approach for model year 2014 demonstrates that the general pattern in salinity levels is well described by the model outputs; however, model predictions are more accurate in the upper and middle portion of the basin. This is likely due to the influence of offshore boundary conditions and stratification in the deeper, lower portions of the bay (Sadid et al. 2018). In general, the calibration based on year 2014 indicated that salinity in the lower basin was underestimated by between 1-5 ppt. Similar results were observed for model year 2016, which was not included in the calibration data set and was considered a validation year (Sadid et al. 2018). As this year is independent from the model fitting procedure, model predictions for this year are the best available metric of retrospective prediction bias. However, it should be recognized

that prediction errors are likely to vary among different years as there is inter-annual variation in the underlying processes that may or may not be well captured by the model.

The second major type of bias and uncertainty is future prediction bias. This is unquantifiable bias/uncertainty in the future conditions projected by the Delft3D model. There are multiple sources of this type of uncertainty, which are additive to any retrospective biases. First, the freshwater inflow conditions expected to be observed under various diversion scenarios are likely to be outside of the range of conditions that were included in the historical data used to calibrate the Delft3D model. Predictions from the model therefore represent extrapolations and therefore are inherently uncertain. Second, the future climate, sea level, water flow, and other conditions are unknown. Future projections of the model do not attempt to account for expected variability in the overall climate outside of projected changes in sea level. This future prediction uncertainty cannot be quantified or accounted for. Implicitly, comparisons between alternative scenarios assume that the direction and magnitude of future prediction bias will be the same for all alternatives.

In this analysis, we develop an approach to account for retrospective prediction bias based upon the comparison of model predictions vs. station observations from model year 2016. This analysis is similar to that described in Sadid et al. (2018, Appendix 3) and uses the same data for both predicted and observed values. However, there are several differences between our approach and the characterization of uncertainty presented by the Delft3D modelers (Delft3d Model Uncertainty Appendix). First, we are interested in a different spatial domain, and therefore observation stations in the extreme upper portions of the basin are not included in this analysis. Second, the Sadid et al. (2018) analysis only included comparisons between predicted and observed salinity values from March – December because the January-February periods of the annual model runs are heavily influenced by the initial conditions. We used the entire year to account for uncertainties due to the initial condition applied and because we required a full-year simulation to estimate annual survival rate effects. Third, for this analysis, it is necessary to estimate a spatially-averaged estimate of bias at a regional level within the Bay as opposed to station-by-station estimates presented by Sadid et al. (2018, Delft3d Model Uncertainty Appendix). This regional spatial average is required because we are

making predictions of the influence of salinity on dolphin survival rates at all locations in the bay, not at specific points corresponding to the locations of the salinity stations used in the model validation. Data are not available to adequately characterize the full range of uncertainty in predictions at every location within the Bay, and therefore we focused on spatial averages accounting for the observed variability and correlation between stations. However, the analysis of bias and uncertainty at specific station point locations demonstrates that there is variation in uncertainty between stations based on the Root Mean Square Error (RMSE) metric to characterize model predictive skill which was applied by the Delft3D modelling group (Delft3d Model Uncertainty Appendix). For our regional analysis, the standard deviation of the annual bias is the appropriate metric to characterize uncertainty. Our approach captures the model uncertainties related to model skill, but it is not directly comparable with the analysis presented in the Delft3d Model Uncertainty Appendix for the reasons presented above.

II.2 Methods

Observed salinity data collected during 2016 from 22 stations dispersed throughout Barataria Bay were included in this analysis (Figure II.1, Table II.1). This analysis excluded 5 stations that were included in the Sadid et al. (2018) validation analysis. Four of these were in the extreme northern portion of the Basin outside of the domain of the bottlenose dolphin movement analysis (CRMS278, CRMS3985, CRMS287, CRMS4103) and one (CRM282) had an incomplete salinity record and was missing data after 04/06/2016. The stations used in this analysis are largely representative of the areas where high numbers of dolphins were observed during the CMR study. There are stations located near the Barataria Pass, Caminada Bay, and the upper portion of the Bay near Bay Batiste where dolphin encounter rates were high (Figure I.9). However, the open portion of the central bay is not well represented by the available stations.

Salinities are typically reported at hourly intervals for each station, and these were first summarized into daily averages. Hourly predicted salinity values from the Delft3D

model for the grid cell occupied by each of these stations was also provided and summarized into daily means for days from January 4 to December 31 (Figure II.2).

The annual mean observed salinity value (Mean Observed, Table II.1) and three metrics of model predictive skill were calculated and summarized for each station: mean observation bias (MBE), standard deviation of bias (sd MBE), and root-mean-square error (RMSE, Wilmott, 1982). Observation bias is calculated as:

$$(1)\ MBE = N^{-1} \sum_{i=1}^{N} (P_i - O_i),$$

where N is the number of days, P_i = modeled (predicted) observation, and O_i is the observed daily salinity. The standard deviation of the mean bias (*sd*) is:

$$(2)\ sd = \sqrt{(N-1)^{-1} \sum_{i=1}^{N} (P_i - O_i - MBE)^2}.$$

Note that the *sd* estimate assumes independence between the individual observations, which is violated for these autocorrelated time series data. Finally, the RMSE is given as:

$$(3)\ RMSE = \sqrt{N^{-1} \sum_{i=1}^{N} (P_i - O_i)^2}.$$

The RMSE indicates the average difference between the observed and predicted values, which is a measure of the overall accuracy of the predictions. In contrast, the *sd* metric reflects the variability in the bias estimate. Values of MBE, *sd* MBE, and RMSE for each station are shown in Table 1. These differ from values reported in Sadid et al. (2018) because the current analysis includes all dates from January-December, while Sadid et al. (2018) included only data from March-December in their summaries.

Regional Cluster Analysis

The objective of this analysis is to develop representations of retrospective prediction bias across the relevant spatial domain for the bottlenose dolphin stock in Barataria Bay. As such, we require a spatially continuous representation of bias in predicted salinity values as opposed to the point locations in the validation data sets. Ideally, sufficient numbers of point locations would be available to allow the development of a surface of bias corrections so that a spatially explicit bias correction could be provided at each point in the spatial grid of modeled salinities. However, the number of observation stations is too sparse to reliably calculate such a continuous gridded surface. Therefore, we took the approach of identifying regional clusters based upon the similarities in the time series among the stations. We used k-means clustering to identify regional groupings of stations with a common pattern in salinity and associated biases. K-means clustering is an agglomerative clustering technique that combines observations into groups based upon minimizing the within-group variance of parameters (Kassambara, 2017). The number of clusters is specified *a priori* by the analyst, and objective measures are used to identify the optimal number of clusters from a range of considered values. In this case, we used metrics to identify the optimal number of clusters including the "gap" and "silhouette" methods, each of which assess changes in the between- and within-cluster variance with changing numbers of clusters (Kassambara, 2017). The "gap" statistic (Gap) compares the change in the within cluster sum of squares to that of the expectation under a null model. The optimal number of clusters is defined as the minimum number of clusters (k) such that $Gap(k) \geq Gap(k+1) - s_k$ where s_k is the expected standard error of the statistic (Tibshirani et al. 2001). The silhouette method evaluates the mean distance between members of a cluster and the members of a different cluster. The statistic is positive when the members are assigned correctly to clusters, and the maximum value indicates the optimal number of clusters from a range of k values (Kassambara, 2017). For each statistic, the optimal number of clusters was evaluated from k = 1 to 10. The variables for each station that were input into the k-means cluster analysis included: mean salinity, RMSE, MBE, sd MBE, East, and North (Table II.1). These variables capture the spatial arrangement of the stations, the environmental similarity, and the similarity in model performance. Analyses were

conducted in packages “cluster” (version 2.10, Maechler et al. 2019) and “factoextra” (version 1.0.6, Kassambara et al. 2019) in the R statistical computing language.

Regional Mean Bias Estimation

Within regional station clusters, the mean and variance of the prediction bias was estimated by combining the time series of daily bias across stations. The aggregation of annual mean bias, and in particular estimation of appropriate variance, is complicated by the time series nature of the data and the correlations among stations. To properly account for these correlations, a generalized additive mixed model (GAMM) was used to model the effect of day of the year on regional mean bias including an autoregressive (AR) error structure to account for serial autocorrelation within the time series. Station was included as a random effect in the GAMM. The GAMM method uses smoothing splines to fit the daily pattern in bias, while the AR structure accounts for the dependence between residuals at different time lags among residuals. GAMM models were fit with no autocorrelation and with lags of 1-3 days based upon an initial examination of the partial autocorrelation function (PACF) of residuals. The model in which residuals showed no lag correlation was selected and used to estimate both the annual mean and variance of the model prediction bias. The GAMM analysis was conducted in package “mgcv” (Version 1.8-31, Wood 2017). The resulting annual MBE and its variance were used to correct predicted salinity fields from the Delft3d model for retrospective bias.

II.3 Results

Regional Cluster Analysis

Examination of the bias time series for each station suggest two general groupings of stations. The first (typified by CRMS0226) shows a small positive average bias and relatively little variability around the mean. The second group (e.g., CRMS0178) shows a negative mean bias greater with variation. There is little indication of linear trends or other patterns in the bias time series, thought the greatest variability typically occurs early in the year in most cases (Figure II.3). An initial matrix of differences between station

pairs supports this pattern of two clusters of stations that are similar within groups based on mean salinity, bias, sd bias, RMSE, and location (Figure II.4).

K-means clustering sorted the stations into similar groups. The centroids of the groups are well separated by a single axis with relatively little separation along a second dimension (Figure II.5). With 4 or 5 groups specified, there are small clusters of only 2 or 3 stations, suggesting that this level of division is too fine. Either 2 or 3 clusters appear to result in separation of stations (Figure II.5). However, both the "gap" and "silhouette" metrics (Figure II.6) indicate that 2 clusters is optimal for these data.

When classified into the defined clusters, the stations are well separated in both environmental and geographic space. Cluster 1 corresponds to stations with a mostly positive salinity bias ranging between -0.823 and 1.333 ppt and RMSE $\leq$ 3.15 (Figure II.7). Cluster 2 corresponds to stations with negative bias between -3.779 and -0.4364 ppt and RMSE $\geq$ 0.3.367 (Figure II.7). Spatially cluster 1 corresponds to stations that are representative of the more northern portion of the Bay that is influenced primarily by freshwater inputs and dominated by marsh habitats. Cluster 2 corresponds to the southern Bay including the open, estuarine waters and the region near the barrier islands and associated channels (Figure II.8).

Regional Mean Bias Estimation

The GAMM of MBE for cluster 1 fit without an autoregressive error structure demonstrated lag correlation in the residuals at days 1-3 (Figure II.9A). Including the AR3 structure in the model accounted for this autocorrelation leaving uncorrelated, "white noise" in the residual correlation structure (Figure II.9B). The resulting GAMM smooth fit for each station closely followed the observed trends in daily bias throughout the year (Figure II.10, see Appendix II.A1 for GAMM summary). It is notable that there were seasonal trends in the bias with the greatest positive bias occurring during the first approximately 100 days of the year for each station. A parametric bootstrap distribution of the mean was generated from the GAMM fit accounting for the uncertainty in parameter estimates and resulting predictions. As expected, the mean distribution of residuals that did not account for spatial autocorrelation had a substantially smaller

variance than for the autoregressive model (Figure II.11). The resulting regional mean bias was 0.717 ppt with a standard deviation of 0.0889.

Results for the GAMM for cluster 2 were similar to those for cluster 1. The initial GAMM without the AR error structure indicated significant autocorrelation at lags of 1-3 days, and this structure was adequately modeled by including the AR3 correlation in the error term (Figure II.12, see Appendix II.A2 for GAMM summary). GAMM model fits closely followed the patterns in the daily bias value, but there was little to no apparent seasonal trend in the magnitude of the bias throughout the year (Figure II.13). There was a greater degree of variability around the GAMM fits for Cluster 2 stations, as was expected from their greater RMSE values compared to Cluster 1. The parametric bootstrap distribution of mean annual bias showed the expected pattern of greater variance in the mean once autocorrelation was accounted for (Figure II.14). There was a small difference in the estimated mean bias between the two GAMM models for Cluster 2. The resulting regional mean bias for cluster 2 was -2.316 ppt with a standard deviation of 0.168.

II.4 Application

Within the dolphin low salinity exposure model, dolphin movement histories are simulated at a daily time step, and the daily salinity value at a location in the Bay on a particular day is used to develop an annual exposure history for each simulated individual. However, the known retrospective prediction biases in the Delft3D model may result in over- or underestimation of the exposure to low salinity. The outcomes of this analysis are used to correct for the regional mean annual bias in estimated salinity and account for the quantified variation in this parameter. Based upon the regional clusters identified here, the grid cells used in the movement simulation were assigned to cluster 1 or cluster 2 (Figure II.15). The boundary between the clusters was drawn to be approximately equidistant between stations on the boundaries of the two clusters. For each location in a movement history, the appropriate bias correction is applied depending on which region the location is in. To account for uncertainty in this correction, a parametric bootstrap approach is used to develop a distribution of bias corrections by

cluster based upon the estimated standard deviation accounting for spatial autocorrelation. Therefore, the approach described here corrects for the retrospective prediction bias in modeled salinity and its associated uncertainty at a regional scale within Barataria Bay.

III. Low Salinity Exposure Model and Predicted Impacts of the MBSD on Survival Rates

III.1 Overview and Objectives

The objective of this project is to evaluate the potential impacts of changes in the distribution of low salinity (< 5 ppt) water in Barataria Bay on the survival rates of the resident common bottlenose dolphin stock. The Mid-Barataria Sediment Diversion (MBSD) is an effort to restore the natural deltaic process to the Barataria Basin resulting in the creation and maintenance of wetlands and overall reduction in the loss of marsh and other habitats in Barataria Bay. The project is designed to divert sediment, nutrients and freshwater from the Mississippi River into the northeastern portion of the Bay during the normal seasonal pulses of the River. This influx of freshwater and associated input of sediments is projected to result in the maintenance of wetland, SAV, and associated habitats that would otherwise be lost absent the sediment diversion. However, the influx of large amounts of freshwater into the system is projected to result in large-scale changes in the hydrographic structure of this modified estuary. In particular, it is projected that lower salinity water will occur throughout the Bay for longer durations each year and over a larger spatial area than under current conditions. Here, we describe a simulation approach to evaluate the effects of this expansion of low salinity water on the survival rates of bottlenose dolphins under the conditions expected for different management scenarios and differing degrees of input of freshwater into the Barataria Bay estuary.

The Delft3D hydrodynamic model (Sadid et al. 2018) is the primary tool used to predict land building and changes in hydrographic structure under different diversion alternative describing the magnitude of the diversions. The freshwater input into this model is driven by a time-series of annual hydrographs describing river flows into the basin. The model simulates the annual time series of daily salinity over the model domain for each year. Available Delft3D projections include surface salinity for 5 annual hydrographs (A representative year, 1994, 2006, 2010, and 2011) for each of five decades ("cycles"). The representative year varies by cycle. Given that there is not a continuous prediction of year to year variation in freshwater inputs and the future projections do not

include prediction of likely freshwater inputs, all evaluations in this analysis are done for a single year and focus on the comparison of expected outcomes under different diversion alternatives for a particular hydrograph.

The simulation approach described here has four primary components. First, the daily projected salinity field for a given cycle, hydrograph, and alternative is obtained from the Delft3D model. The cycles represent decades: cycle0 – cycle5, and the representative year hydrograph varies by cycle: cycle0 = 1970, cycle1 = 1975, cycle2 = 1985, cycle3 = 1994, cycle4 = 2008, and cycle5 = 2008. Sea level rise becomes more apparent in the projections of the last two cycles. Predictions for alternate hydrographs (1994, 2006, 2010, and 2011) are also produced for each cycle. The alternatives include four different expected flow regimes under different diversion levels: NAA = No Action Alternative (Future Without Plan); A3 = discharge from diversion capped at 50K cubic feet per second (cfs); APA (Applicants Preferred Alternative) = discharge from diversion capped at 75K cfs; and A5 = discharge from diversion capped at 150K cfs. The comparison between alternatives within a given cycle/hydrograph combination is the primary focus of this analysis.

Second, bias corrections (and the associated uncertainty) are applied to each spatial location in a given salinity field based on the region within the Bay (see Section 2 of this report). Retrospective prediction bias in the daily salinity was evaluated based upon comparison to observed data from 2016. The results of the analysis from Section 2 are applied to develop corrected salinity values.

Third, a simplified movement model is applied to simulate the daily movements of individual dolphins for an annual simulation. The daily corrected salinity value for each simulated animal position is stored to derive an "exposure history" for each simulated animal. The initial positions for the simulated dolphins are set based upon a random draw of the spatial cells in the model domain with a probability weighting based upon the relative density surface developed in Section 1 of this report.

Fourth, a dose-response curve is applied to each exposure history to estimate an annual individual survival rate for the simulated dolphins. The relationship between exposure to low salinity and the resulting impact on survival is complex and the data available to quantify this relationship is limited. Therefore, the relationship between low

salinity exposure and survival was developed through an expert elicitation process. The expert elicitation was asked to consider the impacts of "continuous exposure" to low salinity (defined as < 5 ppt) on the survival of estuarine dolphins that typically experience a range of salinity conditions within a given year. The elicitation focused on the effect on survival within a given year and did not consider repeat exposures across years. While the experts characterized their uncertainty in the resulting dose-response curve, there is likely substantial unquantified uncertainty in this relationship (Booth and Thomas unpublished).

The average of the annual individual survival rates provides the predicted population mean annual survival for the scenario/hydrograph combination. It should be noted that the model does not include other processes that may impact dolphin survival or a baseline survival rate. Predicted survival rates should therefore be interpreted as the change in survival solely due to exposure to low salinity in a given year.

Uncertainty is incorporated into the simulation for each model parameter. The uncertainty in the salinity bias correction (see Section 2) is applied by randomly drawing bias correction values from the normal distribution with the specific mean and standard deviations and applying 1,000 randomized correction biases to each salinity surface. The movement histories are based upon the probability weighted randomized placement of 5,000 simulated dolphins, and a subsample of these random movement histories are drawn for each estimate of annual exposure. Finally, the uncertainty in the dose-response curve is accounted for by randomly selecting from 10,000 realizations of the curve that reflect the uncertainty in parameter estimates derived from the expert elicitation (Booth and Thomas unpublished). The distributions of annual survival rates therefore reflect 1,000 simulations that include uncertainty in salinity bias corrections, initial animal location and movement patterns, and the dose-response function. These simulations do not represent uncertainty in the future hydrographs or other aspects of future prediction uncertainty in the Delft3D projected salinity, possible long-term changes in dolphin responses to habitat conditions inside Barataria Bay or the adjacent coastal waters, or other factors that may affect dolphin survival rates.

III.2 Methods

Delft3d Model Output Processing

Delft model projected salinity values were provided over the native model grid and the model spatial domain within Barataria Bay and extending offshore into coastal waters for each cycle/hydrograph/alternative. The native model grid has variable spatial resolution depending on the distance from the diversion outfall source, and was therefore standardized to a nominal 500 x 500 m grid resolution. Cells within this standardized grid classified as land (elevation >= 0m) were removed, and the extent of the grid was subsampled and classified by areas corresponding to the BBES stock boundary (Figure III.1).

The BBES stock area includes the known spatial extent of resident bottlenose dolphins including waters extending 1 km seaward from the barrier Islands. Within the stock boundary, four strata (West, Central, Southeast, and Island) were defined that reflect the restricted movement of different groups of animals based on both photo-identification histories (See Section 1 of this report) and telemetry tag data (Wells et al., 2017). These strata are consistent with previously defined regional boundaries that had different animal densities in prior studies (McDonald et al. 2017), with the exception that the Island stratum only covers the central and western portions of the barrier islands including waters extended 1km from shore into nearshore coastal waters (Figure III.1). The strata boundaries extended north into more freshwater areas given that it is possible that BBES dolphins occur infrequently in these habitats. However, these areas are outside of the boundaries of the 2019 CMR study and the extrapolation of the relative density model (Section 1).

Movement Model and Salinity History

To model the exposure to low salinity for individual animals under a given annual salinity field, we first randomly selected 5,000 “starting” positions from within the grid domain. The initial selection of starting cells was weighted by the predicted relative density map described in Section 2 (Figure III.2). The analysis therefore assumes that the

spatial distribution observed during these surveys is representative of the typical distribution of the BBES bottlenose dolphin stock. Areas outside of the valid extrapolation of this density grid were assigned a sampling probability of zero. Probability weighting effectively replicated the expected distribution of animals.

After these initial starting positions were selected, a constrained random walk movement was simulated at a daily time step. The maximum daily displacement for an individual was set at 5km. At each time step, all of the spatial cells within 5km of the simulated individual's current position were available as a destination. The destination cell was selected randomly from this neighborhood, with the probability selection weighted by $1/\text{distance}^2$ where the distance is that from the initial starting location. Because of the inverse-distance^2 weighting, there was a much greater likelihood of selecting cells close to the starting location as opposed to those further away. This approach effectively constrained the movement of simulated individuals to stay in relatively close proximity to the initial starting location. This is consistent with tag telemetry studies that demonstrated that bottlenose dolphins had relatively restricted home ranges within Barataria Bay and tended to remain within strata (Wells et al. 2017). Based on the simulated daily location, each simulated individual was given a daily salinity value drawn from the relevant standardized Delft output grid.

For each daily salinity surface, 1,000 randomized bias-corrected surfaces were created using a parametric bootstrap based upon the estimated mean and standard deviation of salinity bias (see Section 2). A random bias correction value was drawn from a normal distribution and applied to all grid cells (as appropriate by spatial location) for each daily salinity surface. Thus, each dolphin movement history includes a distribution of daily salinity values that represents the uncertainty in the bias correction.

Exposure History and Survival Estimates

At the end of an annual simulation, each simulated movement history had a time series (and distribution) of daily salinity values. This salinity history was used to develop exposure indices for comparison with the salinity:survival dose response (DR) curve (Figure III.3). The expert elicitation (EE) that developed this curve (Booth and Thomas unpublished) explicitly considered "continuous exposure" within the context of

environmental variability, movement of individuals within a given estuary, and the potential for temporary refugia from low salinities. We considered three possible exposure indices as analogous to the "continuous exposure" considered by the EE based on the threshold "low salinity" value of 5ppt: 1) the total number of days (per year) with salinity <5 ppt, 2) a "maximum count" where each day of salinity <5ppt adds 1 to the metric and each day of salinity >5ppt subtracts 1 from the metric (the maximum value obtained during the year would therefore reflect extended periods of low salinity including intermittent breaks), and 3) the "longest streak" defined as the longest stretch of continuous days below 5ppt with breaks of 2 or fewer days. We selected the "longest streak" metric as most analogous to the "continuous exposure" situation considered by the expert elicitation working group. This is a conservative estimate of exposure as an animal may have multiple streaks in a given year, but only the longest one would be considered when evaluating the impacts on survival. Further, it is unknown if the effects of prolonged exposure to low salinity would be fully resolved in a 48-hour respite between repeated exposures, but this metric assumes that the physiological condition of the animal is fully reset after this interval regardless of the length of the initial salinity exposure.

For each of 1,000 bootstrap iterations of the model, a random realization of the salinity:survival DR curve was also selected from the distribution of outcomes provided by the expert elicitation using the DR curve for a "compromised" population (Figure III.3, EE Scenario 1) since BBES bottlenose dolphins are known to have ongoing health impacts from the DWH oil spill. The outcomes of this analysis did not differ appreciably if the DR curve for "healthy" populations was used. This curve was then used to predict individual survival rates for the exposure histories for that bootstrap iteration, and the distribution of the population mean survival rate was calculated. This distribution of means was used to evaluate the potential effects of lowered salinity on survival rates of Barataria Bay bottlenose dolphins under diversion alternatives.

III.3 Results

Initial Distribution and Movement Histories

The probability weighting for selection of starting positions based upon the spatial GAM model resulted in initial distributions of simulated dolphins that reflect the expected distribution of the population. There were a high number of starting positions in the southern part of the Bay near the pass and in the central and northern part of the central region (Figure III.4). The restricted random walk movement histories resulted in relatively small home ranges of simulated animals within the Bay that were generally restricted to within 5-10 km of their original starting point (Figure III.5). These overall patterns are consistent with the evidence of limited movement of individuals between regions and small home ranges (Wells et al. 2017).

Exposure History

For the representative year, cycle 0, No Action Alternative (NAA), the mean longest streak metric was 12.9 days (95% Confidence Limits (CL) 7.5-19.9, Table III.1) overall for the whole Bay and ranged between 0.1 and 23.4 for each region (Table III.1, Figure III.6, Figure III.7). These exposure levels are expected to result in high survival rates for nearly all outcomes of the DR curve (Figure III.3). The long streak metric increased for each diversion alternative which the greatest increases occurring in the West and Central regions of the Bay (Table III.1, Figure III.7). The mean longest streak remained low (< 11 days) in the Island stratum for both A3 and the APA, but increased to 37.7 days in the alternative with the highest potential freshwater input. Under the APA, the longest streak metric overall mean was 51.1 days (95% CL 39.6-62.8, Table III.1) with means of 55.1 (95% CL 31.5-83.7, Table III.1) and 87.2 (95% CL 67.0-108.8, Table III.1) in the central and west regions, respectively.

Survival Rates

For the representative year in cycle 0, the mean survival rate under the NAA was 0.890 (95% CL 0.753-0.982) for the Bay as a whole (Table III.2, Figure III.8). This survival rate decreased under each alternative, and the mean annual population survival rate under the APA was 0.588 (95% CL 0.281-0.832). Pairwise comparisons between the NAA and the other three alternatives demonstrated that the population survival rates were

significantly different based upon the bootstrap distribution of differences between the means (Figure III.8). Consistent with the patterns observed in the longest streak metric, the survival rates decreased the most for the central and western regions (Table III.2), though there were lower survival rates in all regions under the APA (Figure III.9). Under the APA, the mean population survival rate was 0.555 (95% CL 0.120-0.885) and 0.292 (95% CL 0.042-0.683) for the west and central regions, respectively (Figure III.9, Table III.2). The survival rates in these regions were extremely low under A5 and declined to 0.241 (95% CL 0.000-0.658) for the West region and 0.073 (95% CL 0.000-0.403) for the central region (Figure III.10, Table III.2).

The annual salinity field is driven primarily by the hydrograph of river outflow. During high flow years, there will be a greater amount of freshwater input into the Barataria Bay system due to the diversion, and during low flow years it is expected that there will be less difference between alternatives. For cycle 0, we compared the exposure level between the representative year and four alternative years: 1994, 2006, 2010, and 2011. Generally, the changes in survival for these alternate years were similar to those observed for the representative year (Table III.3, Figure III.11). Population mean survival rates for the NAA ranged between 0.837 – 0.950 with the highest survival rates during the relatively low flow year of 2006 (Table III.3). Under the APA, mean survival rates ranged between 0.319 for 2011 and 0.898 for 2006 (Table III.3, Figure III.11). During 2006, there was no significant difference between alternatives; however, for the remaining years, all alternatives had significantly lower survival rates than the NAA (Figure III.11).

It is not possible to explicitly project the expected changes in population size over each decade given that the available hydrographs do not form a predictive time series, nor does the model developed and applied in this study include food web or reproductive information. However, given the extremely low projected survival rates in the west and central regions under the alternatives, it is likely that the abundance of animals within these regions would decline to near zero after the first 10 years of the project. The only portion of the Bay with projected survival rates sufficient to maintain a substantial population would be in the Island stratum where survival rates are expected to exceed 0.9 annually under A3 and the APA. To evaluate the potential future impact of the diversion

on the remaining dolphin population, we simulated annual survival rates for the representative year of each future decade (cycle 1-5). It should be noted that the representative hydrograph was different for each cycle, and therefore some of the observed effects are related to changes in the hydrographs. The NAA alternative in each cycle includes dolphins inhabiting the entire Bay as they are currently. Under these model conditions, the mean population survival rates in future cycles are lower than those under the NAA during cycle 1 and then become slightly higher in cycles 2-5 (for the APA scenario), though the differences are not statistically significant (Table III.4, Figure III.12). The survival rates under the NAA are projected to decrease over the course of the decades which reflects the projected impacts of sea level rise and increased water flow due to land loss (Figure III.12).

III.4 Discussion

This simulation analysis examines the potential effects of future changes in salinity under alternative diversion scenarios on the projected annual survival rate of bottlenose dolphins in Barataria Bay. The analysis accounts for the initial spatial distribution of dolphins in the Bay, variability in individual dolphin movement patterns, bias, uncertainty in predicted salinity values, and uncertainty in the expected relationship between salinity exposure and survival. Assumptions made in this process are described in the sections above. The model is not able to account for uncertainty or bias in the future salinity levels experienced by the population. In addition, the model assumes that the observed spatial distribution during the spring of 2019 is typical of the overall distribution of the stock throughout the entire year and across multiple years and that the applied movement model is representative of the scale and movement patterns of BBES dolphins.

Projected future scenarios include hydrographic conditions outside of the range of natural variability used to calibrate the Delft3d model, and therefore model performance is unknown under these conditions. Unknown future conditions in the River hydrograph will result in changes in salinity and survival rates that differ from the projections which rely on the historical hydrographs. Similarly, future projections rely upon historical

hydrographs. If the future includes a higher proportion of low-flow years, then the impacts of the diversion on the bottlenose dolphin population will be lower than projected. In contrast, if there is an expectation of higher water flow into the system in the future, then the impact could be larger. Available climate prediction models suggest that precipitation during winter and spring will be significantly higher over most of North America in the coming decades which would suggest an increasing likelihood of high-flow years (USGCRP, 2017).

In addition to uncertainty about future climates, several caveats are required when interpreting the potential impacts on dolphin survival. The "longest streak" metric approximates the intent of the expert elicitation panel consideration of "continuous exposure" to salinity less than 5 ppt. However, it is unclear whether this metric ignores important dynamics that may influence the expected dolphin survival. For example, if an animal experienced five 15 day exposures with 3 day breaks in between, the metric would have a value of 15, even though the dolphin had experienced a total of 75 days of exposure with limited opportunity to recover. Furthermore, it is unknown if a two-day break from low salinity is sufficient to allow complete recovery, though that is assumed by the implemented metric. It is notable that a recent natural event resulting in increased freshwater input into Mississippi Sound was followed by substantially increased dolphin mortality with as little as 20-40 days of lowered salinity, not all of which were consecutively below 5 ppt (Garrison, unpublished data). The observation of an increase in mortality associated with extended exposure to freshwater in an estuarine bottlenose dolphin population is consistent with the expectations from this model.

The simulation model demonstrates significant reductions in survival rates for dolphins under the APA with the highest impacts experienced by dolphins in the central and western portions of the Bay. Under the APA, the population mean survival rate is expected to decline by an average of 34% (95% CL 15.3%-62.7%, Table III.2) compared to the NAA. For comparison, baseline adult survival rates for estuarine bottlenose dolphins were estimated to range between 0.88-0.96 for females and 0.85-0.94 for males (ages 1-39 years, Schwacke et al., 2017), and these ranges are consistent with our estimated NAA survival rates. The projected reduction in survival rates, if realized, would result in substantial declines in population size, particularly in the habitats of the

central and western Bay where annual survival rates are expected to decline by 65.9% and 41.9%, respectively. If the reduction in survival was sustained over time, then a smaller dolphin population may be able to persist in Barataria Bay beyond the first decade near the barrier islands. However, this population would also experience relatively low survivorship associated with exposure to freshwater with annual survival rates ranging from 0.681 – 0.901 (Table III.4). By comparison, dolphins near the Islands under the no action alternative in cycle 0 are expected to have survival rates approaching 1 (Table III.2). The projected survival rates for the more broadly distributed population in future cycles under the NAA are comparable to those of the Island population under alternatives, though there may be some survival benefit 50 years in the future (Figure III.12).

There remain significant uncertainties with this analysis, and other factors that impact bottlenose dolphin survival are not included in this approach. However, the available data and analyses indicate that increased freshwater input into Barataria Bay associated with the MBSD is projected to result in substantial declines in bottlenose dolphin annual survival rates that would not be sustainable by this population over the near term.

IV. Literature Cited

Adams, J. D., T. R. Speakman, E. S. Zolman, and L. H. Schwacke. 2006. An automated cataloging, matching, and analysis tool for photo-identification of bottlenose dolphins. Aquatic Mammals 32(2):374–384.

Balmer, B., S. Watwood, B. Quigley and others. 2019. Common bottlenose dolphin (*Tursiops truncatus*) abundance and distribution patterns in St Andrew Bay, Florida, USA. Aquatic Conserv: Mar Freshw Ecosyst. 2019:1–13.

Balmer, B. C., Schwacke, L. H., Wells, R. S.,and others. 2013. Comparison of abundance and habitat usage for common bottlenose dolphins between sites exposed to differential anthropogenic stressors within the estuaries of southern Georgia, U.S.A. Marine Mammal Science, 29(2), E114-E135.

Balmer, B., Wells, R., Nowacek, S. and others. 2008. Seasonal abundance and distribution patterns of common bottlenose dolphins (*Tursiops truncatus*) near St. Joseph Bay, Florida, USA. Journal of Cetacean Research and Management. 10:157–167.

Booth, C. and Thomas, L. in review. An expert elicitation of the effects of low salinity water exposure on bottlenose dolphins. Submitted to 'Oceans – Special Issue: Marine mammals in a changing world.'

Burnham, K. P. and Anderson, D. R. .2004. Multimodel inference. Sociological Methods & Research, 33, 261–304. https://doi.org/10.1177/ 0049124104268644

Hayes, S., Josephson, E., Maze-Foley, K., Rosel, P.E. 2019. US Atlantic and Gulf of Mexico Marine Mammal Stock Assessments – 2018. NOAA Tehnical Memorandim NMFS-NE-258.

Huggins, R. 1989. On the statistical analysis of capture-recapture experiments. Biometrika, 76, 133-140.

Kassambara, A. 2017. Practical Guide to Cluster Analysis in R. Multivariate Analysis I. CreateSpace Independent Publishing Platform, 188 pgs.

Kassambara, A and Mundt, F. 2019. factoextra: Extract and Visualize the Results of Multivariate Data Analyses. R package version 1.0.6. https://CRAN.R-project.org/package=factoextra

Lane, S. M., C. R. Smith, J. Mitchell, B. C. Balmer, and others. 2015. Reproductive outcome and survival of common bottlenose dolphins sampled in Barataria Bay, Louisiana, USA, following the Deepwater Horizon oil spill. Proc. R. Soc. B 282: 20151944.

Litz, JA, EI Ronje, HR Whitehead, and LP Garrison. 2019. Updated abundance estimate for common bottlenose dolphins (Tursiops truncatus) inhabiting West Bay, Texas. Aquatic conservation: Marine and Freshwater ecosystems. 2019; 1- 12. https://doi.org/10.1002/aqc.3195

McDonald, T. L., F. E. Hornsby, T. R. Speakman, E. S. Zolman and others. 2017. Survival, density, and abundance of common bottlenose dolphins in Barataria Bay (USA) following the *Deepwater Horizon* oil spill. Endang Species Res 33:193-209. https://doi.org/10.3354/esr00806

Melancon, R. A., S, S. Lane and others. 2011. Photo-identification Field and Laboratory Protocols Utilizing FinBase Version 2. NOAA Technical Memorandum NMFS-SEFSC-627. 46 pp.

Maechler, M., Rousseeuw, P., Struyf, A., Hubert, M., Hornik, K. 2019. cluster: Cluster Analysis Basics and Extensions. R package version 2.1.0.

Mullin, K.D., K. Barry, T. McDonald, J. Morey, B. Quigley, E. Ronje, L. Schwacke, C. Sinclair, T. Speakman and J. Thompson. 2018. Assessment of the overlap of Terrebonne-Timbalier Bay and Barataria Bay common bottlenose dolphin (*Tursiops truncatus*) stocks based on photo-identification of individual dolphins. NOAA Technical Memorandum NMFS-SEFSC-729. 29pp. doi:10.25923/8g4y-dg29

Mullin, K. D., T. McDonald, R. S. Wells and others. 2017. Density, abundance, survival, and ranging patterns of common bottlenose dolphins (*Tursiops truncatus*) in Mississippi Sound following the *Deepwater Horizon* oil spill. PLoS ONE:12, e0186265. https://doi.org/10.1371/journal.pone.0186265

Otis, D. L., Burnham, K. P., White, G. C., & Anderson, D. R. 1978. Statistical-Inference from Capture Data on Closed Animal Populations. Wildlife Monographs(62), 1-135.

Rosel, P. E., K. D. Mullin, L. Garrison and others. 2011. Photo‐identification capture–mark–recapture techniques for estimating abundance of bay, sound, and estuary populations of bottlenose dolphins along the U.S. East Coast and Gulf of Mexico: A workshop report. NOAA Technical Memorandum NMFS-SEFSC‐621.

Sadid, K., Messina, F., Hoonshin, J., Yuill, B, Meselehe, E. 2018. Basinwide Model Version 3: Basinwide model for mid-Breton Sediment Diversion Modeling. The Water Institute of the Gulf. Prepared for and funded by the Coastal Protection and Restoration Authority under TO51. Baton Rouge, LA.

Schwacke LH, Thomas L, Wells RS, McFee WE and others .2017. Quantifying injury to common bottlenose dolphins from the *Deepwater Horizon* oil spill using an age-, sex- and class-structured population model. Endang Species Res 33:265-279. https://doi.org/10.3354/esr00777

Shane, S. H. 1990. Behavior and ecology of the bottlenose dolphin at Sanibel Island, Florida. Pages 245–266 *in* S. Leatherwood and R. R. Reeves, eds. The bottlenose dolphin. Academic Press, San Diego, CA.

Speakman, T. R., S. M. Lane, L. H. Schwacke and others. 2010. Mark–recapture estimates of seasonal abundance and survivorship for bottlenose dolphins (*Tursiops truncatus*) near Charleston, South Carolina. USA. Journal of Cetacean Research and Management, 11:153–162.

Tibshirani, R., Walther, G., and Hastie, T. 2001. Estimating the number of clusters in a data set via the gap statistic. Journal of the Royal Statistical Society B, 63:411-423.

USGCRP. 2017. Climate Science Special Report: Fourth National Climate Assessment, Volume I [Wuebbles, D.J., D.W. Fahey, K.A. Hibbard, D.J. Dokken, B.C. Stewart, and T.K. Maycock (eds.)]. U.S. Global Change Research Program, Washington, DC, USA, 470 pp. https://science2017.globalchange.gov/chapter/7/

Urian, K., A. Gorgone, A. Read and others. 2015. Recommendations for photo-identification methods used in capture-recapture models with cetaceans. Marine Mammal Science 31(1):298–321.

Urian, K. W., and R. S. Wells. 1996. Sarasota dolphin research program field techniques and photo-identification handbook. Dolphin Biology Research Institute, Sarasota, FL.

Wells, R. S., L. H. Schwacke, T. K. Rowles, and others. 2017. Ranging patterns of common bottlenose dolphins *Tursiops truncatus* in Barataria Bay, Louisiana, following the *Deepwater Horizon* oil spill. Endang Species Res 33:159-180. https://doi.org/10.3354/esr00732

Willmott, C.J. 1982. Some comments on the evaluation of performance. Bull. Amer. Met. Soc. 63: 1309-1313.

Wood, S.N. .2017. Generalized Additive Models: An Introduction with R (2nd edition). Chapman and Hall/CRC.

Wood S.N., N. Pya and B. Saefken .2016. Smoothing parameter and model selection for general smooth models (with discussion). Journal of the American Statistical Associ ation 111:1548-1575.

List of Tables and Figures

Table III.3. Mean (95% Confidence Limits) of population annual survival rates by alternative for cycle 0, representative year and alternate years. NAA = No Action Alternative, A3 = Alternative 3 (50K CFS diversion), APA = Applicant's Preferred Alternative (75K CFS diversion), A5 = Alternative 5 (150K CFS diversion).

Table III.4. Mean (95% Confidence Limits) of population annual survival rates by alternative for the representative year in each cycle (decade). For cycles 1-5, the simulations for the NAA includes dolphins inhabiting the entire Bay where under the other alternatives dolphin starting positions are restricted to the Island habitat with the highest survival rates. NAA = No Action Alternative, A3 = Alternative 3 (50K CFS diversion), APA = Applicant's Preferred Alternative (75K CFS diversion), A5 = Alternative 5 (150K CFS diversion).

Figure I.1. Barataria Bay in southern Louisiana including the region surveyed during photo-id surveys prior to 2019 (hatched area, McDonald et al., 2017).

Figure I.2. Survey track-lines for the Barataria Bay Estuarine System Stock capture-mark-recapture project 14 March to 1 April 2019. Prior year surveys did not include the "southeast" area or the contour tracklines in the northern portion of the survey area.

Figure I.3 Planned temperature and salinity stations during the spring 2019 CMR survey.

Figure I.4. Executed tracklines, dolphin group sighting locations, and analysis grid.

Figure I.5. Dolphin group sizes during the spring 2019 CMR survey.

Figure I.6. Discovery curve showing the number of new dolphins added to the Barataria Bay master photo-identification catalog by survey year.

Figure I.7. GAM model fit and residuals. The line indicates the model smooth fit for each explanatory factor, and the shaded area indicates the 95% confidence limit of the model fit.

Figure I.8. Fitted (line) and observed (points) dolphins per 100m of survey effort (SPUE) as a function of explanatory factors. The dashed line indicates the 95% confidence limits of model fitted values.

Figure I.9. Predicted relative density (SPUE) projected over the spatial grid. Areas with CV > 0.4 are masked from the resulting surface given high model uncertainty when projecting outside of the range of survey data.

Figure II.1. Station locations for 22 salinity observations included in the current analysis.

Figure II.2. Daily mean observed (black dots) and Delft3d modelled (red line) salinity for each observation sation from 2016.

Figure II.3. Daily bias (red line) for each salinity observation station. The dashed line indicates the Mean Bias Estimate for each station.

Figure II.4. Distance plot indicating the Pearson distance between station pairs. Higher values indicate greater differences between stations. Pairs are ordered to highlight clustering among stations.

Figure II.5. Cluster plots showing the membership and distribution of clusters of stations based upon K-means clusters specifying 2-5 clusters.

Figure II.6. Cluster optimization statistics using the (A) Average silhouette and (B) Gap statistics. Both metrics indicate that an optimal number of clusters is 2 (dashed vertical line).

Figure II.7. Cluster membership as a function of RMSE and MBE. Cluster 1 includes stations with positive salinity biases and lower RMSE values while Cluster 2 includes stations with more negative biases and higher RMSE.

Figure II.8. Salinity stations by cluster. Cluster 1 includes stations further north in areas of the Bay more heavily influenced by freshwater while Cluster 2 includes stations in the middle and lower bay that are more estuarine.

Figure II.9. Partial autocorrelation of residuals from GAMM models for Cluster 1 stations with (A) no autocorrelation structure and (B) an AR3 autocorrelation structure. The dashed line indicates the level for significant autocorrelation in residuals. There is evidence for autocorrelation at lags 1-3 days. Accounting for this lag correlation leaves no remaining significant autocorrelation in the residuals for the GAMM model.

Figure II.10. Predicted (red line) and observed (points) daily salinity bias values for cluster 1 salinity stations. The 95% confidence interval of the GAMM predictions is indicated by the dashed lines.

Figure II.11. Parametric bootstrap distribution of mean annual bias for Cluster 1 stations derived from the GAMM model. The distribution median is indicated by the dashed vertical line. While the mean bias estimates are similar, ignoring autocorrelation in residuals (A) underestimates the uncertainty in the estimate while the distribution including the AR3 correlation (B) demonstrates higher variance in the mean.

Figure II.12. Partial autocorrelation of residuals from GAMM models for Cluster 2 stations with (A) no autocorrelation structure and (B) an AR3 autocorrelation structure. The dashed line indicates the level for significant autocorrelation in residuals. There is evidence for autocorrelation at lags 1-3 days. Accounting for this lag correlation leaves no remaining significant autocorrelation in the residuals for the GAMM model.

Figure II.13. Predicted (red line) and observed (points) daily salinity bias values for cluster 2 salinity stations. The 95% confidence interval of the GAMM predictions is indicated by the dashed lines.

Figure II.14. Parametric bootstrap distribution of mean annual bias for Cluster 2 stations derived from the GAMM model. The distribution median is indicated by the dashed vertical line. The mean bias estimate for the AR3 model is slightly higher than that for the model including no autocorrelation. Ignoring autocorrelation in residuals (A) underestimates the uncertainty in the estimate while the distribution including the AR3 correlation (B) demonstrates higher variance in the mean.

Figure II.15. Regions within the Barataria Bay bottlenose dolphin stock area corresponding to cluster 1 and cluster 2 stations and corresponding mean bias estimates. The mean and standard deviation in bias will be applied spatially within these regions to account for retrospective prediction bias in outputs from the Delft3D model. Cluster 1 has a mean bias of 0.717 (sd = 0.0889) while cluster 2 has a mean bias of -2.136 (sd = 0.168).

Figure III.1. Predicted daily salinity from the Delft model for each cycle, hydrograph, and alternative were standardized onto a 500x500m grid and overlaid with the spatial boundaries of the BBES bottlenose dolphin stock. The underlying salinity in this image is from an example output (Cycle 0, NAA, April 20). The stock boundary and within stock strata definitions are outlined in black.

Figure III.2. Relative density (Sightings Per Unit Effort) surface over the model domain overlaid with the BBES stratum boundaries. The mean SPUE values (dolphins per 100m trackline) by strata are: Island: 0.406, West - 0.0813, Central - 0.203, and Southeast - 0.100

Figure III.3. Dose response curve indicating the relationship between continuous days of exposure and individual survival probability. The shaded area indicates the 95% confidence limits of a distribution of 10,000 realizations of this curve reflecting parameter uncertainty. The solid red line indicates the median of the distribution while the blue lines indicate the first and third quartiles of the distribution.

Figure III.4. Example distribution of starting positions for simulated dolphins.

Figure III.5. Example movement histories of simulated dolphins. The outline indicates the regional boundaries. The green lines indicate the annual locations of selected simulated dolphins (numbers).

Figure III.6. Mean longest streak metric for different alternatives during cycle 0, representative year. NAA = No Action Alternative, A3 = Alternative 3 (50K CFS diversion), APA = Applicant's Preferred Alternative (75K CFS diversion), A5 = Alternative 5 (150K CFS diversion).

Figure III.7. Mean longest streak metric for different alternatives during cycle 0, representative year by region. NAA = No Action Alternative, A3 = Alternative 3 (50K CFS diversion), APA = Applicant's Preferred Alternative (75K CFS diversion), A5 = Alternative 5 (150K CFS diversion).

Figure III.8. Survival rates for different alternatives during cycle 0, representative year. P-values indicate results of significance tests comparing survival rates for each alternative to the No Action Alternative. NAA = No Action Alternative, A3 = Alternative 3 (50K CFS diversion), APA = Applicant's Preferred Alternative (75K CFS diversion), A5 = Alternative 5 (150K CFS diversion).

Figure III.9. Survival rates during cycle 0, representative year comparing the No Action Alternative to the Applicants Preferred Alternative by regional stratum. P-values indicate results of significance tests comparing survival rates between alternatives within regions. NS indicates a non-significant ($p > 0.05$) proportion of differences in survival rates less than zero. NAA = No Action Alternative, APA = Applicant's Preferred Alternative (75K CFS diversion).

Figure III.10. Regional survival rates during cycle 0, representative year for all alternatives. NAA = No Action Alternative, A3 = Alternative 3 (50K CFS diversion), APA = Applicant's Preferred Alternative (75K CFS diversion), A5 = Alternative 5 (150K CFS diversion).

Figure III.11. Population survival rates by alternative for additional years in cycle 0. P-values indicate results of significance tests comparing survival rates for each alternative to the No Action Alternative. NS indicates a non-significant ($p > 0.05$) proportion of differences in survival rates less than zero. NAA = No Action Alternative, A3 = Alternative 3 (50K CFS diversion), APA = Applicant's Preferred Alternative (75K CFS diversion), A5 = Alternative 5 (150K CFS diversion).

Figure III.12. Population survival rates by alternative for the representative year of each decade. P-values indicate results of significance tests comparing survival rates for each

alternative to the No Action Alternative. NS indicates a non-significant ($p > 0.05$) proportion of differences in survival rates less than zero. For all alternatives except the NAA, the populations for cycles 1-5 were restricted to animals with starting positions in the Island strata. NAA = No Action Alternative, A3 = Alternative 3 (50K CFS diversion), APA = Applicant's Preferred Alternative (75K CFS diversion), A5 = Alternative 5 (150K CFS diversion).

Table I.1. Summary of survey effort in Barataria Bay 14 March to 1 April 2019.

Survey Area	# of Surveys	Survey Hours	Survey Distance (km)	# of Sightings	# of Dolphins Encountered	# of Photos
West	11	76	1,160	85	465	6,746
Central	13	90	1,504	150	964	9,792
Southeast	13	90	1,531	133	617	10,827
Total	**37**	**256**	**4,195**	**368**	**2,046**	**27,365**

Table I.2. Group size mean and range per survey area. n = number of groups per area.

Survey Area	# of Sightings	Mean (SD)	Range
West	86	5.4 (5.58)	1 - 40
Central	150	6.4 (6.44)	1 - 40
Southeast	132	4.6 (5.65)	1 - 40

Table I.3. Summary of data from temperature and salinity stations collected in Barataria Bay 14 March – 1 April 2019

	Salinity (ppt)		**Temperature (°C)**	
Survey Area	*Average*	*Range*	*Average*	*Range*
West	7.6	0.4-18.2	18.9	14.2-22.9
Central	9.2	1.5-20.2	18.1	9.2-21.1
Southeast	11.4	0.6-31.0	18.2	14.6-22.5

Table I.4. Model results from the closed capture-recapture full-likelihood approach. M_t = detection probabilities assumed to be time varying; M_{tb} model where detection probabilities (p) vary with time but also recapture probabilities are different from initial capture probabilities; $M_{0=}$ the null model with constant detection probabilities across all factors.

Model	AICc	Delta AICc	AICc Weights	Model Likelihood	Num. Par	Deviance	-2log(L)
{Mt}	-5911.19	0	0.73129	1	5	31.2111	-5921.2048
{Mtb}	-5909.18	2.0029	0.26864	0.3674	6	31.2067	-5921.2091
{M0}	-5892.89	18.292	0.00008	0.0001	2	55.5175	-5896.8984

Table I.5. Real function parameters from the closed capture Full-likelihood M_t model. Parameters: p = probability of capture and the probability of recapture in each secondary session, f_0=number of individuals with no sightings during each primary.

Parameter	Estimate	Standard Error	95% Confidence Interval	
			Lower	Upper
1: p	0.1468791	0.0111539	0.1263351	0.1701133
2: p	0.2152886	0.0141434	0.1888613	0.2443000
3: p	0.1904734	0.0130884	0.1661299	0.2174537
4: p	0.1877906	0.0129726	0.1636753	0.2145474
5: f_0	656.02217	64.499169	541.28906	795.07443

Table I.6. Population estimates (N), standard error (SE), coefficient of variation (CV), and 95% confidence intervals (95% CI) derived from the closed capture (CC) robust design full-likelihood M_t model. Estimated Total N is the estimated marked N divided by the proportion marked.

CC Full - likelihood	
Minimum known marked	835
Estimated Marked N	1491
SE Marked N	64.5
95% CI Marked N	1376 – 1630
Proportion marked	0.72
SE Proportion Marked	0.031
Estimated Total N	**2071**
SE Total N	121.8
95% CI Marked N	1832 – 2309

Table I.7. GAM model summary.

```
Family: Tweedie(p=1.369)
Link function: log

Formula:
tot.dolphins ~ s(x) + s(y) + s(d.pass) + offset(log(effort))

Parametric coefficients:
            Estimate Std. Error t value Pr(>|t|)
(Intercept) -6.99656    0.08011  -87.34   <2e-16 ***

Approximate significance of smooth terms:
              edf Ref.df      F  p-value
s(x)        5.661  6.656 11.504 1.54e-13 ***
s(y)        3.606  4.554  2.650   0.0256 *
s(d.pass)   4.152  5.120  2.757   0.0240 *

R-sq.(adj) =  0.0747   Deviance explained = 14.6%
-REML = 1537.2  Scale est. = 8.3175    n = 1868
```

Table II.1. Station information for 22 observation stations incuded in the current analysis. Station data are the same as those described in Sadid et al. (2018) exluding 5 stations. East and North represent station coordinates in UTM15 (WGS 84) map projection.

Station	MBE	sd MBE	Mean Salinity	RMSE	East	North	MBE Orig.	RMSE Orig.
CRMS0171	-3.13	3.10	16.8	4.40	811277	3248116	-2.95	4.08
CRMS0172	-1.98	3.03	14.3	3.62	816792	3247185	-1.71	3.17
CRMS0174	-2.78	2.73	12.6	3.89	813953	3256360	-2.27	3.18
CRMS0175	-0.42	3.87	12.7	3.88	777651	3243432	-1.17	3.94
CRMS0176	-2.56	2.71	12.2	3.73	810874	3257567	-2.13	3.19
CRMS0178	-2.66	3.63	13.8	4.50	787006	3243450	-3.16	4.70
CRMS0179	-3.78	2.97	12.3	4.80	820429	3256411	-3.05	3.92
CRMS0181	-1.28	3.12	12.9	3.37	820831	3249682	-0.77	2.55
CRMS0226	0.90	1.95	6.4	2.14	801923	3268796	0.37	1.57
CRMS0232	1.40	2.71	4.7	3.04	789639	3266868	0.80	2.50
CRMS0237	0.22	2.33	6.7	2.34	796361	3264750	-0.37	2.04
CRMS0263	0.59	2.02	4.8	2.10	801493	3273325	0.03	1.61
CRMS0272	-3.05	2.32	10.5	3.83	820801	3259140	-2.43	3.03
CRMS3617	0.54	2.02	5.4	2.09	799087	3272647	-0.02	1.67
CRMS4529	-0.83	1.91	9.1	2.08	808225	3264337	-1.17	2.16
GISL1	-0.44	3.40	9.2	3.42	795884	3258664	-1.12	2.98
USGS1	1.19	1.41	1.1	1.84	774616	3274025	1.05	1.72
USGS3	1.33	1.85	1.2	2.27	773211	3268635	1.07	2.06
USGS5	0.98	3.00	5.4	3.15	789822	3265229	0.34	2.65
USGS6	-1.09	4.36	8.0	4.48	787150	3255761	-1.97	4.66
USGS7	-2.75	2.76	16.4	3.90	797133	3247851	-2.85	3.94
USGS8	-2.21	3.30	18.8	3.97	796670	3242081	-2.02	3.73

Table III.1. Mean (95% Confidence Limits) of the Longest Streak metric by region and alternative for cycle 0, representative year. NAA = No Action Alternative, A3 = Alternative 3 (50K CFS diversion), APA = Applicant's Preferred Alternative (75K CFS diversion), A5 = Alternative 5 (150K CFS diversion). Overall indicates the average for the whole BBES Stock.

Region	NAA	A3	APA	A5
Overall	12.9 (7.5-19.9)	44.3 (33.1-55.7)	51.1 (39.6-62.8)	79.8 (67.0-92.6)
Island	0.1 (0.0-0.5)	6.2 (4.5-8.4)	10.8 (7.2-15.1)	37.7 (28.5-48.4)
West	6.3 (0.6-18.6)	45.8 (19.7-78.1)	55.1 (31.5-83.7)	93.6 (68.8-122.2)
Central	15.3 (7.2-25.7)	74.8 (55.4-95)	87.2 (67.0-108.8)	122.7 (107-139.3)
Southeast	23.4 (10.2-40.7)	36.5 (19.4-58.5)	37.8 (20.4-60.5)	56.1 (36.2-81.8)

Table III.2. Mean (95% Confidence Limits) of population annual survival rates by region and alternative for cycle 0, representative year. NAA = No Action Alternative, A3 = Alternative 3 (50K CFS diversion), APA = Applicant's Preferred Alternative (75K CFS diversion), A5 = Alternative 5 (150K CFS diversion). Overall indicates the average for the whole Bay.

Region	NAA	A3	APA	A5
Overall	0.890 (0.753-0.982)	0.665 (0.423-0.854)	0.588 (0.281-0.832)	0.355 (0.092-0.694)
Island	1.000 (0.999-1.000)	0.980 (0.865-1.000)	0.935 (0.613-1.000)	0.605 (0.094-0.975)
West	0.955 (0.855-1.000)	0.684 (0.348-0.921)	0.555 (0.120-0.885)	0.241 (0.000-0.658)
Central	0.858 (0.611-0.992)	0.406 (0.113-0.746)	0.292 (0.042-0.683)	0.073 (0.000-0.403)
Southeast	0.807 (0.584-0.97)	0.714 (0.458-0.938)	0.683 (0.368-0.926)	0.545 (0.221-0.857)

Table III.3. Mean (95% Confidence Limits) of population annual survival rates by alternative for cycle 0, representative year and alternate years. NAA = No Action Alternative, A3 = Alternative 3 (50K CFS diversion), APA = Applicant's Preferred Alternative (75K CFS diversion), A5 = Alternative 5 (150K CFS diversion).

Year	NAA	A3	APA	A5
1994	0.885 (0.786-0.960)	0.567 (0.307-0.778)	0.405 (0.150-0.667)	0.185 (0.045-0.453)
2006	0.950 (0.861-0.997)	0.897 (0.761-0.977)	0.898 (0.757-0.978)	0.838 (0.586-0.961)
2010	0.864 (0.687-0.961)	0.577 (0.305-0.816)	0.464 (0.219-0.744)	0.214 (0.052-0.505)
2011	0.837 (0.652-0.950)	0.461 (0.181-0.733)	0.319 (0.071-0.638)	0.121 (0.016-0.378)
Representative Year	0.890 (0.753-0.982)	0.665 (0.423-0.854)	0.588 (0.281-0.832)	0.355 (0.092-0.694)

Table III.4. Mean (95% Confidence Limits) of population annual survival rates by alternative for the representative year in each cycle (decade). For cycles 1-5, the simulations for the NAA includes dolphins inhabiting the entire Bay where under the other alternatives dolphin starting positions are restricted to the Island habitat with the highest survival rates. NAA = No Action Alternative, A3 = Alternative 3 (50K CFS diversion), APA = Applicant's Preferred Alternative (75K CFS diversion), A5 = Alternative 5 (150K CFS diversion).

Cycle	NAA	A3	APA	A5
0	0.890 (0.753-0.982)	0.665 (0.423-0.854)	0.588 (0.281-0.832)	0.355 (0.092-0.694)
1	0.967 (0.891-1.000)	0.939 (0.673-1.000)	0.811 (0.345-0.992)	0.259 (0.048-0.776)
2	0.880 (0.781-0.960)	0.980 (0.873-1.000)	0.901 (0.563-0.999)	0.423 (0.054-0.911)
3	0.797 (0.649-0.926)	0.937 (0.676-1.000)	0.854 (0.368-0.995)	0.328 (0.053-0.880)
4	0.647 (0.475-0.804)	0.875 (0.504-0.989)	0.681 (0.162-0.958)	0.224 (0.035-0.657)
5	0.658 (0.462-0.817)	0.954 (0.717-1.000)	0.864 (0.362-0.996)	0.368 (0.046-0.843)

Figure I.1. Barataria Bay in southern Louisiana including the region surveyed during photo-id surveys prior to 2019 (hatched area, McDonald et al., 2017).

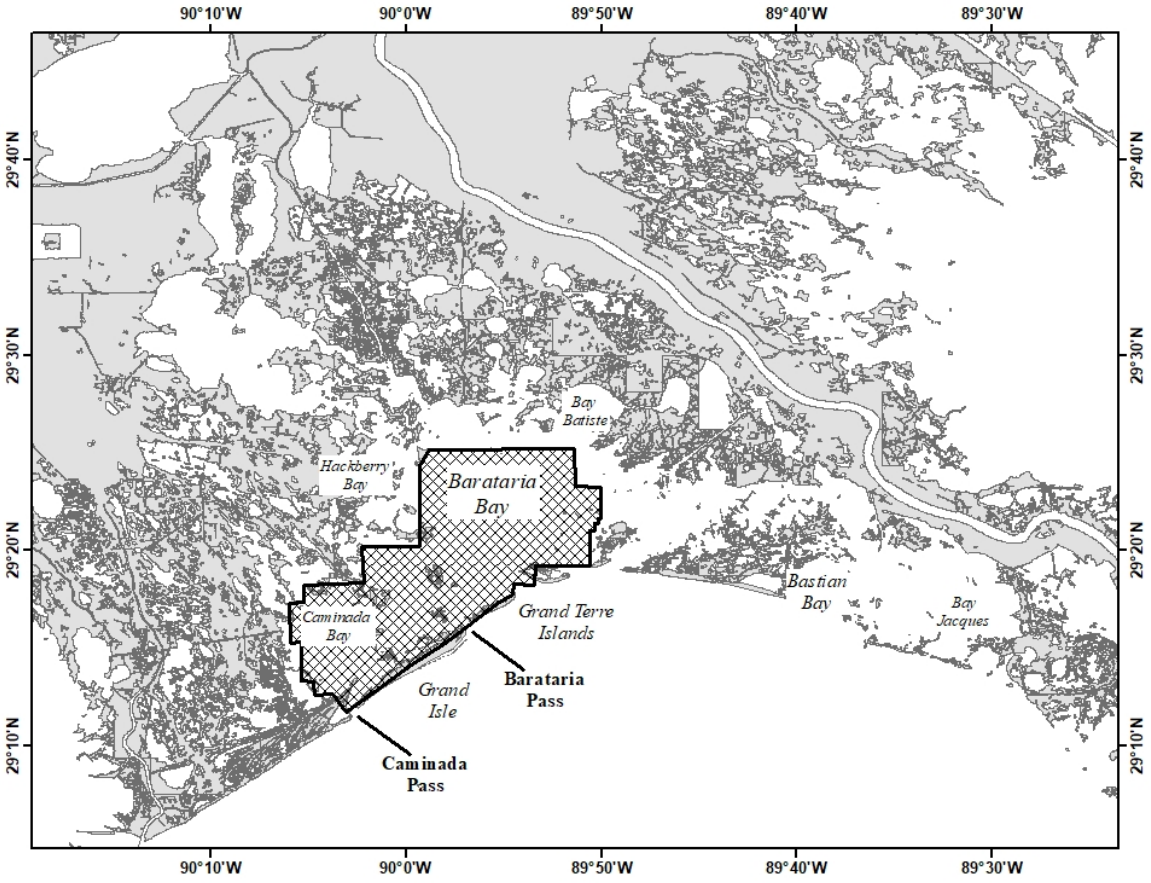

Figure I.2. Survey track-lines for the Barataria Bay Estuarine System Stock capture-mark-recapture project 14 March to 1 April 2019. Prior year surveys did not include the "southeast" area or the contour tracklines in the northern portion of the survey area.

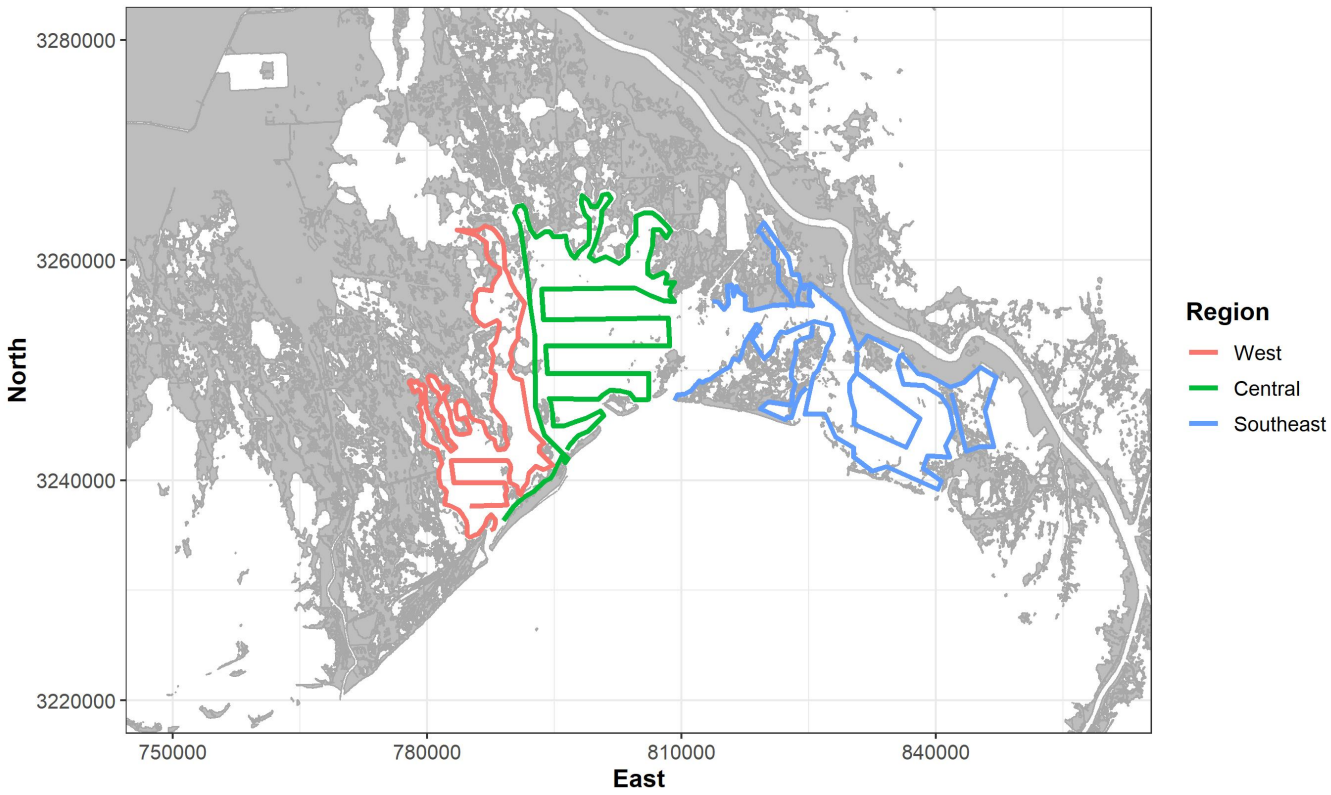

Figure I.3 Planned temperature and salinity stations during the spring 2019 CMR survey.

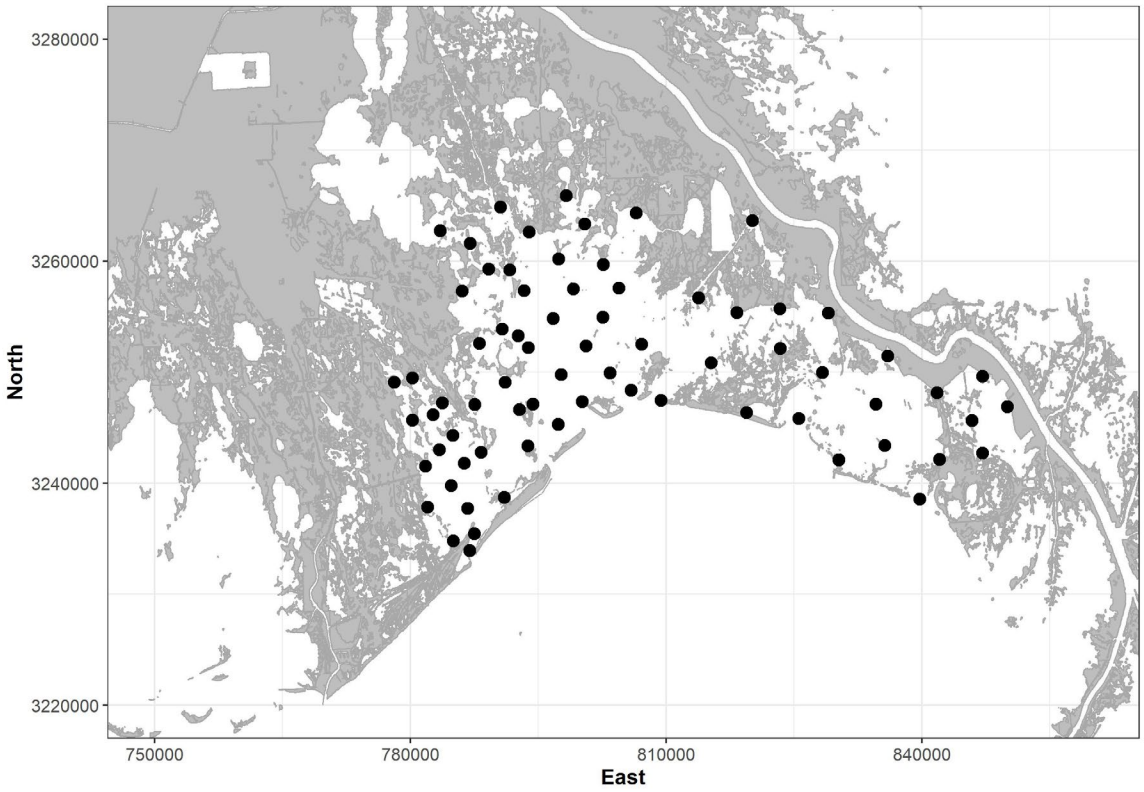

Figure I.4. Executed tracklines, dolphin group sighting locations, and analysis grid.

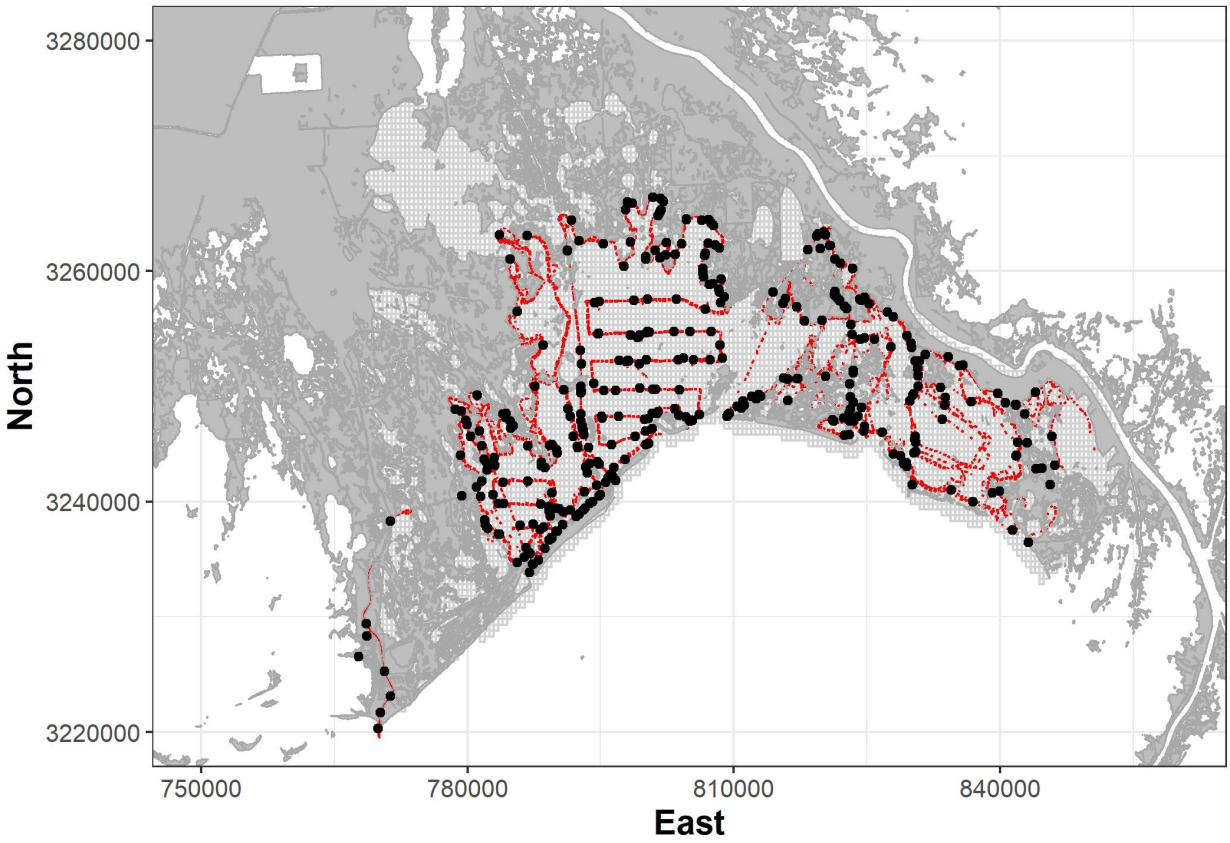

Figure I.5. Dolphin group sizes during the spring 2019 CMR survey.

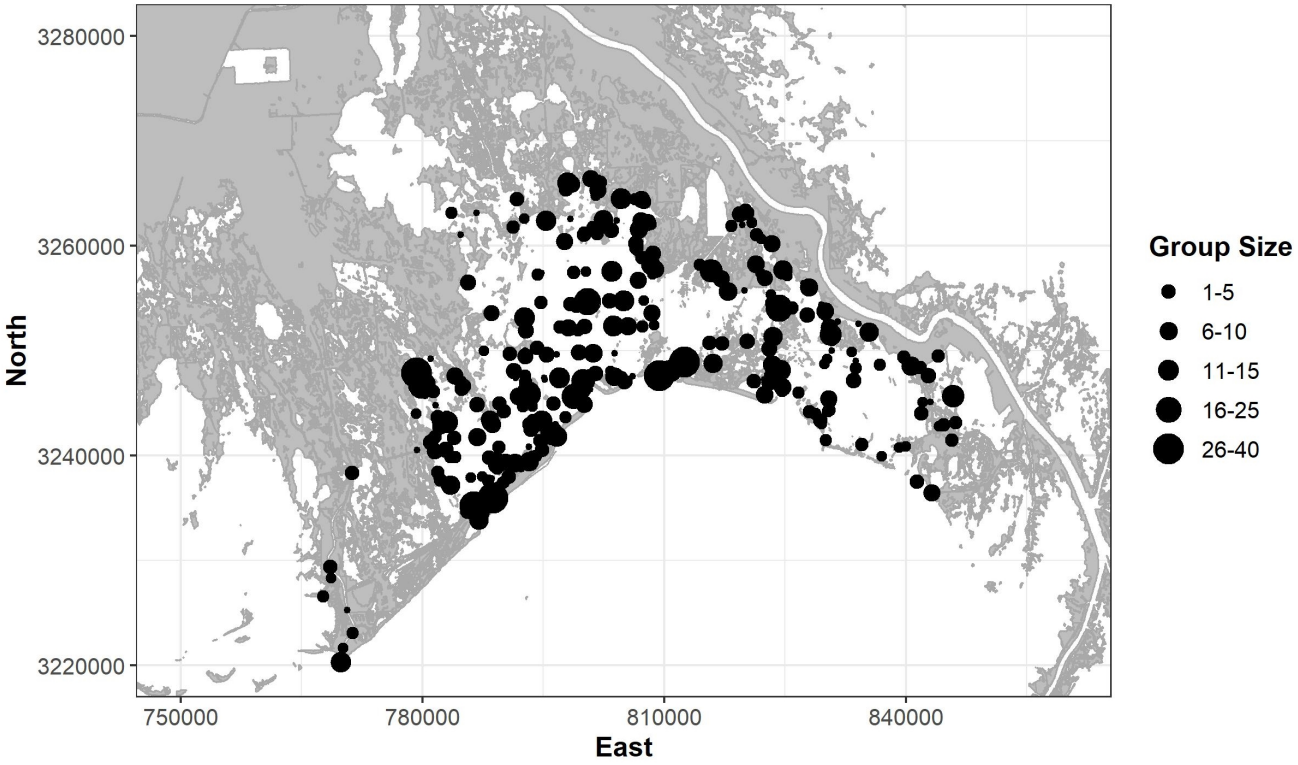

Figure I.6. Discovery curve showing the number of new dolphins added to the Barataria Bay master photo-identification catalog by survey year.

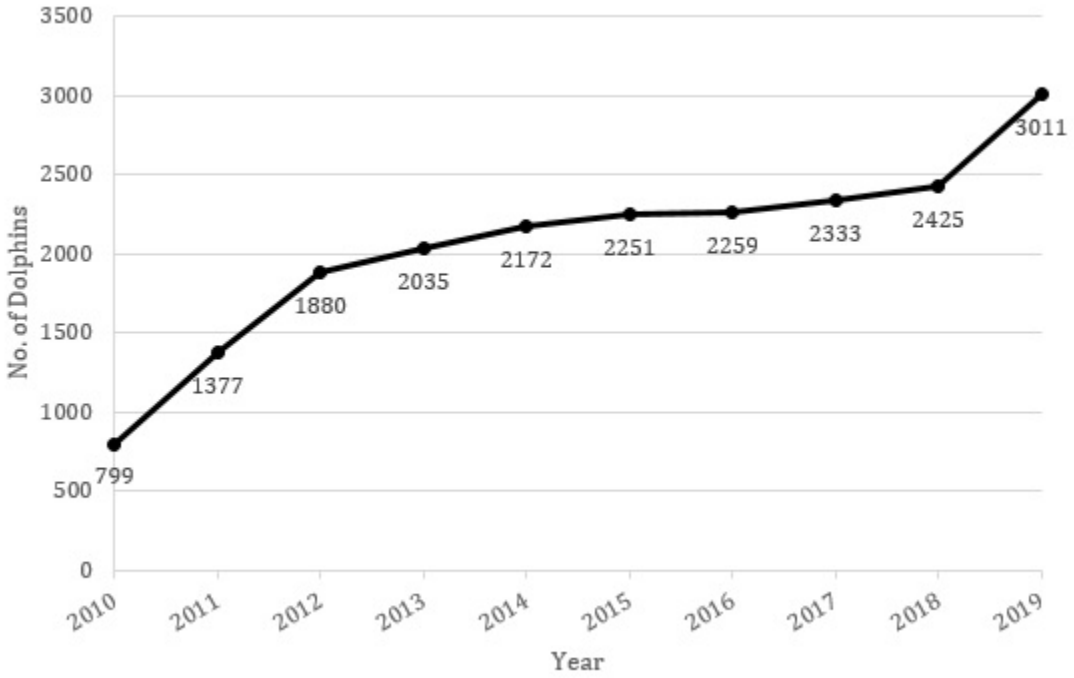

Figure I.7. GAM model fit and residuals. The line indicates the model smooth fit for each explanatory factor, and the shaded area indicates the 95% confidence limit of the model fit.

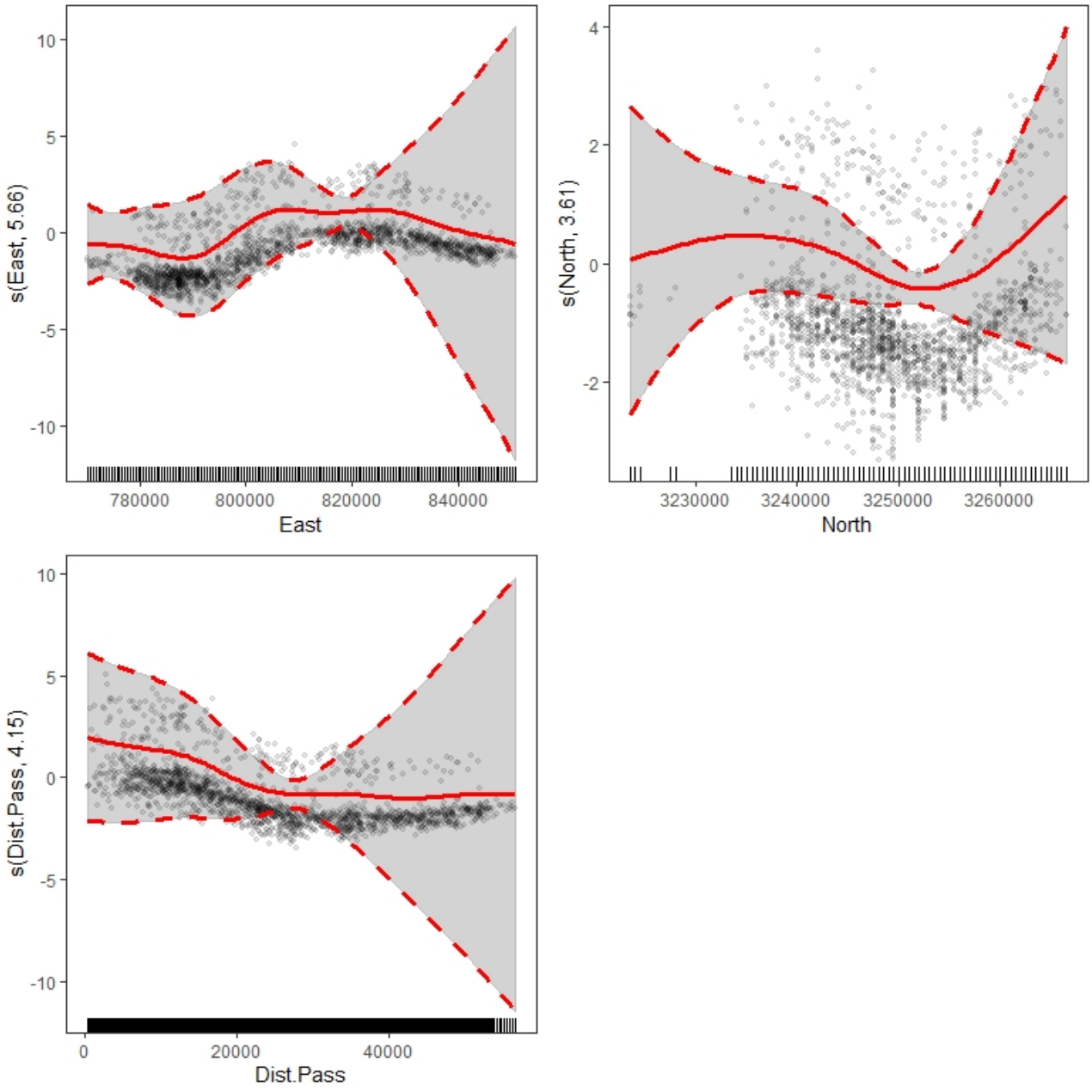

Figure I.8. Fitted (line) and observed (points) dolphins per 100m of survey effort (SPUE) as a function of explanatory factors. The dashed line indicates the 95% confidence limits of model fitted values.

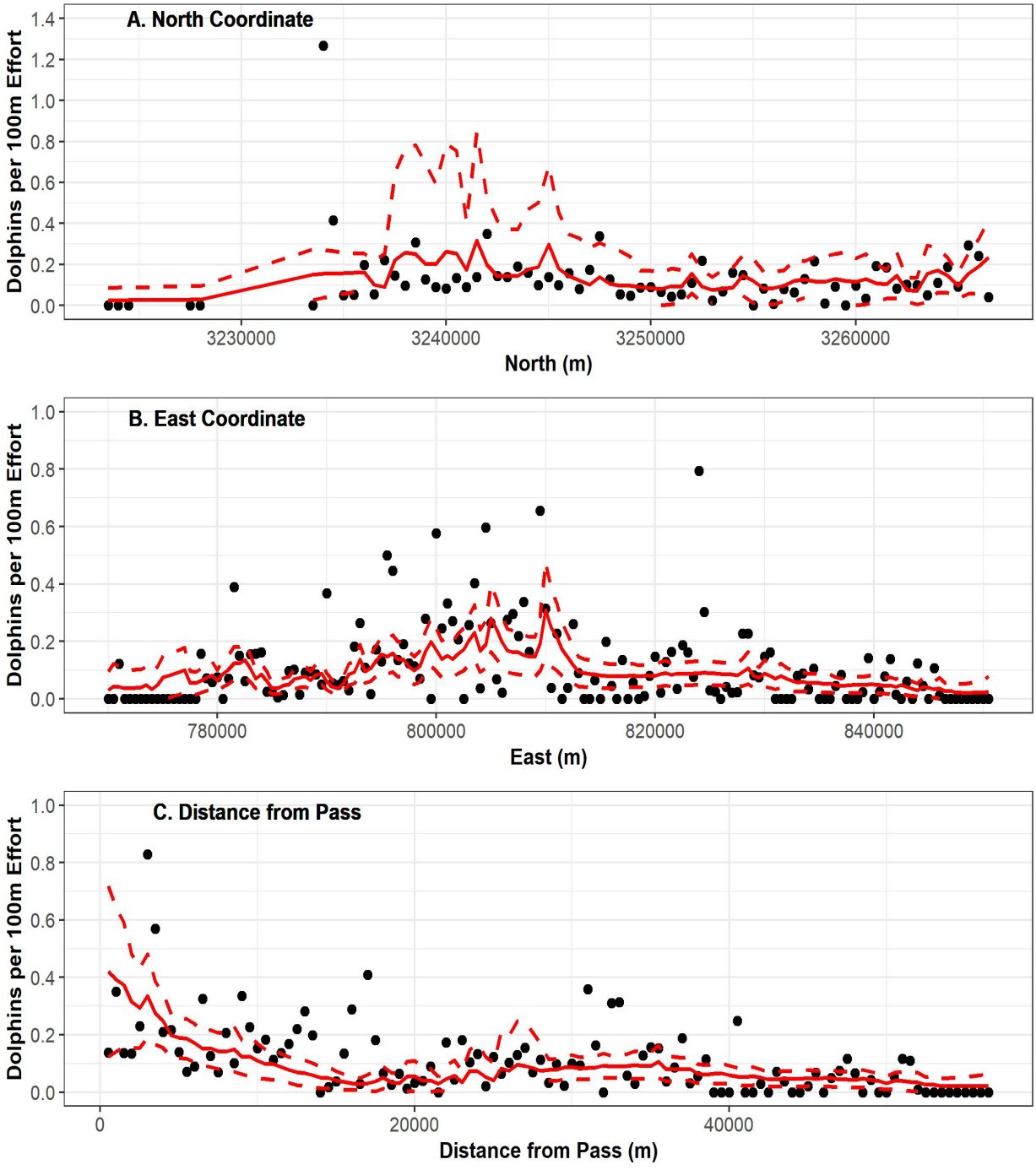

Figure I.9. Predicted relative density (SPUE) projected over the spatial grid. Areas with CV > 0.4 are masked from the resulting surface given high model uncertainty when projecting outside of the range of survey data.

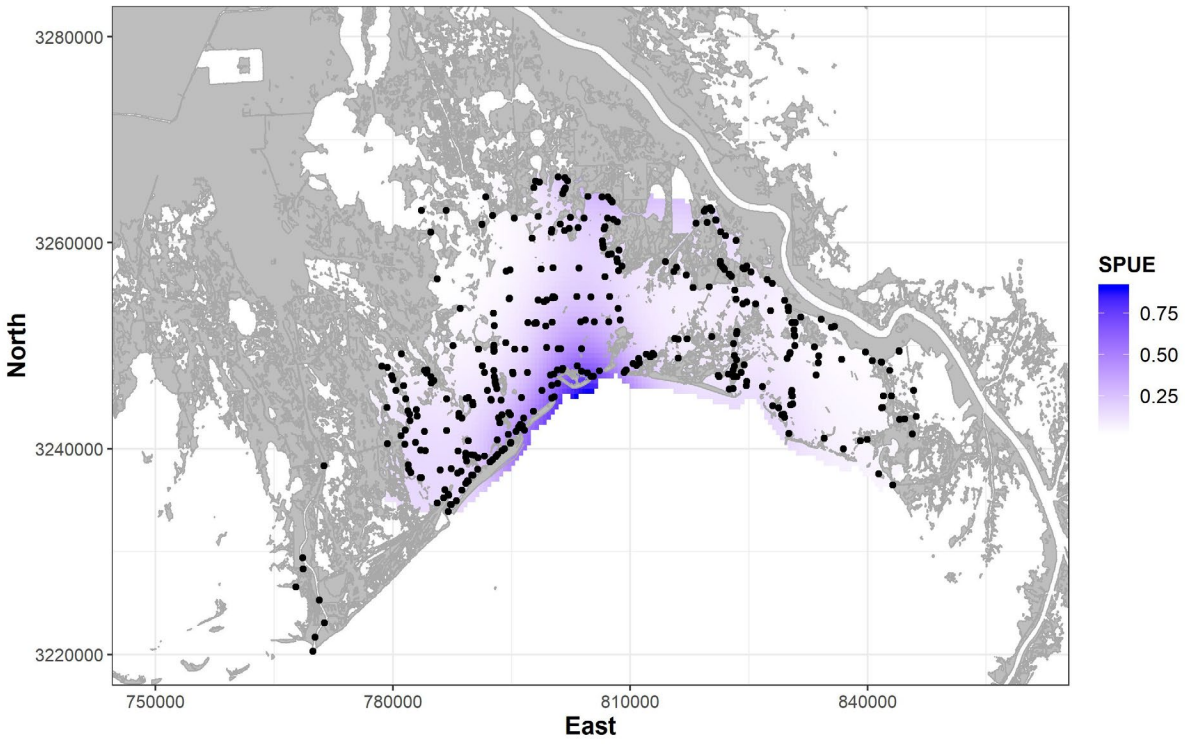

Figure II.1. Station locations for 22 salinity observations included in the current analysis.

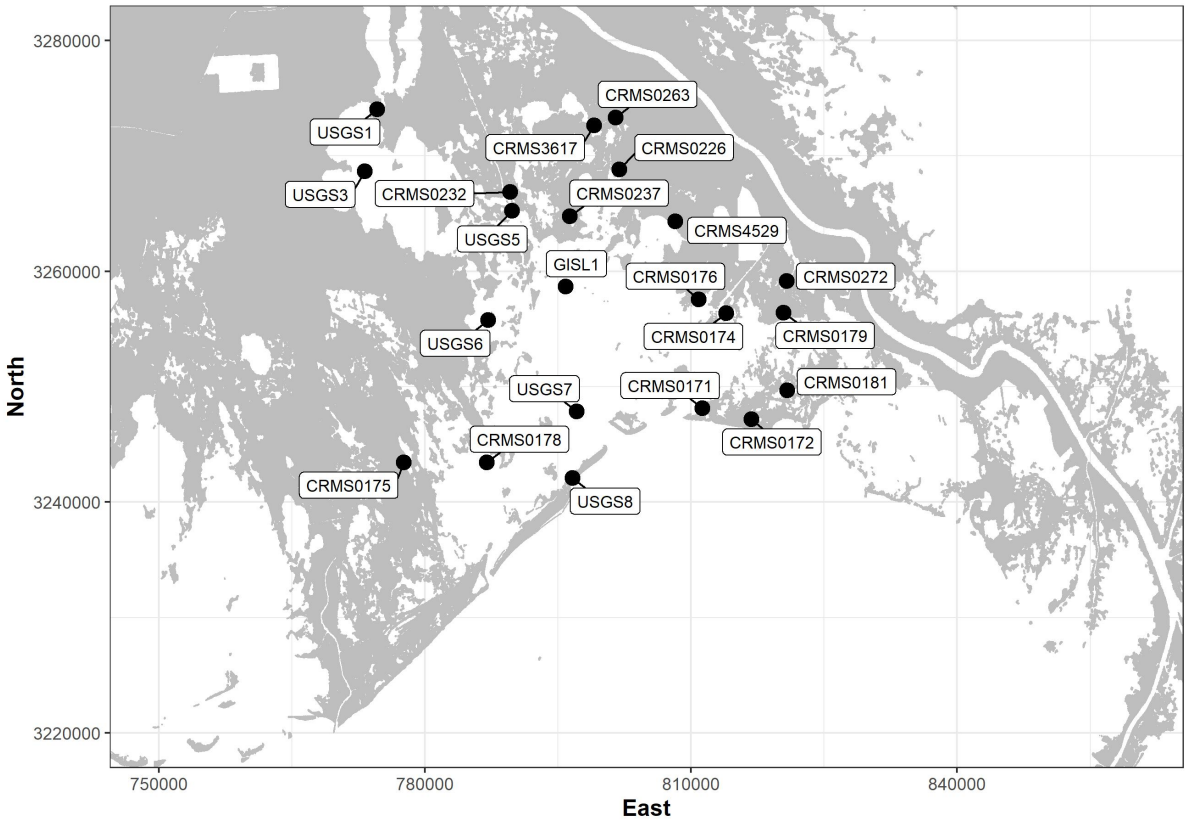

Figure II.2. Daily mean observed (black dots) and Delft3d modelled (red line) salinity for each observation sation from 2016.

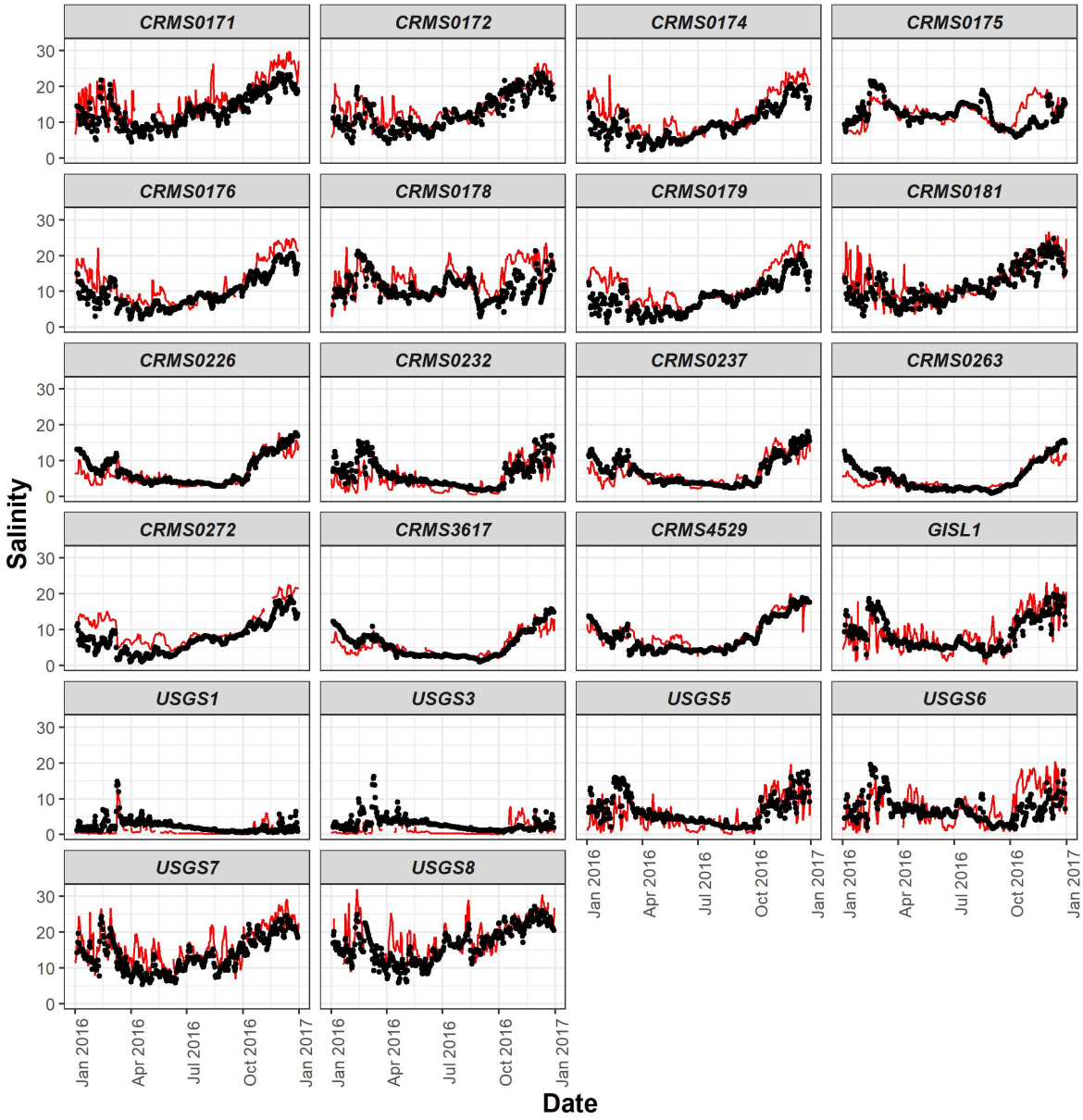

Figure II.3. Daily bias (red line) for each salinity observation station. The dashed line indicates the Mean Bias Estimate for each station.

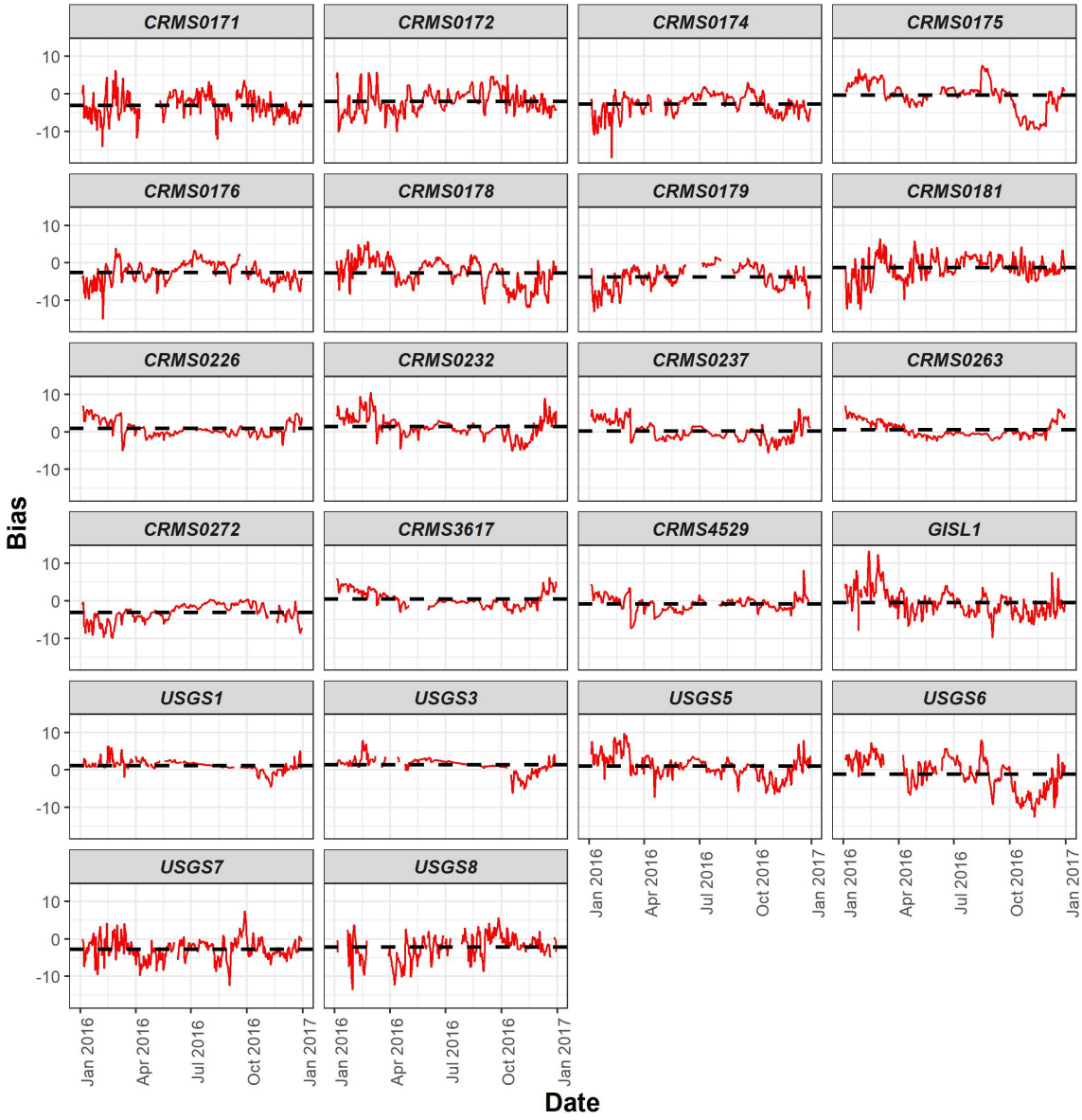

Figure II.4. Distance plot indicating the Pearson distance between station pairs. Higher values indicate greater differences between stations. Pairs are ordered to highlight clustering among stations.

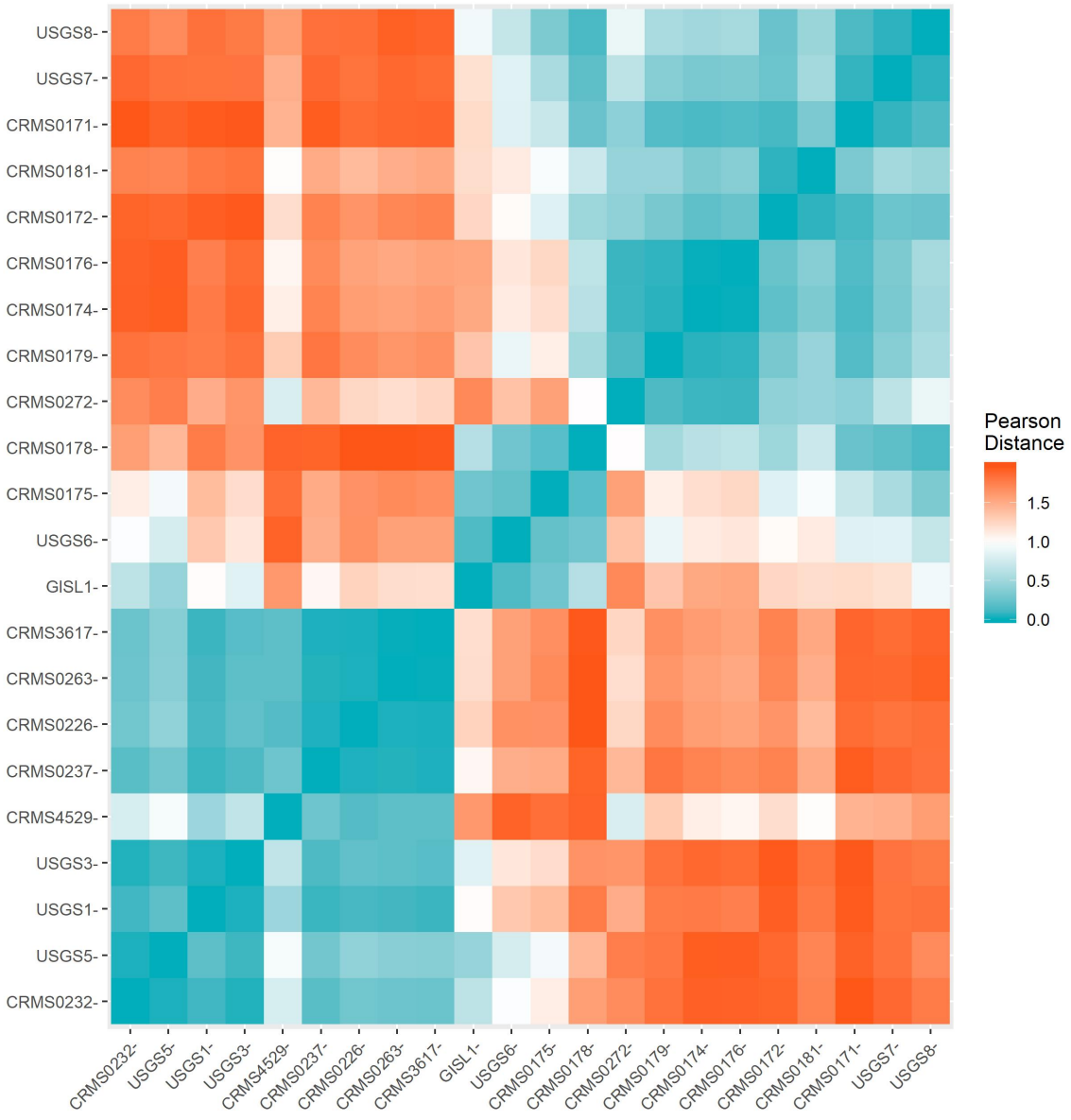

Figure II.5. Cluster plots showing the membership and distribution of clusters of stations based upon K-means clusters specifying 2-5 clusters.

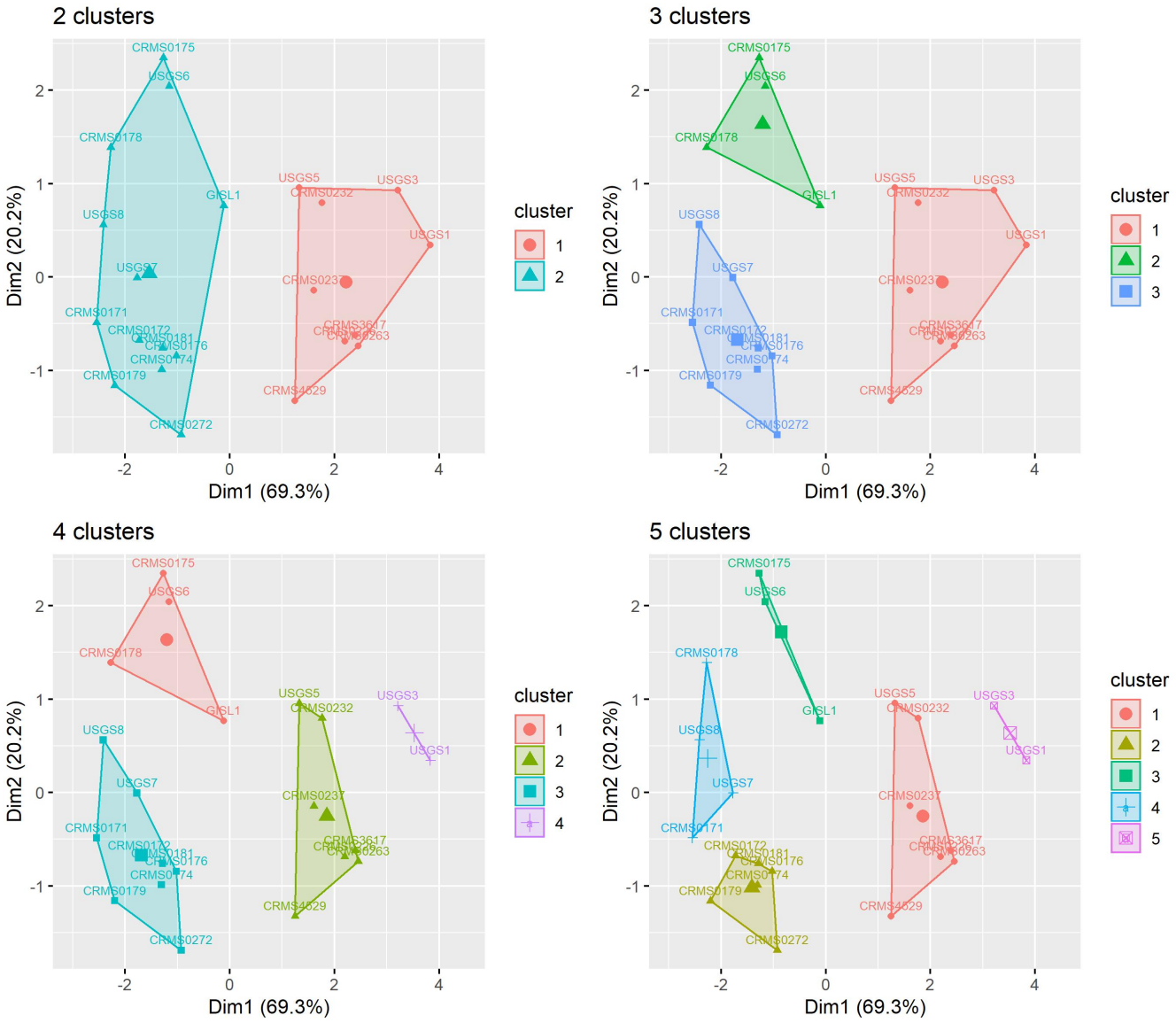

Figure II.6. Cluster optimization statistics using the (A) Average silhouette and (B) Gap statistics. Both metrics indicate that an optimal number of clusters is 2 (dashed vertical line).

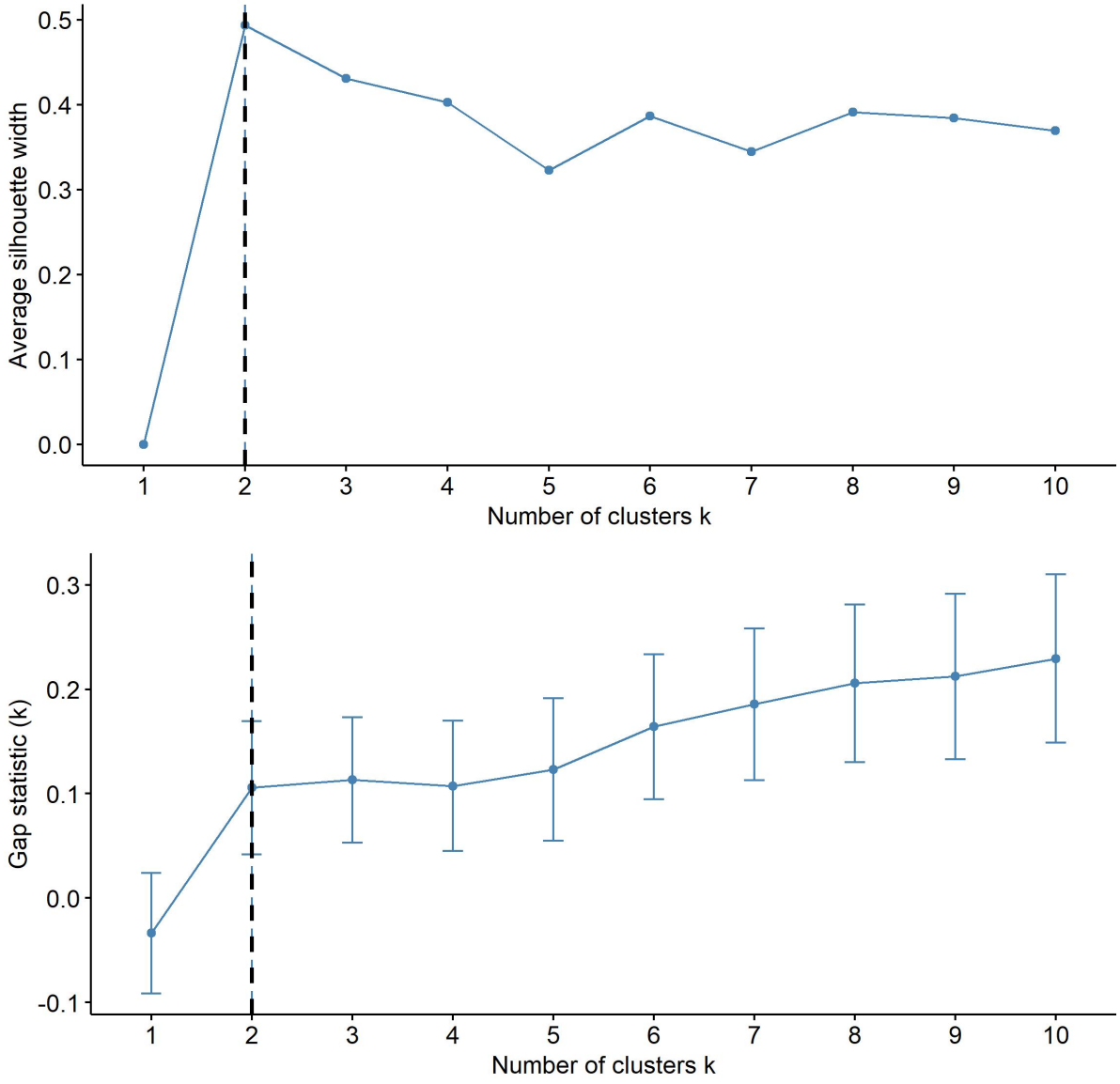

Figure II.7. Cluster membership as a function of RMSE and MBE. Cluster 1 includes stations with positive salinity biases and lower RMSE values while Cluster 2 includes stations with more negative biases and higher RMSE.

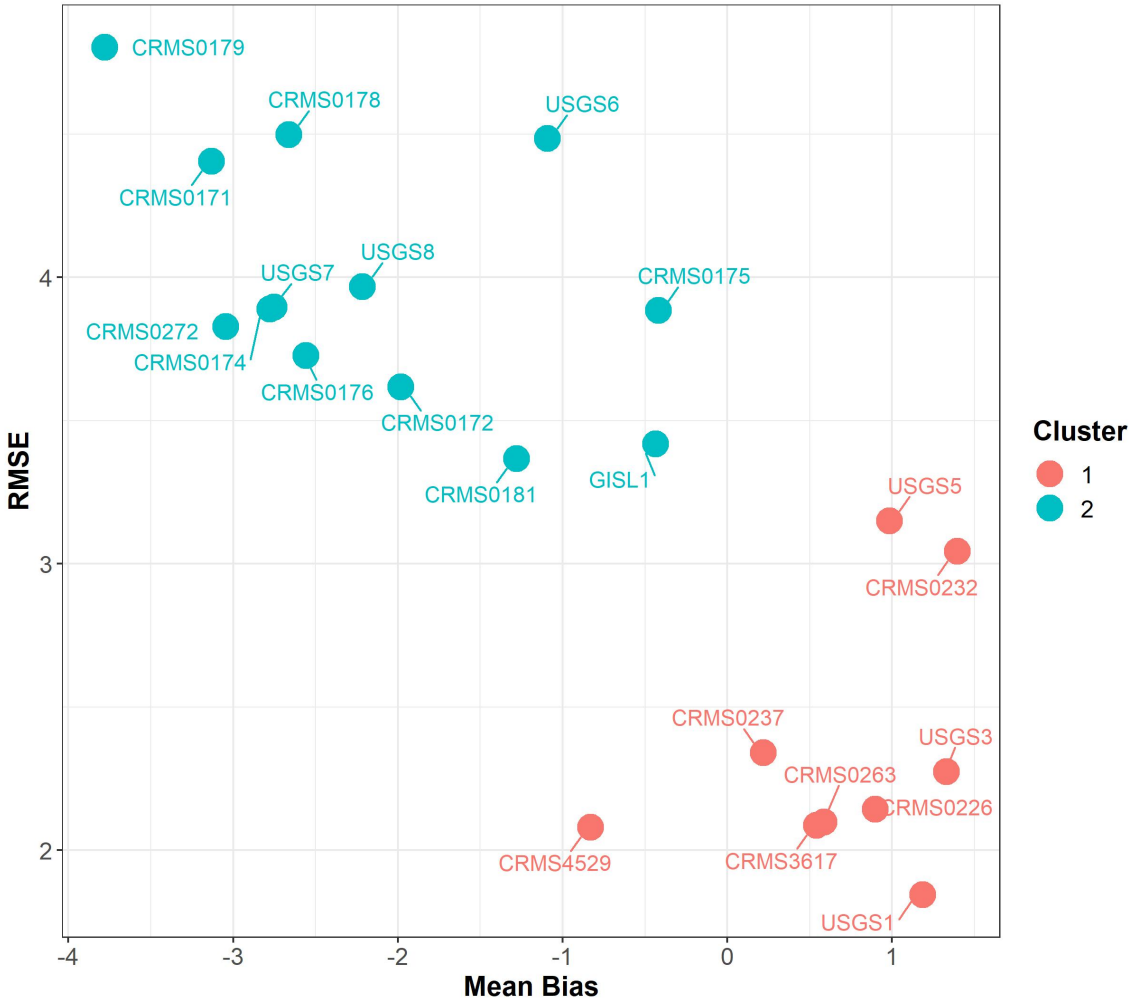

Figure II.8. Salinity stations by cluster. Cluster 1 includes stations further north in areas of the Bay more heavily influenced by freshwater while Cluster 2 includes stations in the middle and lower bay that are more estuarine.

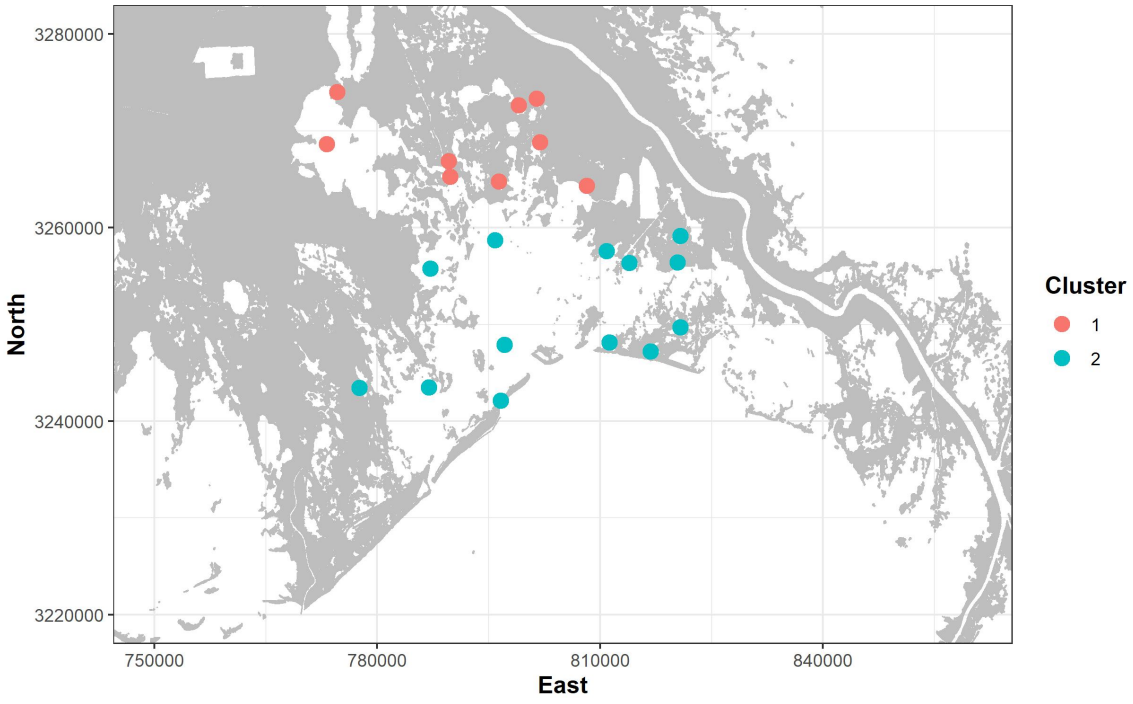

Figure II.9. Partial autocorrelation of residuals from GAMM models for Cluster 1 stations with (A) no autocorrelation structure and (B) an AR3 autocorrelation structure. The dashed line indicates the level for significant autocorrelation in residuals. There is evidence for autocorrelation at lags 1-3 days. Accounting for this lag correlation leaves no remaining significant autocorrelation in the residuals for the GAMM model.

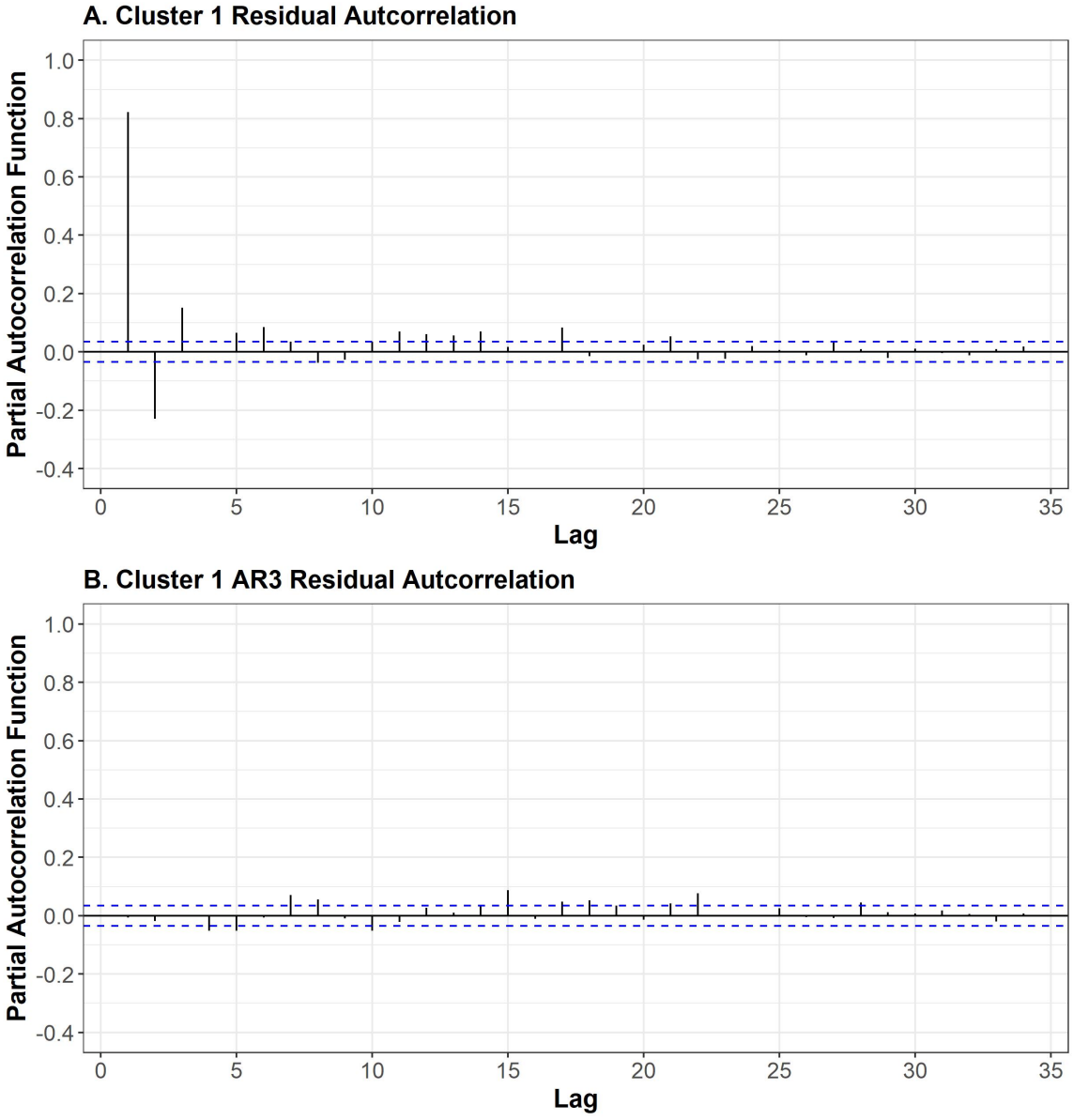

Figure II.10. Predicted (red line) and observed (points) daily salinity bias values for cluster 1 salinity stations. The 95% confidence interval of the GAMM predictions is indicated by the dashed lines.

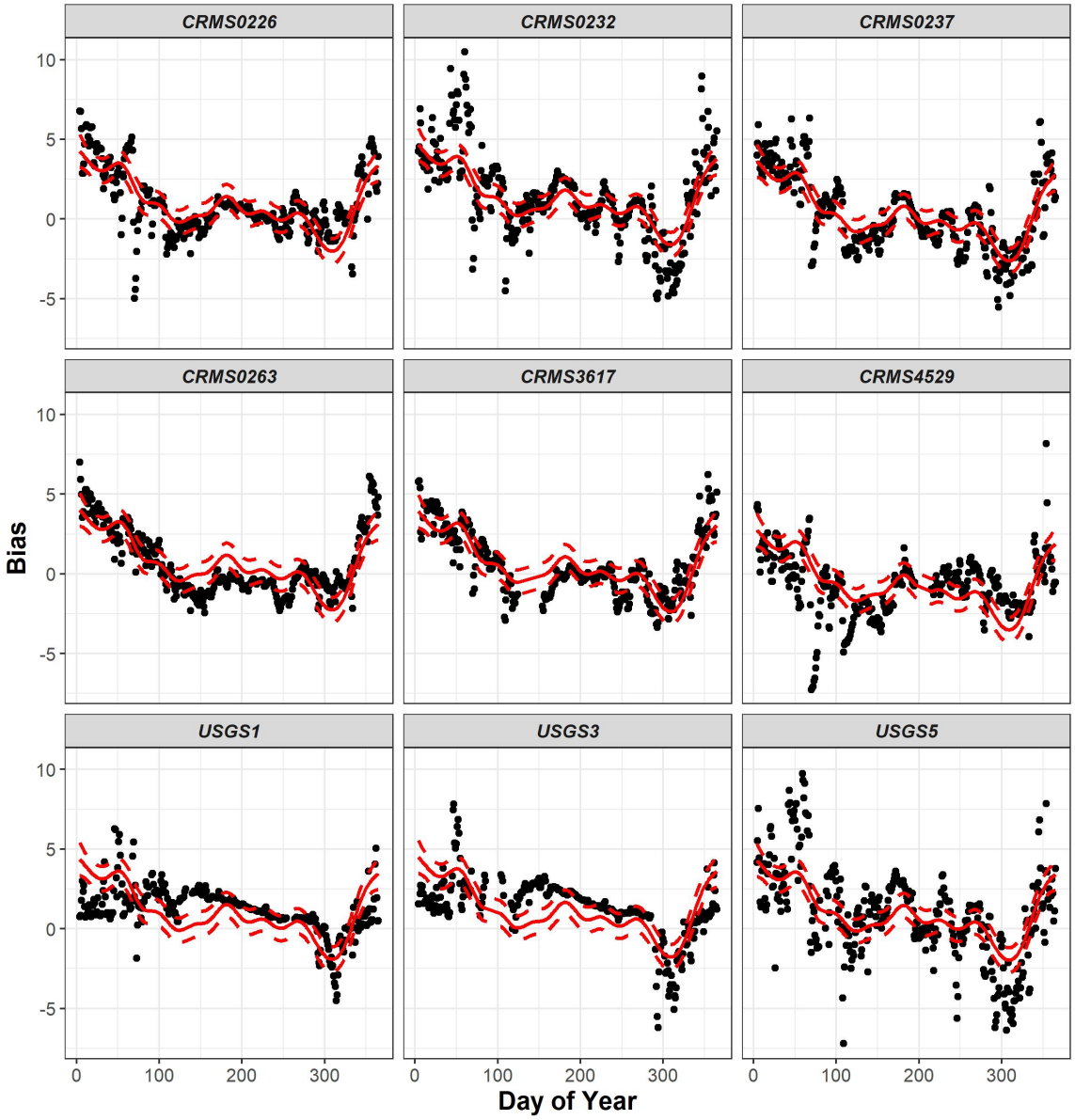

Figure II.11. Parametric bootstrap distribution of mean annual bias for Cluster 1 stations derived from the GAMM model. The distribution median is indicated by the dashed vertical line. While the mean bias estimates are similar, ignoring autocorrelation in residuals (A) underestimates the uncertainty in the estimate while the distribution including the AR3 correlation (B) demonstrates higher variance in the mean.

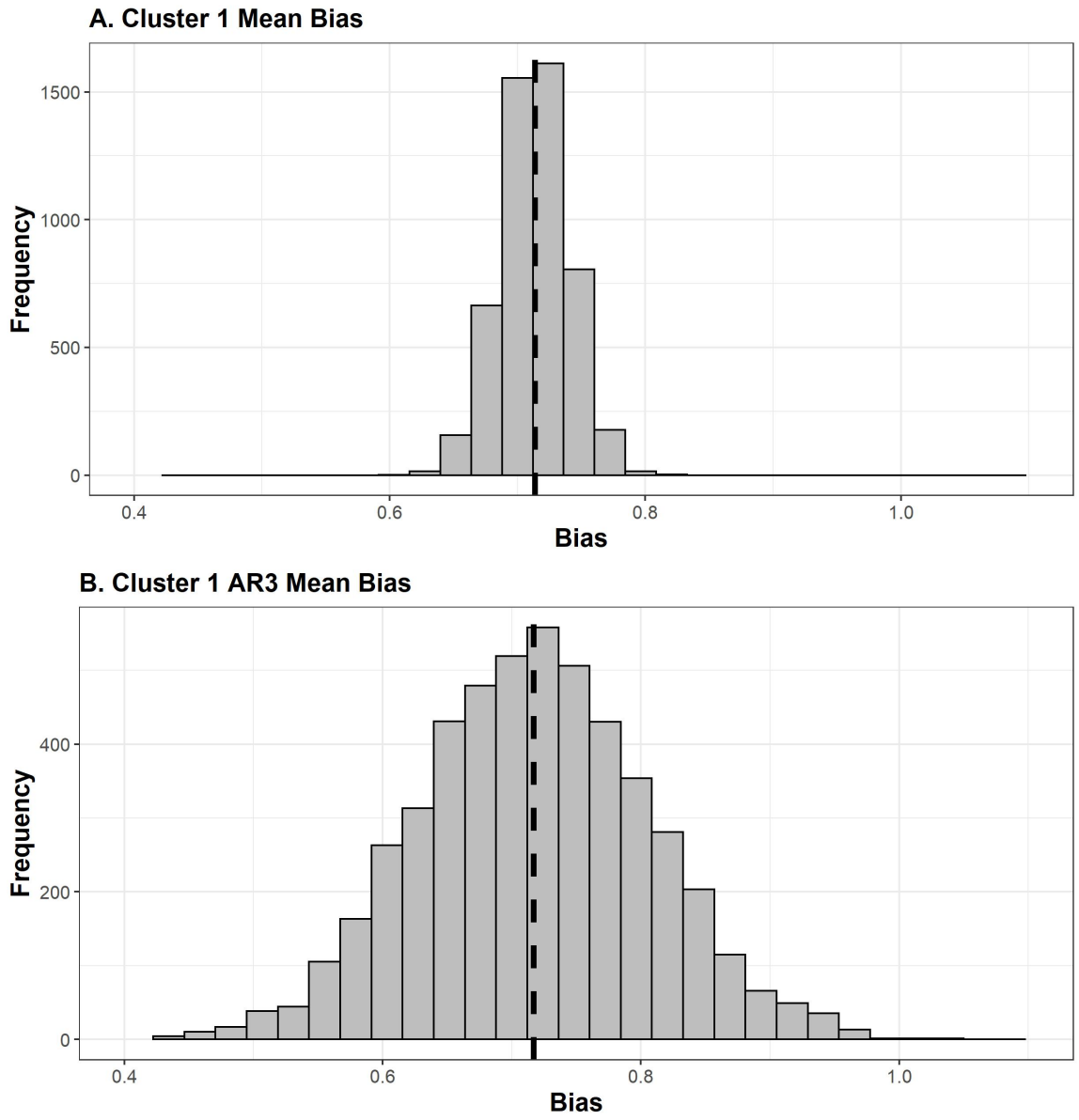

Figure II.12. Partial autocorrelation of residuals from GAMM models for Cluster 2 stations with (A) no autocorrelation structure and (B) an AR3 autocorrelation structure. The dashed line indicates the level for significant autocorrelation in residuals. There is evidence for autocorrelation at lags 1-3 days. Accounting for this lag correlation leaves no remaining significant autocorrelation in the residuals for the GAMM model.

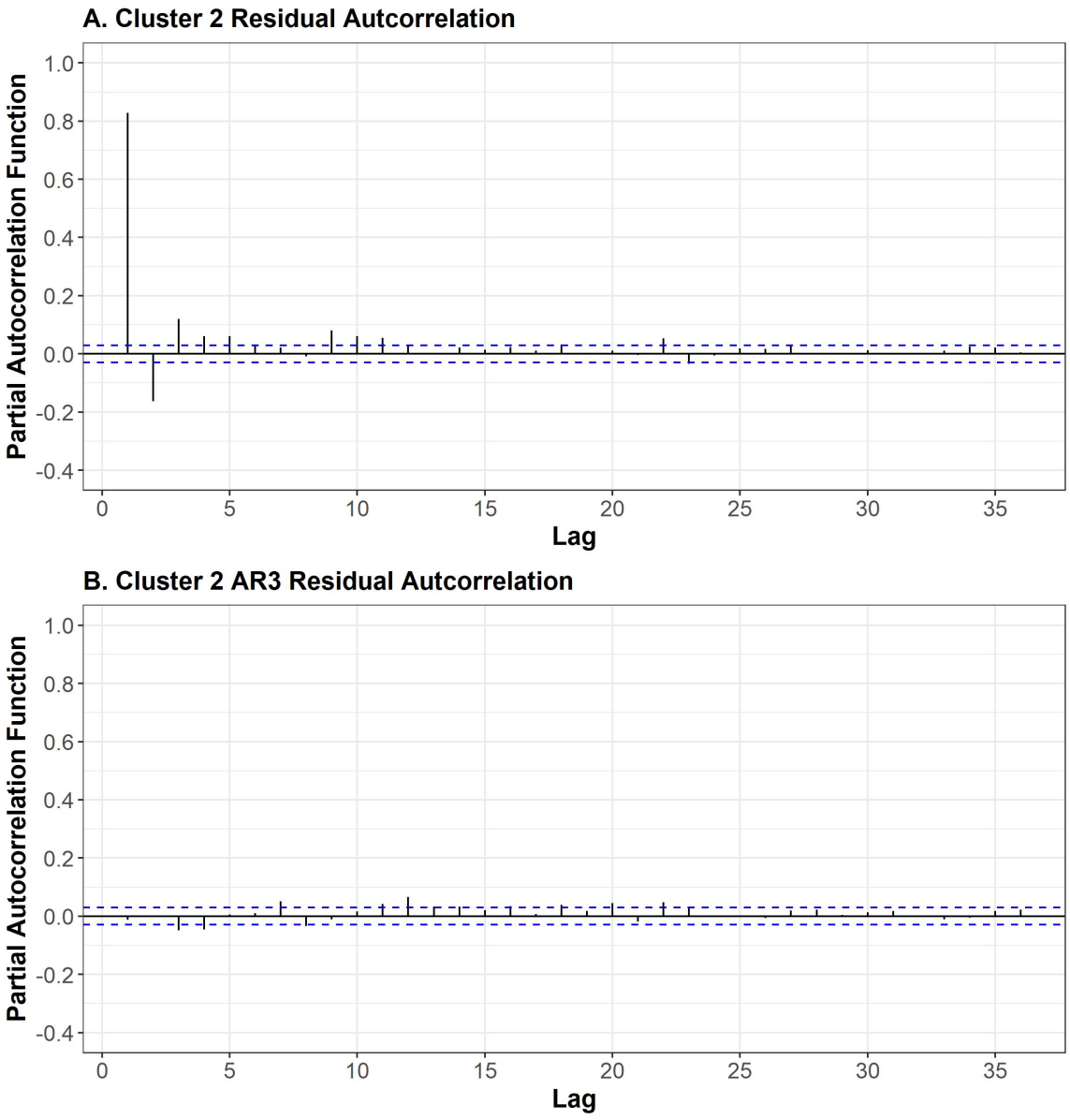

Figure II.13. Predicted (red line) and observed (points) daily salinity bias values for cluster 2 salinity stations. The 95% confidence interval of the GAMM predictions is indicated by the dashed lines.

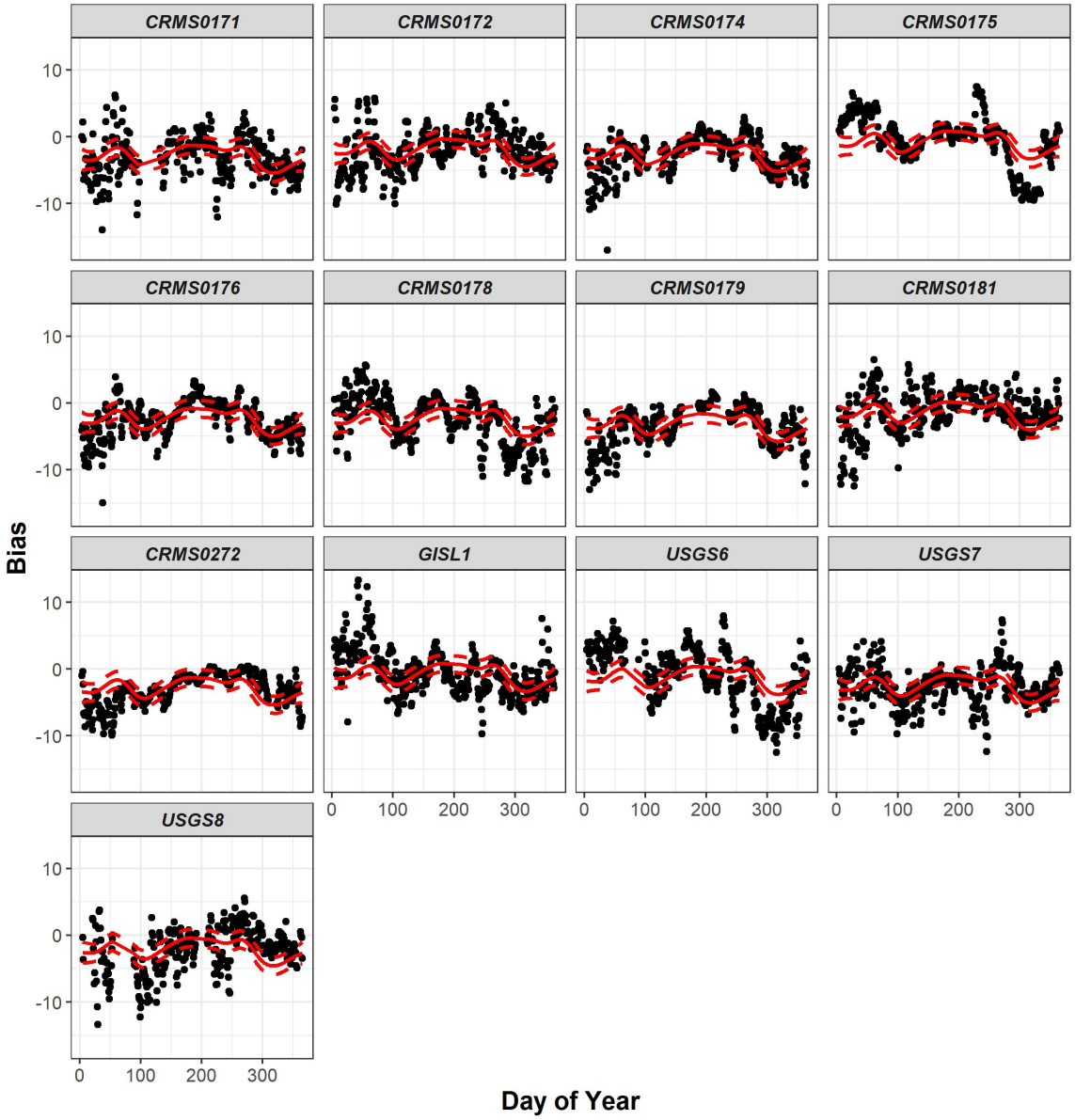

Figure II.14. Parametric bootstrap distribution of mean annual bias for Cluster 2 stations derived from the GAMM model. The distribution median is indicated by the dashed vertical line. The mean bias estimate for the AR3 model is slightly higher than that for the model including no autocorrelation. Ignoring autocorrelation in residuals (A) underestimates the uncertainty in the estimate while the distribution including the AR3 correlation (B) demonstrates higher variance in the mean.

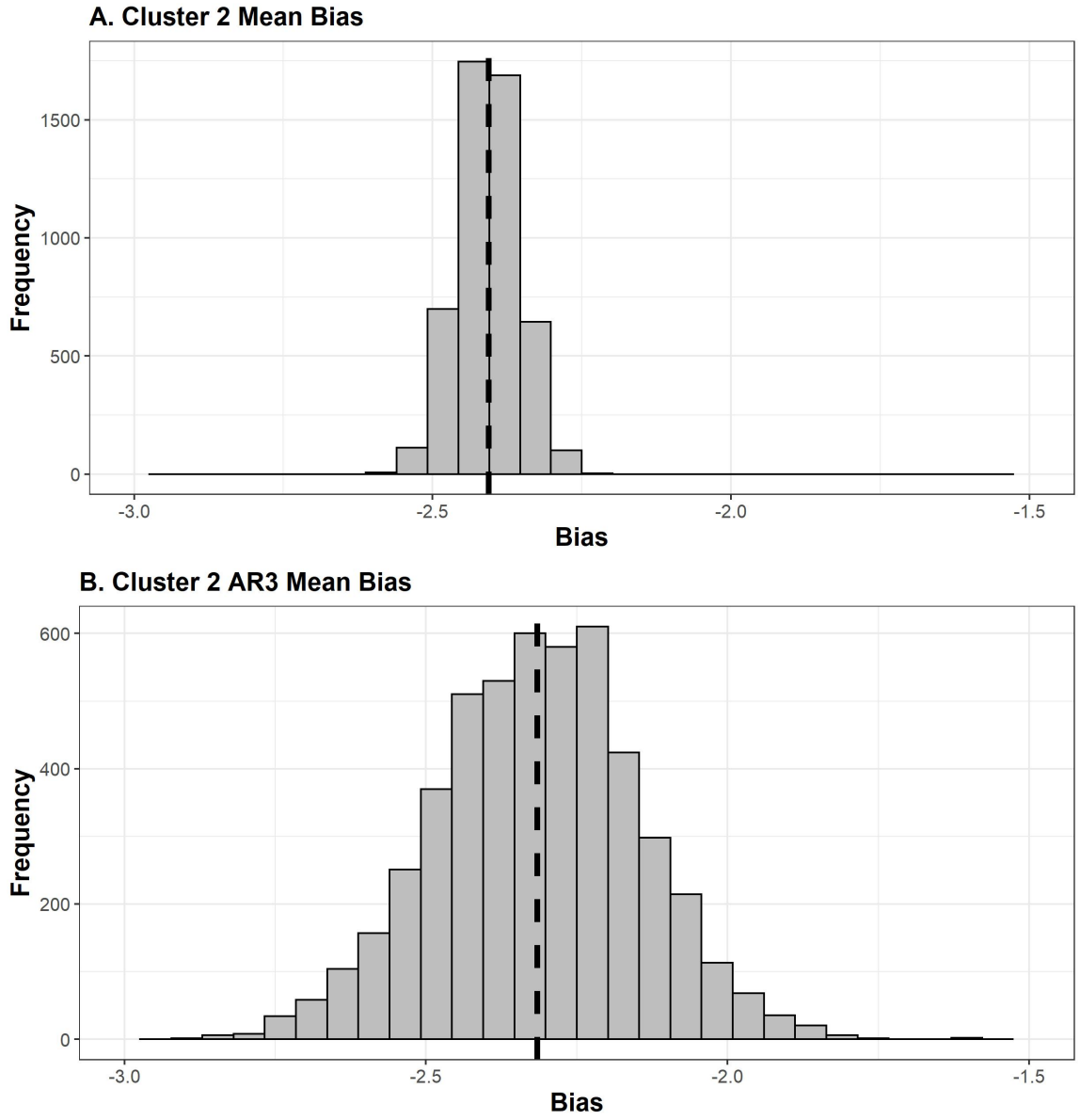

Figure II.15. Regions within the Barataria Bay bottlenose dolphin stock area corresponding to cluster 1 and cluster 2 stations and corresponding mean bias estimates. The mean and standard deviation in bias will be applied spatially within these regions to account for retrospective prediction bias in outputs from the Delft3D model. Cluster 1 has a mean bias of 0.717 (sd = 0.0889) while cluster 2 has a mean bias of -2.136 (sd = 0.168).

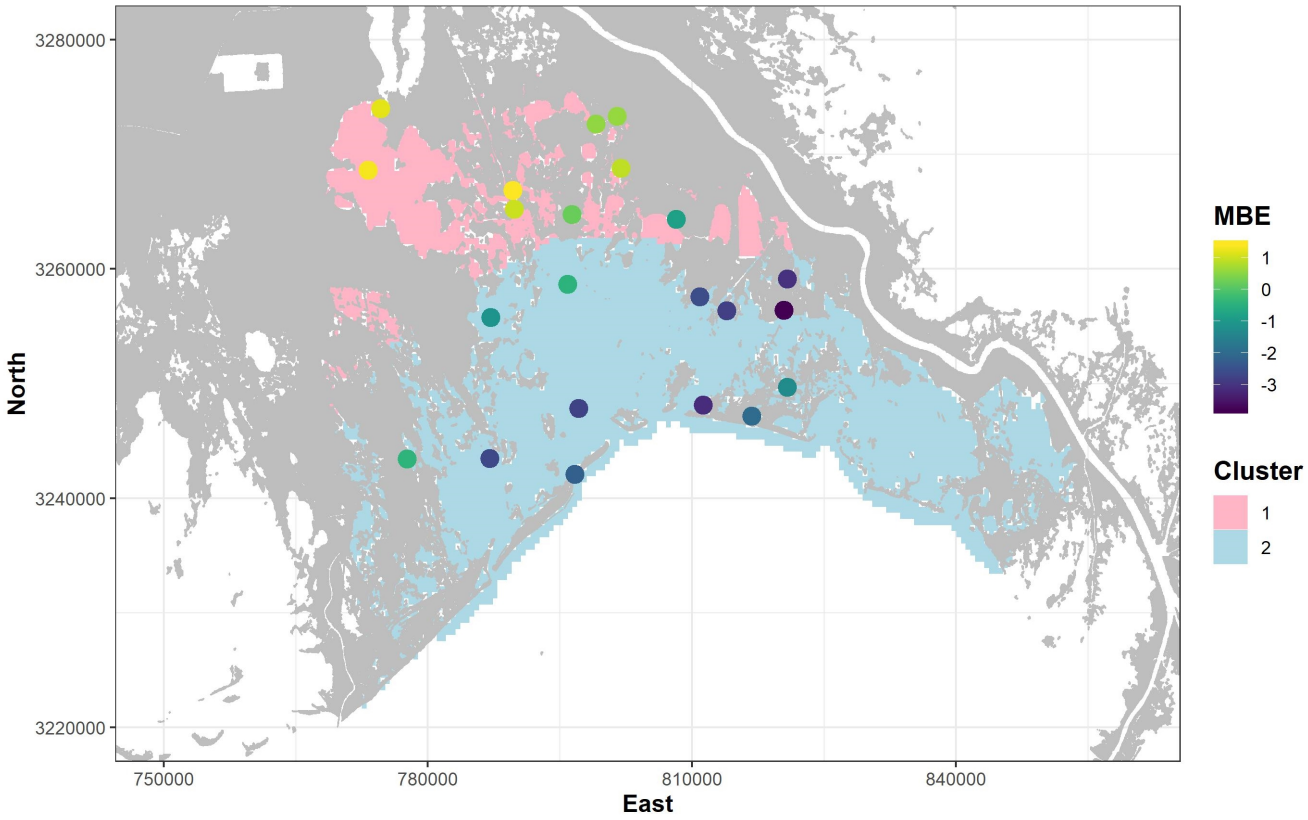

Figure III.1. Predicted daily salinity from the Delft model for each cycle, hydrograph, and alternative were standardized onto a 500x500m grid and overlaid with the spatial boundaries of the BBES bottlenose dolphin stock. The underlying salinity in this image is from an example output (Cycle 0, NAA, April 20). The stock boundary and within stock strata definitions are outlined in black.

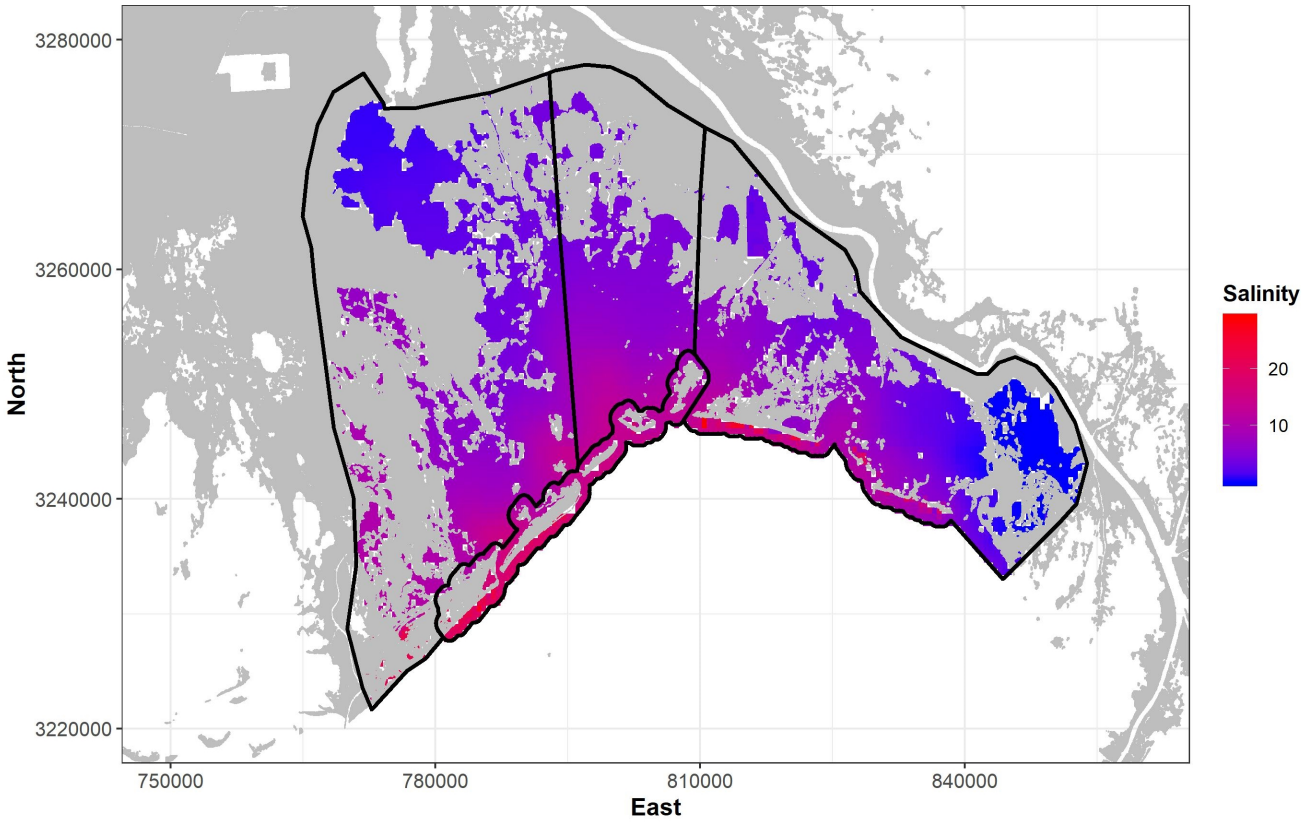

Figure III.2. Relative density (Sightings Per Unit Effort) surface over the model domain overlaid with the BBES stratum boundaries. The mean SPUE values (dolphins per 100m trackline) by strata are: Island: 0.406, West - 0.0813, Central - 0.203, and Southeast - 0.100

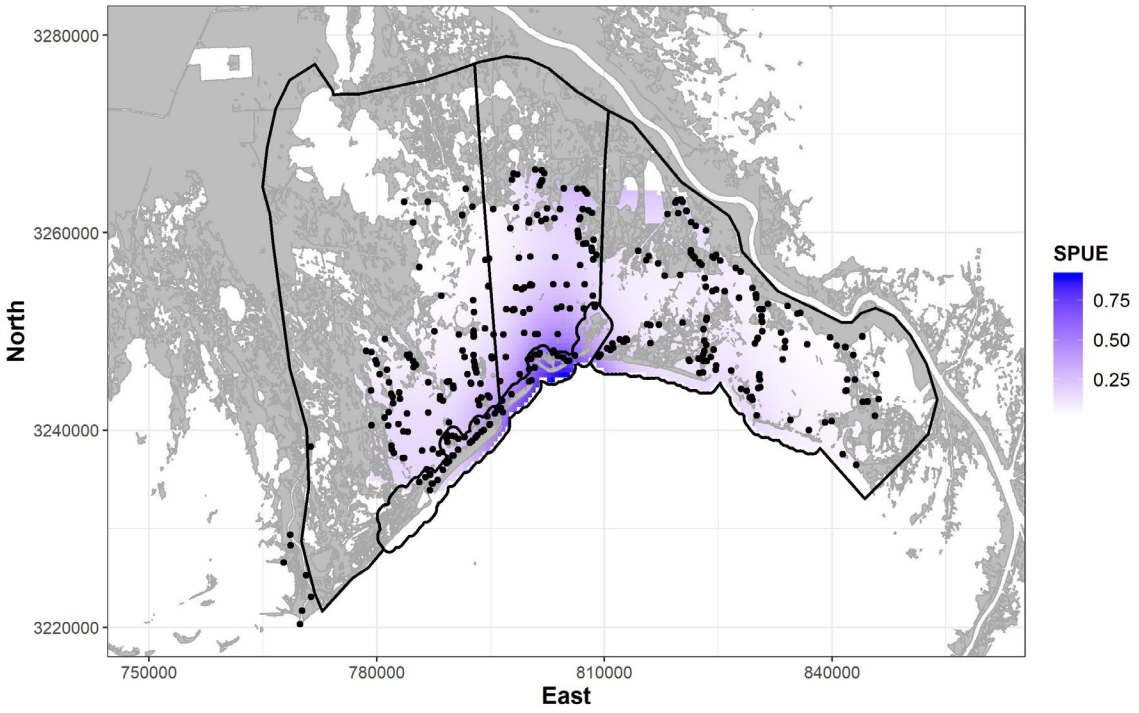

Figure III.3. Dose response curve indicating the relationship between continuous days of exposure and individual survival probability. The shaded area indicates the 95% confidence limits of a distribution of 10,000 realizations of this curve reflecting parameter uncertainty. The solid red line indicates the median of the distribution while the blue lines indicate the first and third quartiles of the distribution.

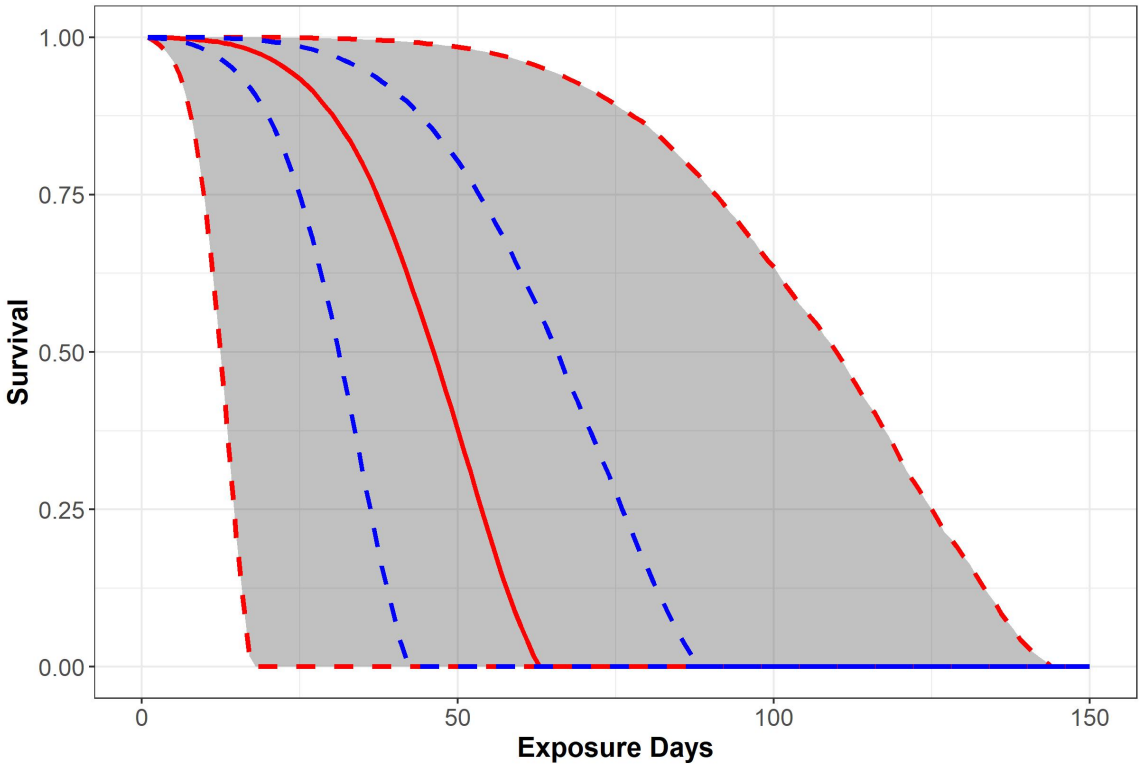

Figure III.4. Example distribution of starting positions for simulated dolphins.

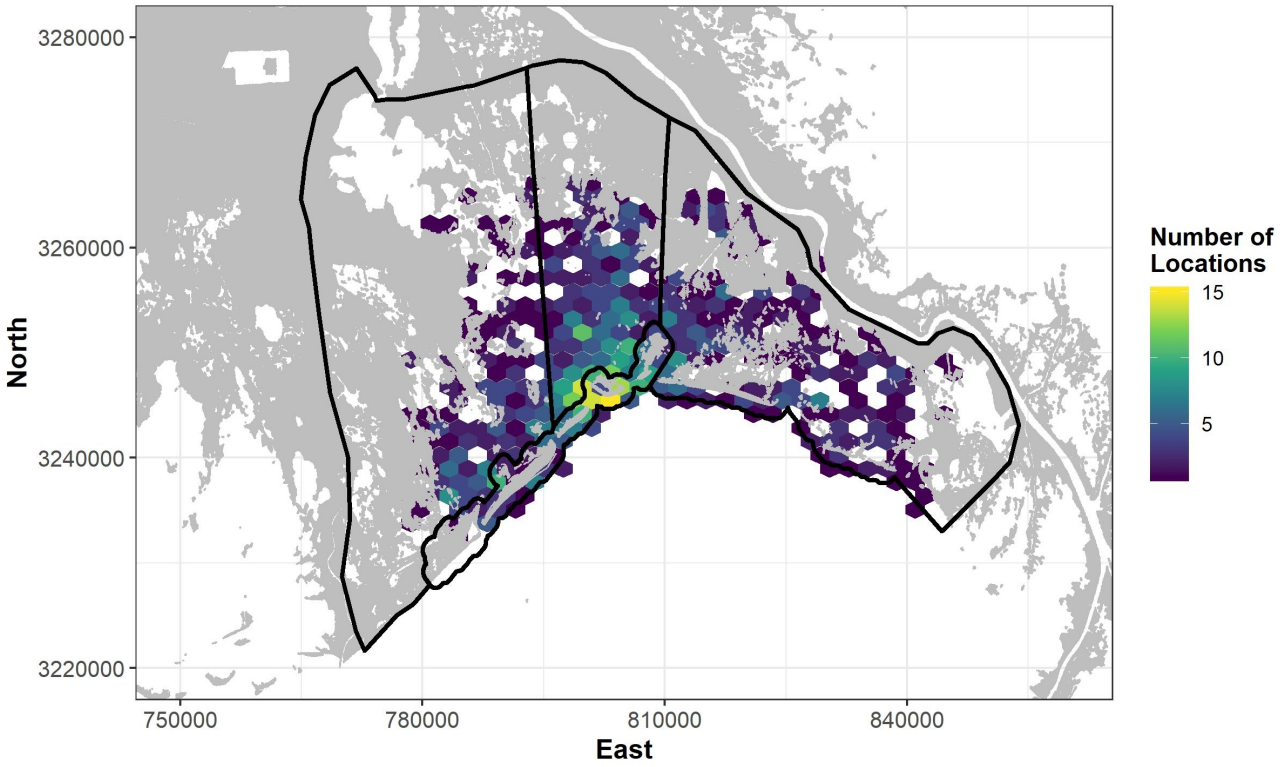

Figure III.5. Example movement histories of simulated dolphins. The outline indicates the regional boundaries. The green lines indicate the annual locations of selected simulated dolphins (numbers).

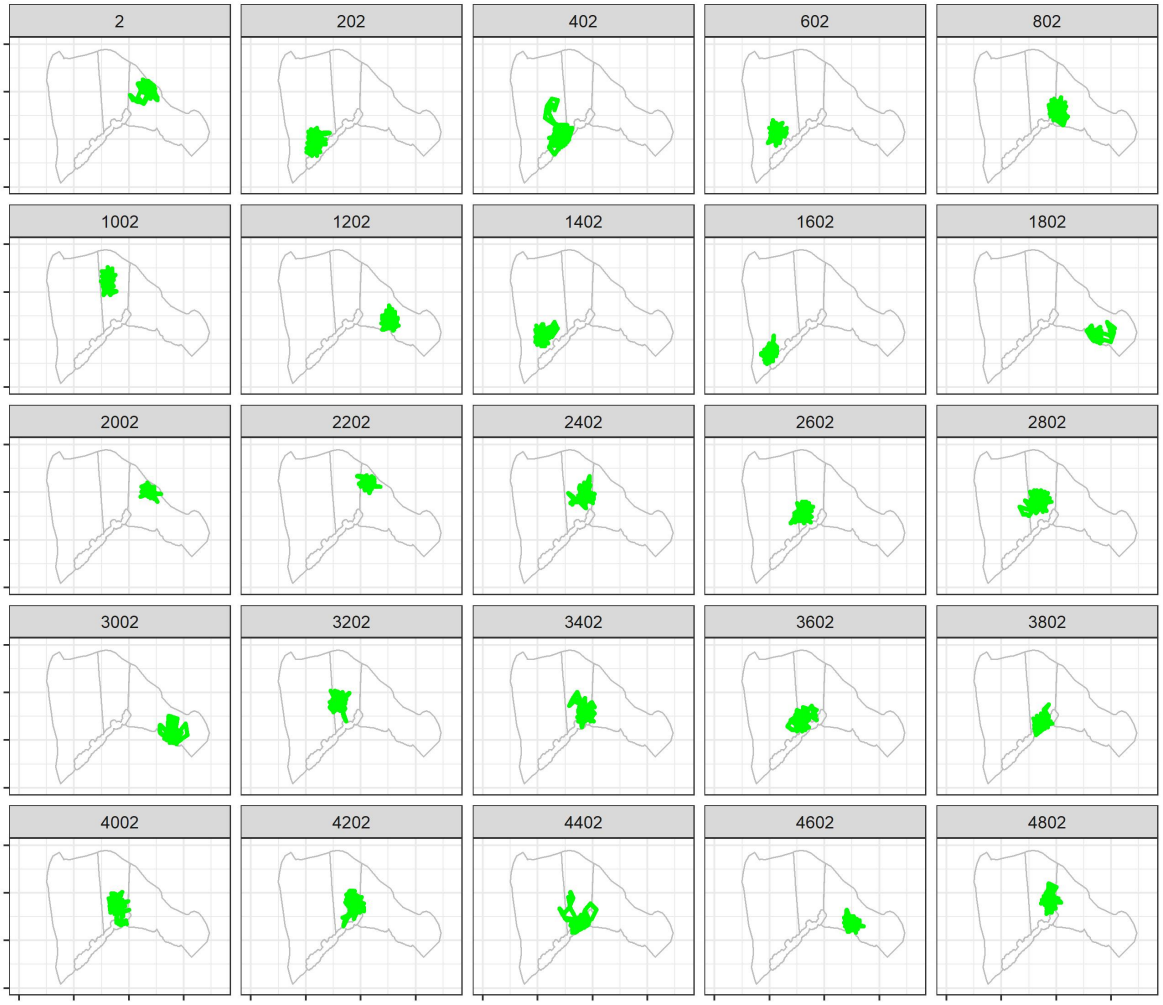

Figure III.6. Mean longest streak metric for different alternatives during cycle 0, representative year. NAA = No Action Alternative, A3 = Alternative 3 (50K CFS diversion), APA = Applicant's Preferred Alternative (75K CFS diversion), A5 = Alternative 5 (150K CFS diversion).

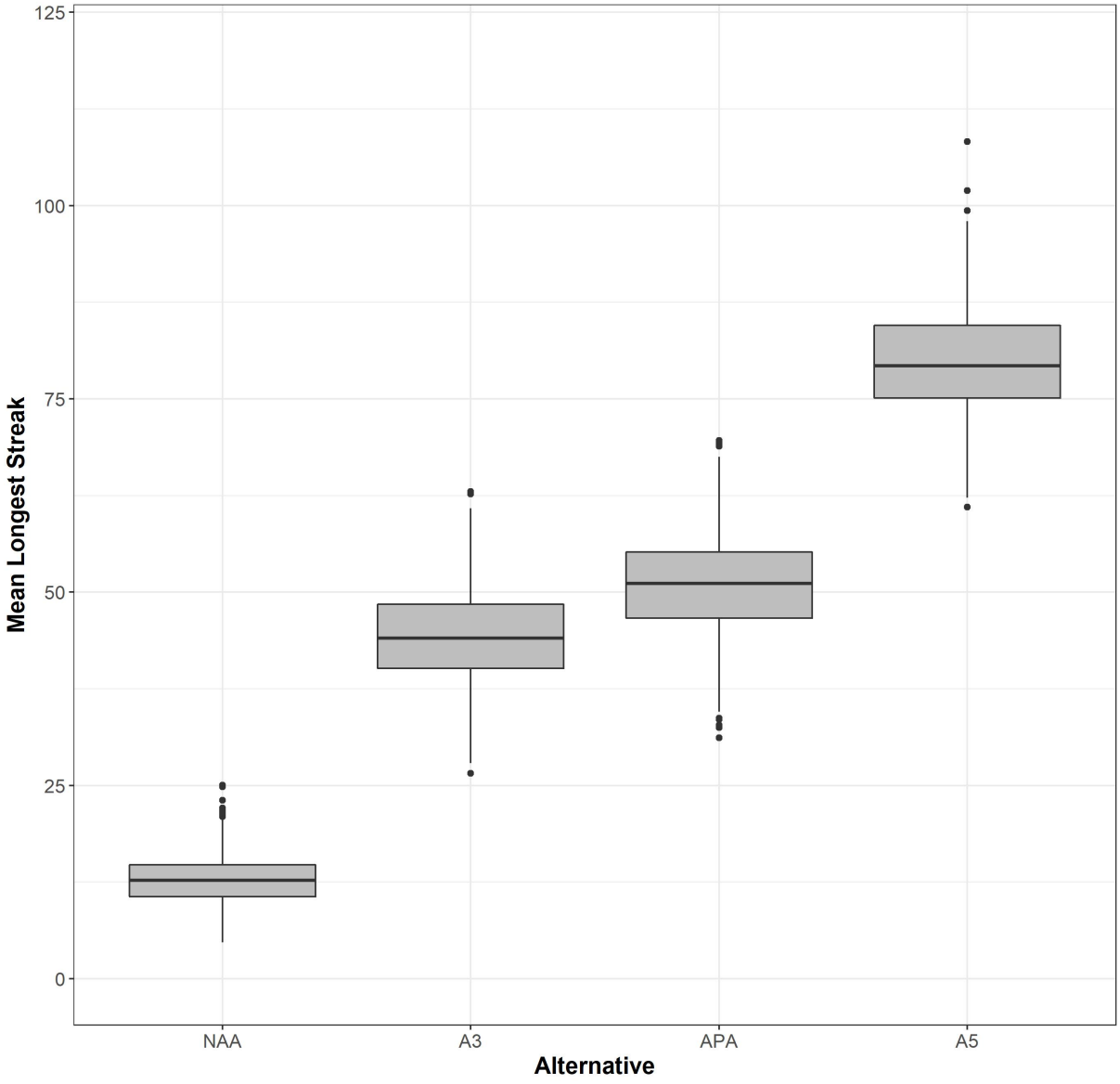

Figure III.7. Mean longest streak metric for different alternatives during cycle 0, representative year by region. NAA = No Action Alternative, A3 = Alternative 3 (50K CFS diversion), APA = Applicant's Preferred Alternative (75K CFS diversion), A5 = Alternative 5 (150K CFS diversion).

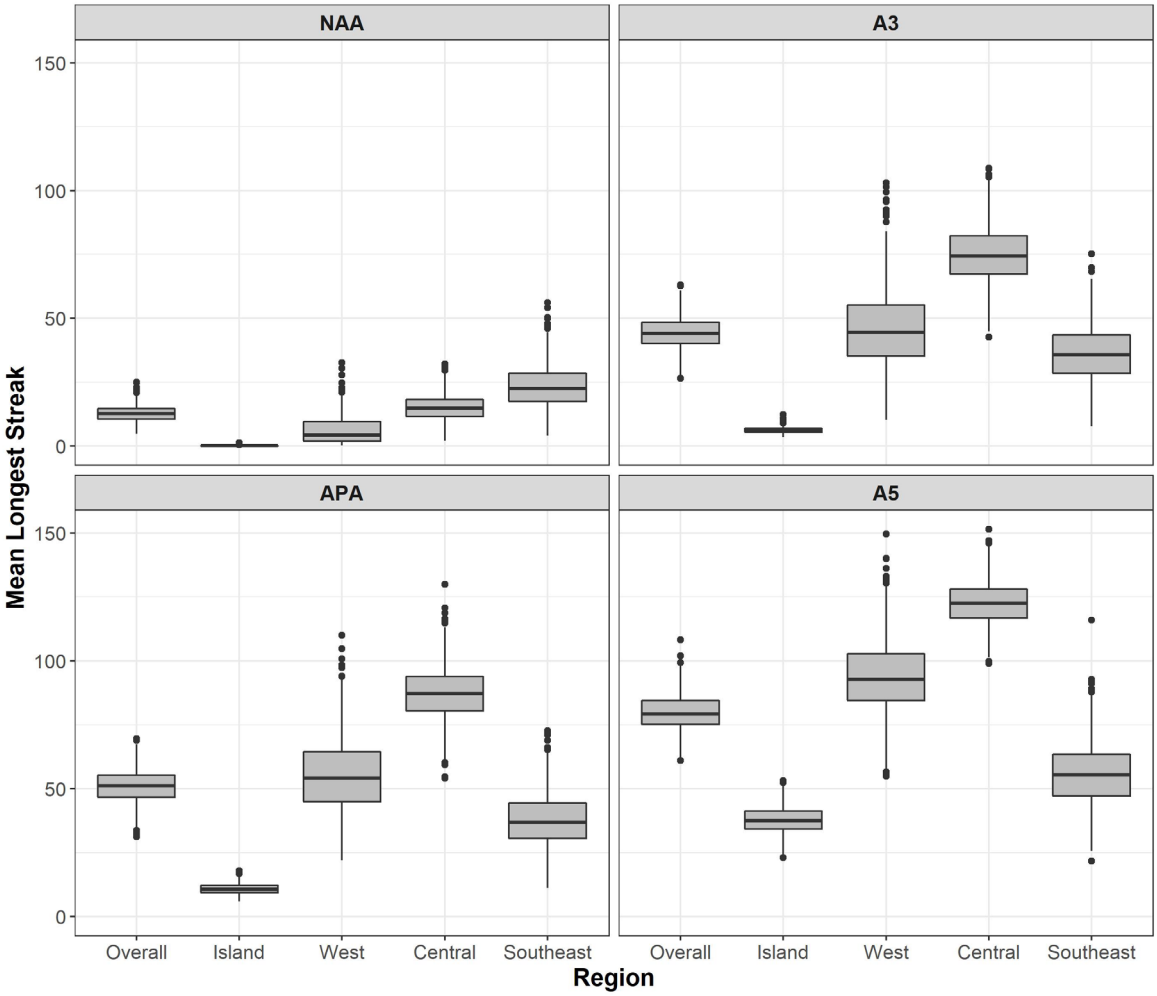

Figure III.8. Survival rates for different alternatives during cycle 0, representative year. P-values indicate results of significance tests comparing survival rates for each alternative to the No Action Alternative. NAA = No Action Alternative, A3 = Alternative 3 (50K CFS diversion), APA = Applicant's Preferred Alternative (75K CFS diversion), A5 = Alternative 5 (150K CFS diversion).

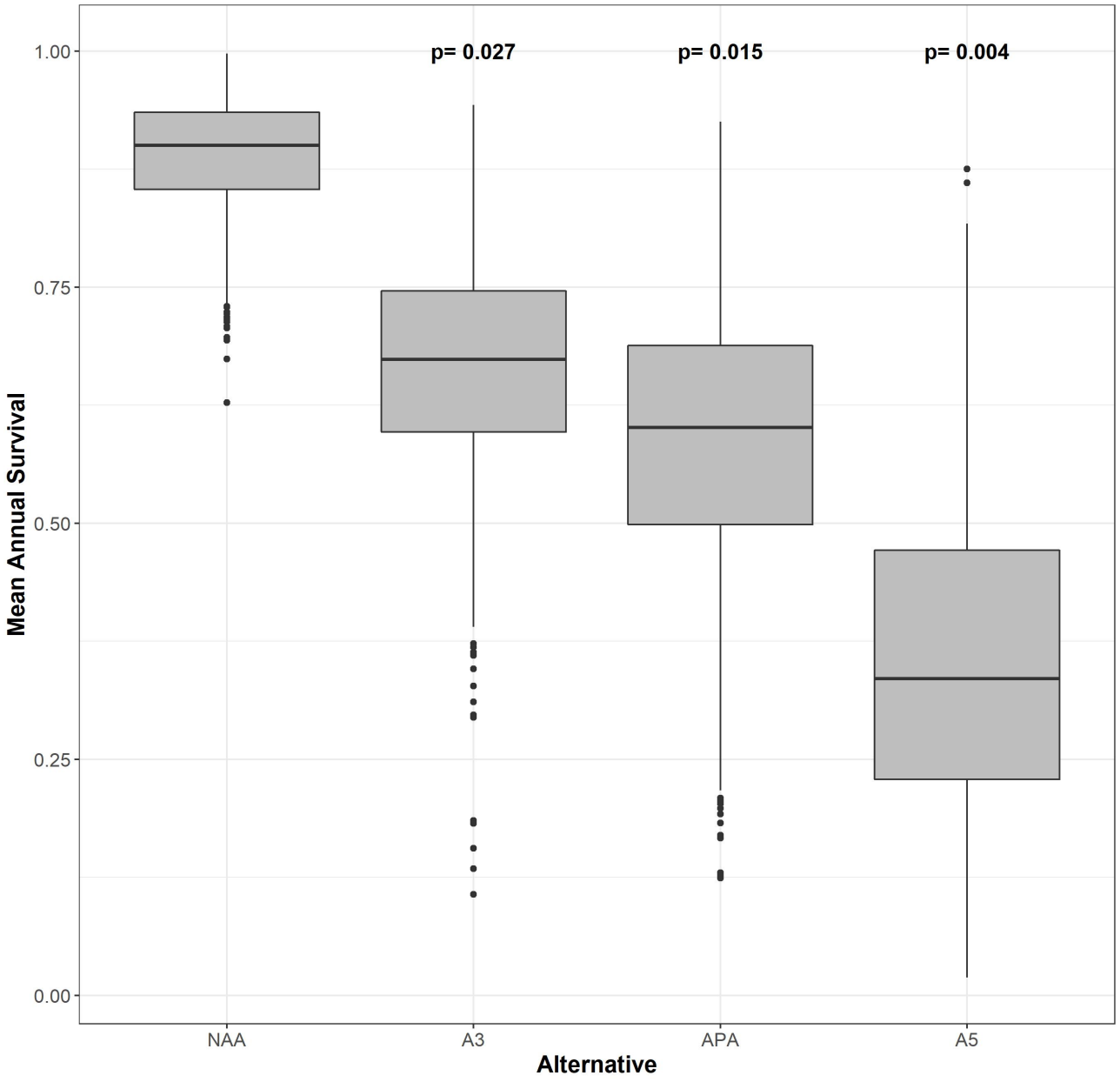

Figure III.9. Survival rates during cycle 0, representative year comparing the No Action Alternative to the Applicants Preferred Alternative by regional stratum. P-values indicate results of significance tests comparing survival rates between alternatives within regions. NS indicates a non-significant ($p > 0.05$) proportion of differences in survival rates less than zero. NAA = No Action Alternative, APA = Applicant's Preferred Alternative (75K CFS diversion).

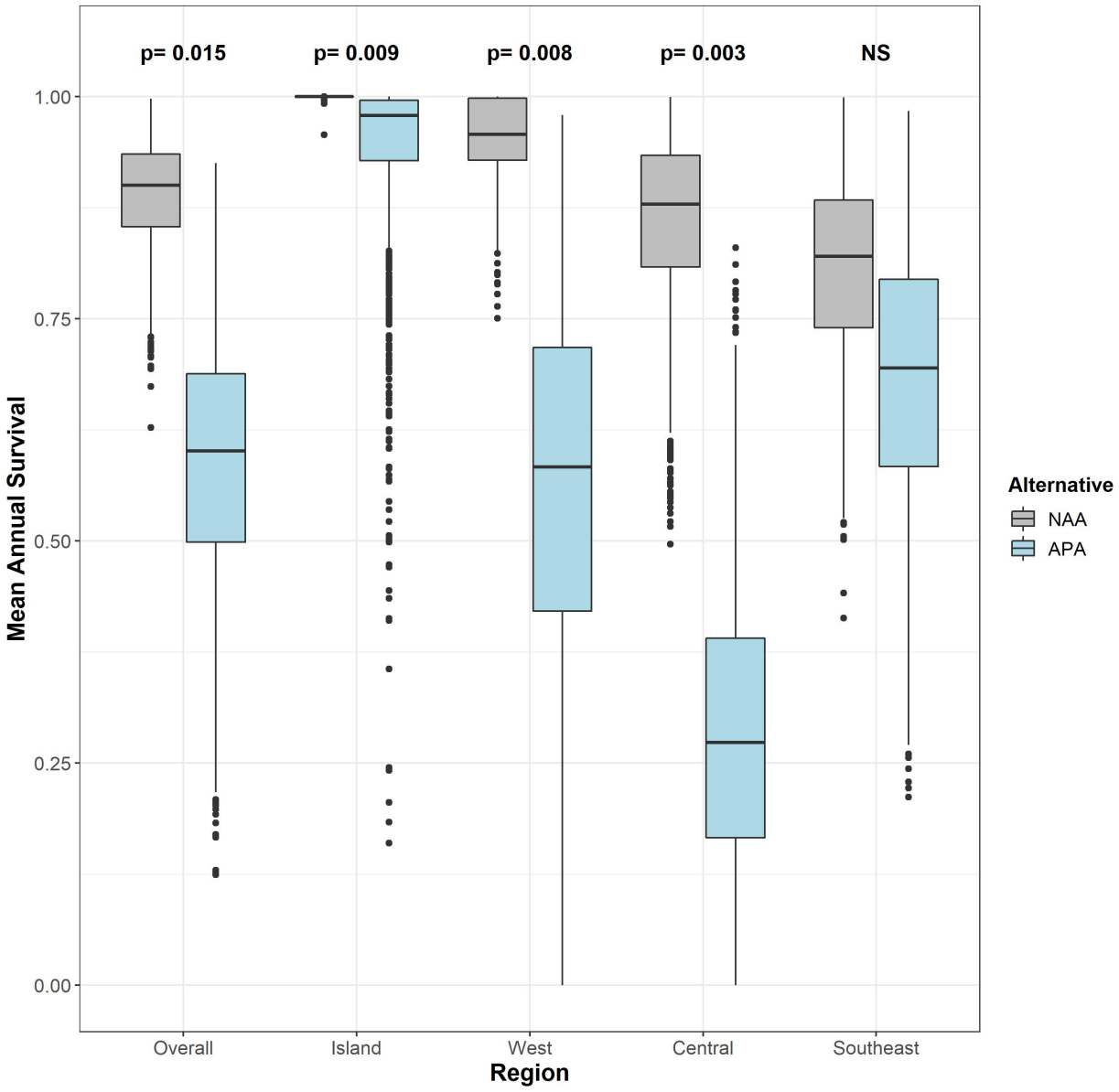

Figure III.10. Regional survival rates during cycle 0, representative year for all alternatives. NAA = No Action Alternative, A3 = Alternative 3 (50K CFS diversion), APA = Applicant's Preferred Alternative (75K CFS diversion), A5 = Alternative 5 (150K CFS diversion).

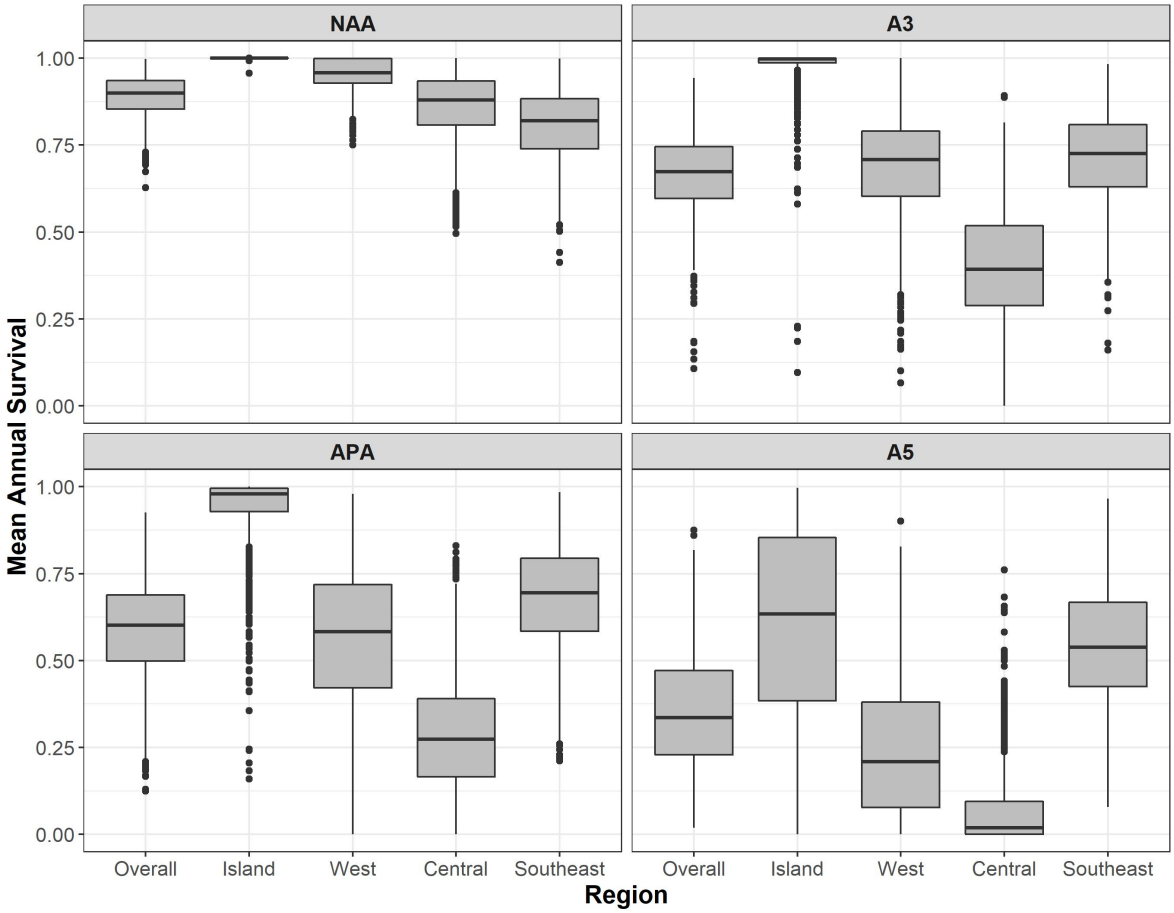

Figure III.11. Population survival rates by alternative for additional years in cycle 0. P-values indicate results of significance tests comparing survival rates for each alternative to the No Action Alternative. NS indicates a non-significant ($p > 0.05$) proportion of differences in survival rates less than zero. NAA = No Action Alternative, A3 = Alternative 3 (50K CFS diversion), APA = Applicant's Preferred Alternative (75K CFS diversion), A5 = Alternative 5 (150K CFS diversion).

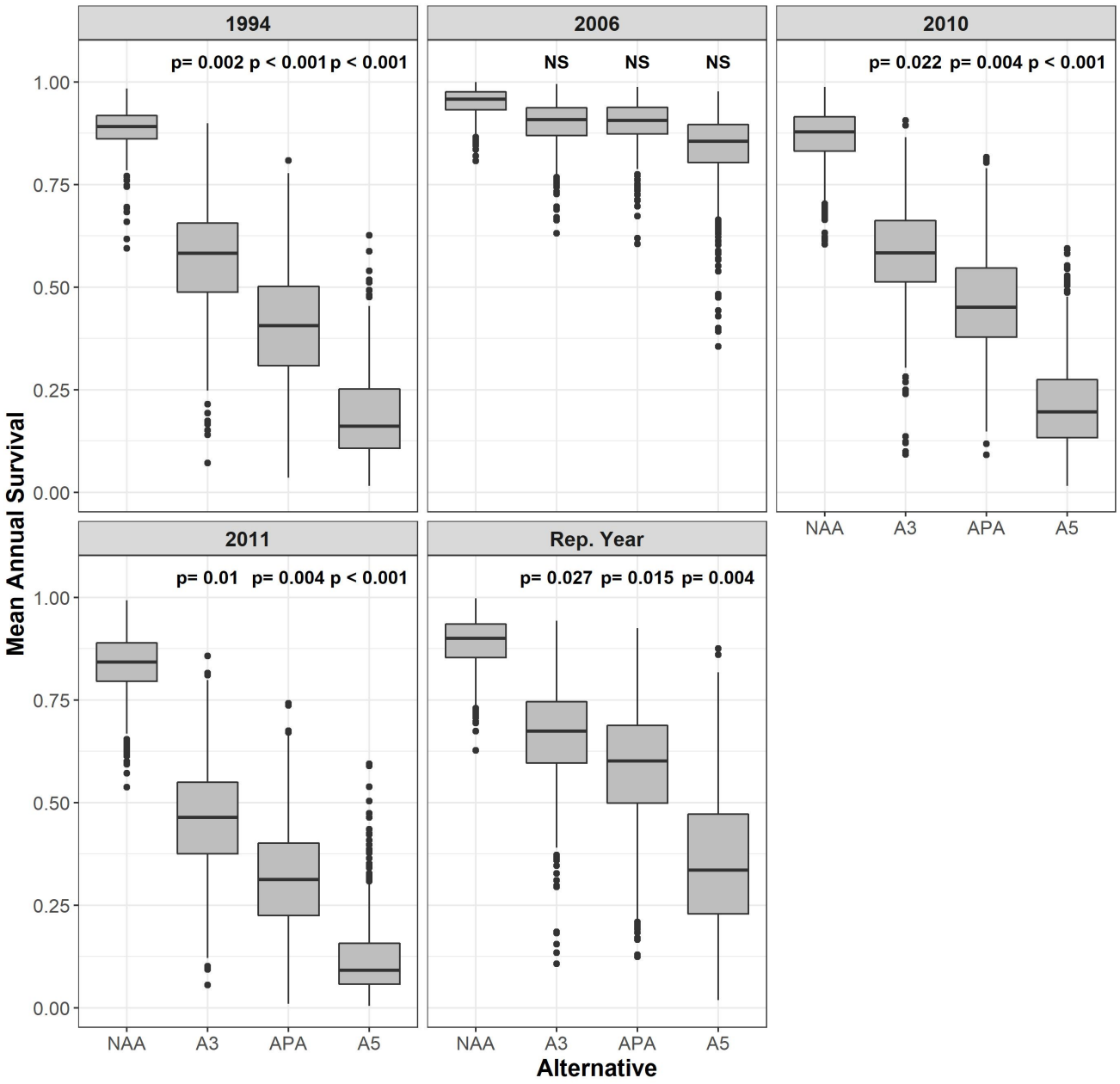

Figure III.12. Population survival rates by alternative for the representative year of each decade. P-values indicate results of significance tests comparing survival rates for each alternative to the No Action Alternative. NS indicates a non-significant ($p > 0.05$) proportion of differences in survival rates less than zero. For all alternatives except the NAA, the populations for cycles 1-5 were restricted to animals with starting positions in the Island strata. NAA = No Action Alternative, A3 = Alternative 3 (50K CFS diversion), APA = Applicant's Preferred Alternative (75K CFS diversion), A5 = Alternative 5 (150K CFS diversion).

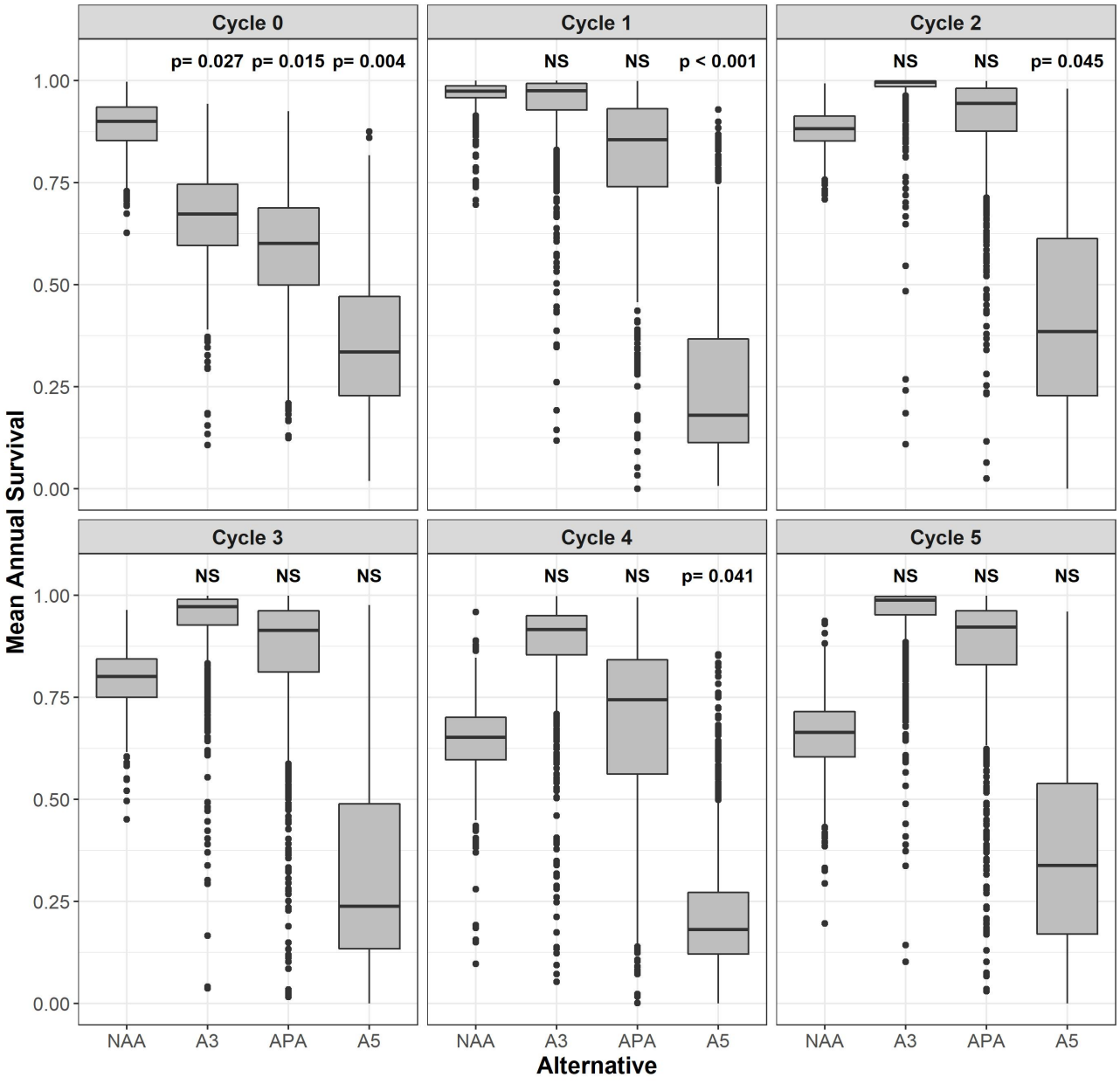

Appendix

II.A1: Summary of Generalized Additive Mixed Model for Cluster 1

M1 – GAMM with station random effects, No Autoregressive Term – Cluster 1

```
Family: gaussian
Link function: identity

Formula:
delta.sal ~ s(jul.day, k = 20) + s(sta.fac, bs = "re")

Parametric coefficients:
            Estimate Std. Error t value Pr(>|t|)
(Intercept)   0.7013     0.2215   3.166  0.00156 **
---
Signif. codes:  0 ‘***’ 0.001 ‘**’ 0.01 ‘*’ 0.05 ‘.’ 0.1 ‘ ’ 1

Approximate significance of smooth terms:
              edf Ref.df      F p-value
s(jul.day) 18.596   18.6 192.08  <2e-16 ***
s(sta.fac)  7.883    8.0  74.69  <2e-16 ***
---
Signif. codes:  0 ‘***’ 0.001 ‘**’ 0.01 ‘*’ 0.05 ‘.’ 0.1 ‘ ’ 1

R-sq.(adj) =  0.568
Scale est. = 2.2474    n = 3141
```

M1AR3 – GAMM with station random effects, AR3 Correlation – Cluster 1

```
Family: gaussian
Link function: identity

Formula:
delta.sal ~ s(jul.day, k = 20) + s(sta.fac, bs = "re")

Parametric coefficients:
            Estimate Std. Error t value Pr(>|t|)
(Intercept)   0.7030     0.2168   3.242   0.0012 **
---
Signif. codes:  0 ‘***’ 0.001 ‘**’ 0.01 ‘*’ 0.05 ‘.’ 0.1 ‘ ’ 1

Approximate significance of smooth terms:
              edf Ref.df      F  p-value
s(jul.day) 14.742  14.74 22.759  < 2e-16 ***
s(sta.fac)  6.636   8.00  5.433 1.69e-08 ***
---
Signif. codes:  0 ‘***’ 0.001 ‘**’ 0.01 ‘*’ 0.05 ‘.’ 0.1 ‘ ’ 1

R-sq.(adj) =  0.551
Scale est. = 2.494     n = 3141
```

Appendix II.A2: Summary of Generalized Additive Mixed Model for Cluster 2

M2 – GAMM with station random effects, No Autoregressive Term – Cluster 2

```
Family: gaussian
Link function: identity

Formula:
delta.sal ~ s(jul.day, k = 20) + s(sta.fac, bs = "re")

Parametric coefficients:
            Estimate Std. Error t value Pr(>|t|)
(Intercept)  -2.1602     0.2826  -7.644 2.57e-14 ***
---
Signif. codes:  0 ‘***’ 0.001 ‘**’ 0.01 ‘*’ 0.05 ‘.’ 0.1 ‘ ’ 1

Approximate significance of smooth terms:
             edf Ref.df     F p-value
s(jul.day) 17.59  17.59 67.93  <2e-16 ***
s(sta.fac) 11.72  12.00 45.97  <2e-16 ***
---
Signif. codes:  0 ‘***’ 0.001 ‘**’ 0.01 ‘*’ 0.05 ‘.’ 0.1 ‘ ’ 1

R-sq.(adj) =  0.282
  Scale est. = 8.1276    n = 4446
```

M2AR3 – GAMM with station random effects, AR3 Correlation – Cluster 2

```
Family: gaussian
Link function: identity

Formula:
delta.sal ~ s(jul.day, k = 20) + s(sta.fac, bs = "re")

Parametric coefficients:
            Estimate Std. Error t value Pr(>|t|)
(Intercept)  -2.1205     0.2883  -7.356 2.25e-13 ***
---
Signif. codes:  0 ‘***’ 0.001 ‘**’ 0.01 ‘*’ 0.05 ‘.’ 0.1 ‘ ’ 1

Approximate significance of smooth terms:
              edf Ref.df     F  p-value
s(jul.day) 11.411  11.41 8.194 3.28e-14 ***
s(sta.fac)  8.912  12.00 3.131 1.21e-06 ***
---
Signif. codes:  0 ‘***’ 0.001 ‘**’ 0.01 ‘*’ 0.05 ‘.’ 0.1 ‘ ’ 1

R-sq.(adj) =   0.26
  Scale est. = 8.7335    n = 4446
```